2012-08-23

Exploiting Diversity in Broadband Wireless Relay Networks

Qingxiong Deng
Worcester Polytechnic Institute

EXPLOITING DIVERSITY IN BROADBAND WIRELESS RELAY NETWORKS

by

Qingxiong Deng

A Dissertation

Submitted to the Faculty

of the

WORCESTER POLYTECHNIC INSTITUTE

in partial fulfillment of the requirements for the

Degree of Doctor of Philosophy

in

Electrical and Computer Engineering

by

Aug. 2012

APPROVED:

Professor Andrew G. Klein, WPI, Major Advisor

Professor D. Richard Brown III, WPI

Professor Dennis L. Goeckel, UMass Amherst

EXPLOITING DIVERSITY IN BROADBAND WIRELESS RELAY NETWORKS

Qingxiong Deng, Ph.D.

Worcester Polytechnic Institute 2012

Fading is one of the most fundamental impairments to wireless communications. The standard approach to combating fading is by adding redundancy - or diversity - to help increase coverage and transmission speed. Motivated by the results in multiple-input multiple-output technologies, which are usually used at base stations or access points, cooperation commutation has been proposed to improve the performance of wireless networks which consist of low-cost single antenna devices. While the majority of the research in cooperative communication focuses on flat fading for its simplicity and easy analysis, in practice the underlying channels in broadband wireless communication systems such as cellular systems (UMTS/LTE) are more likely to exhibit frequency selective fading. In this dissertation, we consider a frequency selective fading channel model and explore distributed diversity techniques in broadband wireless relay networks, with consideration to practical issues such as channel estimation and complexity-performance tradeoffs.

We first study a system model with one source, one destination and multiple decode-and-forward (DF) relays which share a single channel orthogonal to the source. We derive the diversity-multiplexing tradeoff (DMT) for several relaying strategies: best relay selection, random relay selection, and the case when all decoding relays participate. The best relay selection method selects the re-

lay in the decoding set with the largest sum-squared relay-to-destination channel coefficients. This scheme can achieve the optimal DMT of the system at the expense of higher complexity, compared to the other two relaying strategies which do not always exploit the spatial diversity offered by the relays. Different from flat fading, we find special cases when the three relaying strategies have the same DMT. We further present a transceiver design and prove it can achieve the optimal DMT asymptotically. Monte Carlo simulations are presented to corroborate the theoretical analysis. We provide a detailed performance comparison of the three relaying strategies in channels encountered in practice. The work has been extended to systems with multiple amplify-and-forward relays. We propose two relay selection schemes with maximum likelihood sequential estimator and linear zero-forcing equalization at the destination respectively, and both schemes can asymptotically achieve the optimal DMT.

We next extend the results in the two-hop network, as previously studied, to multi-hop networks. In particular, we consider the routing problem in clustered multi-hop DF relay networks since clustered multi-hop wireless networks have attracted significant attention for their robustness to fading, hierarchical structure, and ability to exploit the broadcast nature of the wireless channel. We propose an opportunistic routing (or relay selection) algorithm for such networks. In contrast to the majority of existing approaches to routing in clustered networks, our algorithm only requires channel state information in the final hop, which is shown to be essential for reaping the diversity offered by the channel. In addition to exploiting the available diversity, our simple cross-layer algorithm has the flexibility to satisfy an additional routing objective such as maximization of network lifetime. We demonstrate through analysis and simulation that our proposed routing algorithm

attains full diversity under certain conditions on the cluster sizes, and its diversity is equal to the diversity of more complicated approaches that require full channel state information.

The final part of this dissertation considers channel estimation in relay networks. Channel state information is vital for exploiting diversity in cooperative networks. The existing literature on cooperative channel estimation assumes that block lengths are long and that channel estimation takes place within a fading block. However, if the forwarding delay needs to be reduced, short block lengths are preferred, and adaptive estimation through multiple blocks is required. In particular, we consider estimating the relay-to-destination channel in DF relay systems for which the presence of forwarded information is probabilistic since it is unknown whether the relay participates in the forwarding phase. A detector is used so that the update of the least mean square channel estimate is made only when the detector decides the presence of training data. We use the generalized likelihood ratio test and focus on the detector threshold for deciding whether the training sequence is present. We also propose a heuristic objective function which leads to a proper threshold to improve the convergence speed and reduce the estimation error. Extensive numerical results show the superior performance of using this threshold as opposed to fixed thresholds.

ACKNOWLEDGEMENTS

First and foremost, I am grateful to my supervisor, Prof. Andrew G. Klein, who has given me the chance to pursue Ph.D. degree and who has guided my intellectual development throughout the last four years. He taught me not only how to think critically and accurately, but also how to write clearly and coherently. I am forever indebted to his innumerable insights, patience and encouragement in helping me with my research. I will never forget the pep-talks he gave to me in times of difficulty and frustration. Ph.D. thesis always seems an endless journey; without him, I could never have finished this dissertation.

I would like to thank my Ph.D. committee, Prof. D. Richard Brown III and Prof. Dennis L. Goeckel for agreeing to serve on my committee, and contributing insightful comments in examining my work. Special thanks go to Prof. Brown for allowing me to sit in his lab with the company from his Ph.D. students.

I wish to thank my graduate labmates, Yanjie Peng, Raquel G. Machado, Min Ni, Joshua R. Bacon and Yizheng Liao. I am grateful to them for taking the time to discuss my research problems, and creating an intellectual and aspiring atmosphere in the lab.

I owe enormous thanks to many people in and outside of WPI for helping me in life and study. I am lucky to have so many people to share knowledge and experience with me. Without their support and care, I would not have had a smooth start of living in U.S.

Finally, I want to say thanks to my family for their love and support. I would not have come to WPI for a Ph.D. degree if I did not have a family that valued education. I am also very grateful to Siming Lu for always caring about me and standing by my side.

TABLE OF CONTENTS

LIST OF TABLES

LIST OF FIGURES

LIST OF ABBREVIATIONS

Abbreviation	Meaning
AF	amplify-and-forward
AWGN	additive white Gaussian noise
BER	bit-error rate
BPSK	binary phase shift keying
CSI	channel state information
CSIR	channel state information at the receiver
CSIT	channel state information at the transmitter
DF	decode-and-forward
DFE	decision-feedback equalization
DMT	diversity-multiplexing tradeoff
DP	decision point
DSTC	distributed space-time code
DSFC	distributed space-frequency code
FFF	feed forward filter
FBF	feedback filter
GLRT	generalized likelihood ratio test
ISI	intersymbol interference
LMS	least mean square
MAC	media access control
MFB	matched-filter bound
MIMO	multiple-input multiple-output
MLSE	maximum-likelihood sequential estimation
MMSE	minimum mean square error
OFDM	orthogonal frequency-division multiplexing
PDF	probability density function
QAM	quadrature amplitude modulation
RS	relay selection
SC	single carrier
SIMO	single-input multiple-output
SNR	signal-to-noise ratio
STBC	space-time block code
ZFE	zero-forcing equalization

LIST OF SYMBOLS

Symbol	Meaning
$\boldsymbol{e}_i$	Unit canonical vector
$\mathbf{0}_{m\times n}$	$m \times n$ matrix of all 0's
$\mathbf{1}_{m\times n}$	$m \times n$ matrix of all 1's
$\boldsymbol{I}_n$	$n \times n$ identity matrix
$\otimes$	Kronecker product (i.e. matrix direct product)
$\times_n$	n-mode tensor/matrix product
$(\cdot)^\top$	matrix transpose
$(\cdot)^H$	matrix conjugate transpose
$[\boldsymbol{S}]_i$	ith column of matrix $\boldsymbol{S}$
$[\boldsymbol{S}]_{i,j}$	i,jth entry of matrix $\boldsymbol{S}$
$\text{sgn}(\cdot)$	signum function
$\text{diag}(\boldsymbol{x})$	Square diagonal matrix with vector $\boldsymbol{x}$ along diagonal
$\text{diag}(\boldsymbol{A})$	Vector resulting from extraction of diagonal elements of $\boldsymbol{A}$
$\lceil\cdot\rceil$, $\lfloor\cdot\rfloor$	round up, down to nearest integer
$\text{tr}(\cdot)$	matrix trace
$\Re\{\cdot\}$	Extraction of real-valued component
$\nabla_{\boldsymbol{f}}$	Gradient with respect to $\boldsymbol{f}$
$\|\|\boldsymbol{x}\|\|_p$	ℓ_p norm
$E[\cdot]$	Expectation
$\delta[\cdot]$	Discrete Kronecker delta function

Chapter 1

Introduction

The exponentially growing need for data connectivity has fuelled fast development of wireless technologies. From cellular networks, wireless local area networks (WLANs), and wireless sensor networks to wireless body area networks, wireless technologies have expanded into almost every aspect of our lives. With the wide usage of smartphones, cellular networks have evolved to carry more diversified data. Along with traditional voice data and regular traffic such as web browsing, messaging, and file transfers, cellular networks have increasingly been carrying more and more real-time traffic such as video and games. Such real-time traffic requires higher data rates to achieve the required quality of service (QoS). The ever growing demand for multimedia streaming on mobile terminals has inspired the deployment of 4G mobile networks. To help meet ubiquitous personal wireless data service demands, greater efforts are being made to increase the data rate and extend the coverage of wireless communications.

1.1 Motivation

Transmitting reliable and high-rate data over a wireless channel is a very challenging task since wireless channels are susceptible to noise, interference and other

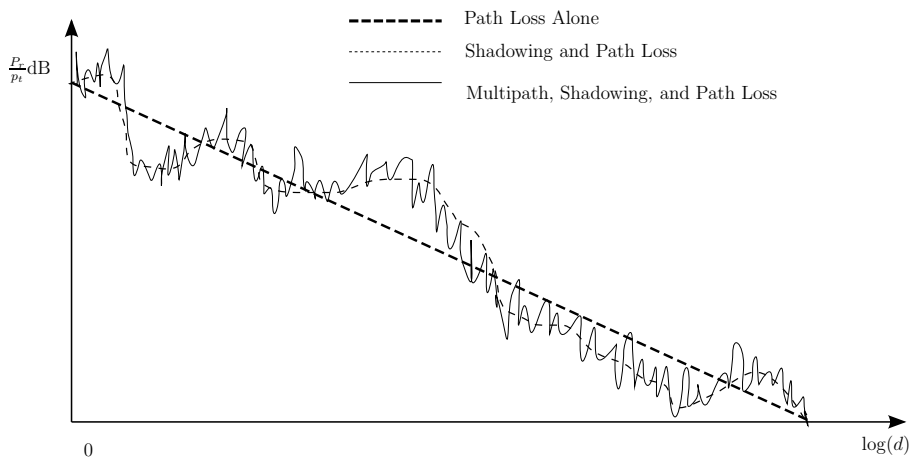

Figure 1.1: Path loss, shadowing, and multipath. [1]

impairments [1]. In particular, three major factors, as shown in Fig. 1.1, affect the power of the received signal. The first two are *path loss* and *shadowing*. Path loss is the reduction in the received signal power due to propagation through space. Shadowing is the power attenuation in the received signal due to the blockage from obstacles in the signal path. The amount of path loss and shadowing in the received signal varies due to the dynamic transmission environment. Variations in path loss and shadowing occur when the mobile device moves through a distance on the order of the cell size, and are collectively referred to as *large-scale fading*. Large-scale fading is usually accounted for in the cell-site planning stage [2], and is mitigated by power control. The typical way power control combats large-scale fading is by requiring a specified minimum received signal-to-noise ratio (SNR) on all mobiles within the cell to achieve acceptable performance [1].

In addition to large-scale fading, another inevitable impairment to wireless communications is *multipath fading*, the randomness of the channel which happens on a much faster time-scale than large-scale fading, as shown in Fig. 1.1. It is

caused by multiple dynamic reflectors in the transmission environment. As shown in Fig. 1.2, trees, buildings, and ground can serve as reflectors. As a result, the received signal is a superposition of many constructive and destructive responses, each traversing though different paths. The relative path lengths might change since the transmitter or the receiver may be moving, or any of the objects that provide reflective surfaces may be moving. As wireless communications usually use high carrier frequencies, at least of the order of 10^8 Hz, a small difference in the relative path length may cause significant phase changes in the signal. Therefore, multipath fading is categorized as small-scale fading, which occurs at a small distance on the order of the carrier wavelength. In addition, due to different propagation times, the difference in the arrival time of responses from the longest path and the shortest path, which is defined as *delay spread*, may be spread over multiple symbol durations. If the delay spread is longer than the symbol duration, the received signal is impaired not only by noise, but also by inter-symbol interference (ISI). Because of different phase responses along different paths, some frequencies undergo constructive interference while the others encounter destructive interference. As shown in Fig. 1.3, the frequency response of the channel within the signal passband varies significantly. In this situation, the received signal suffers frequency selective (FS) fading, and the underlying channel (FS fading channel) is usually modelled as a finite impulse response (FIR) filter in discrete time, with each coefficient as a random variable. If the delay spread does not exceed the symbol duration, the channel experiences frequency flat fading.

Multipath fading can cause significant degradation in communication performance. As shown in Fig. 1.4, the BER for binary phase shift keying (BPSK) over the Rayleigh fading channel decays much slower than the BER for BPSK over the

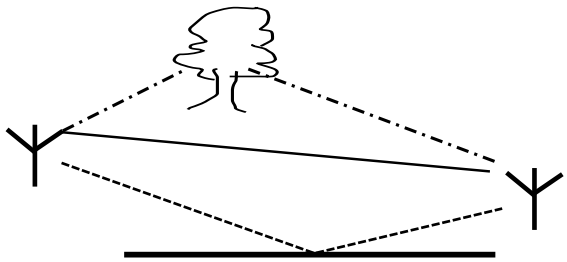

Figure 1.2: Sources of multipath fading.

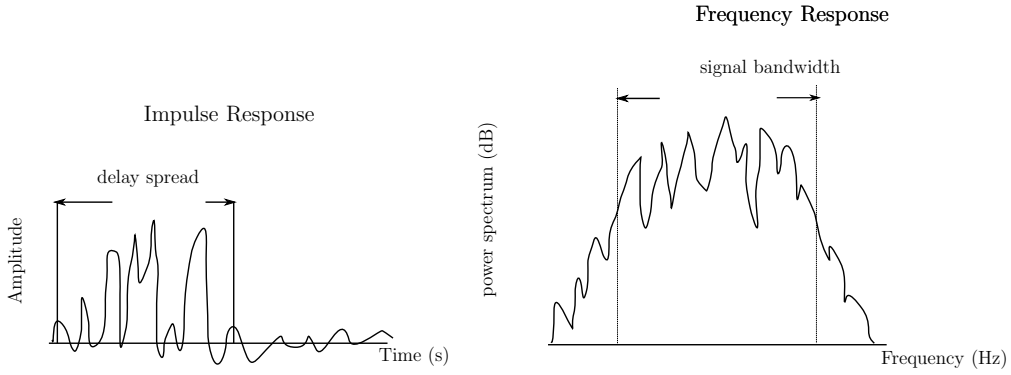

Figure 1.3: Frequency selective channel.

additive white Gaussian noise (AWGN) channel, as the AWGN channel doesn't suffer from fading. If there is a strong destructive response in the channel, the received SNR can experience a severe drop and may result in temporary failure of communication. This case is frequently referred to as a *deep fade*. While addressing large-scale fading is typically handled during cell-site planning, combating multipath fading is done in the design of communication receivers.

The basic idea of combating multipath fading is to reduce the probability that the channel is in a deep fade. An immediate thought to combat multipath fading is to employ redundancy by sending the signal on another channel independent from the original channel, as the chance of two independent channels simultaneously in deep fades is lower than that of one channel in a deep fade. In this way, the

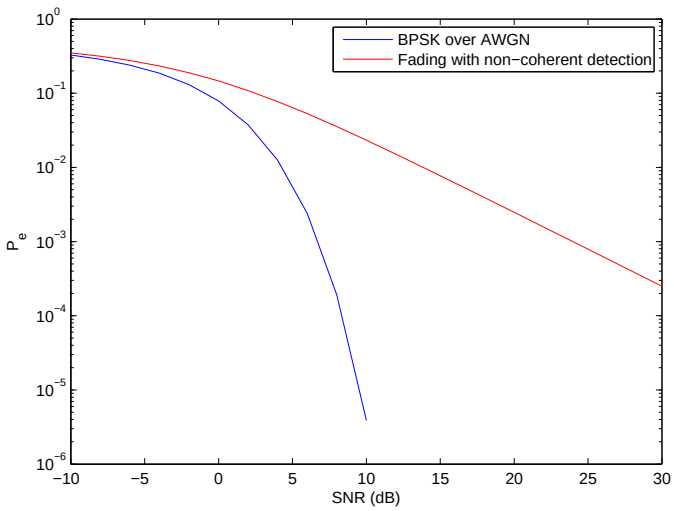

Figure 1.4: Performance degradation caused by fading.

additional channel can be regarded as providing more *diversity* to the radio communication. Diversity has been considered a powerful technique to combat fading and increase reliability. Diversity can be obtained through *coding* and *interleaving*, where information is dispersed into different coherence periods, different coherence bandwidth, and sufficiently spaced antennas [2]. In another words, there are three basic diversity techniques: (1) time diversity, (2) frequency diversity, and (3) space diversity. Fig. 1.5 shows an example of how time diversity can be achieved through interleaving. If in the second coherence time intervals the channel is in deep fade, without interleaving it is difficult to recover the information in the second coherence time interval; with interleaving, two thirds of the information throughout the three coherence time interval remains good and the whole information can be recovered with very high probability. Spatial diversity is particularly attractive since it provides diversity gain without using additional time or bandwidth resources [2].

One way to exploit spatial diversity is through multi-antenna or multi-input multi-output (MIMO) technologies [3], where both of the transmitter and receiver

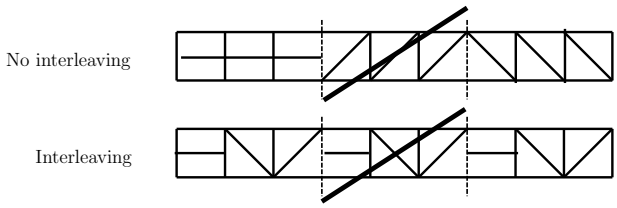

Figure 1.5: Time diversity achieved through interleaving. Without interleaving, a deep fade will wipe out the entire codewords.

can be installed with more than one antenna. Fig. 1.6 shows a MIMO example where the transmitter uses two antennas and the receiver uses three antennas. The MIMO technologies include precoding (multi-layer beamforming), diversity coding (space-time coding), and spatial multiplexing. It is able to either increase throughput (multiplexing gain) or increase reliability (diversity gain) with the same amount of power without using extra scare spectral resources. This performance improvement originates from the increased ability to combat wireless channel variation, i.e. *fading*, by using multiple transmitting-receiving antenna pairs, where each antenna pair provides a possible statistically independent channel at the same carrier frequency and time. However, achieving statistical independence requires that the separation distance between antennas to be at least a few carrier wavelengths. Furthermore, multi-antenna technologies typically require relatively intensive computation, especially in decoding complicated space-time block codes (STBCs). Hence, multi-antenna technologies are usually used only at base stations. Owing to the size constraint and limited processing power, small-sized mobile terminal devices seldom use multiple antennas, or usually use no more than two antennas.

Another way to exploit spatial diversity is through cooperative communication, or cooperative diversity [4], which can utilize spatially separated antennas as

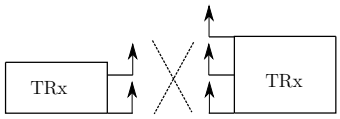

Figure 1.6: MIMO: a 2×3 example.

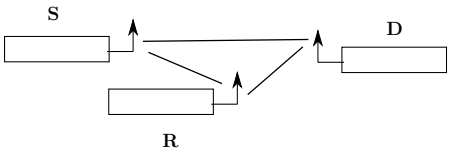

Figure 1.7: Cooperative communication: a "virtual" antenna array.

an array to provide spatial diversity and help combat fading with single-antenna wireless devices. The basic idea of cooperative communication is to allow single-antenna devices to share their antennas in such a way that they form a "virtual antenna array" to reap a similar benefit of MIMO. The key idea in cooperative communication resides in the broadcast nature of wireless channels. As shown in Fig. 1.7, when the source transmits to the destination, a *relay* within the transmission range can receive the signal and can be a potential auxiliary node that assists in forwarding the signal to the destination. Cooperative communication provides the benefit of increased energy efficiency, extended coverage, and increased network throughput. The Third Generation Partnership Project's (3GPP) Long Term Evolution-Advanced (LTE-Advanced) has developed a new standard which uses relays in mobile broadband access, resulting in throughput enhancement and coverage extension [5] in a cost-effective way.

Cooperative communication poses many challenges to communication system designers. To enable cooperative diversity techniques to operate on low-cost small-sized devices, the limited processing capability of cooperative nodes requires algorithms that do not involve intense computation. Because the antennas are spa-

tially distributed on different mobile devices, existing MIMO techniques such as STBCs cannot be directly used without careful considerations of the possible timing asynchrony, carrier asynchrony, processing delay, non-linearity of most existing RF-frond ends, and imperfect information recovery at the relays. Current literature shows extensive research efforts in designing efficient relay protocols [4, 6], designing DSTC [7, 8], and new channel estimation techniques [9, 10].

The majority of research in cooperative communication assumes frequency flat channels for its simplicity and analytical tractability. In high data-rate communications, the signal duration is small and the bandwidth of the signal is much larger than the coherence bandwidth of the channel, resulting in frequency selective (FS) fading [2]. In many practical radio communication systems, e.g. GSM, WiFi, the underlying channels can exhibit FS behavior. Thus, if high data rates are desired in cooperative communication, it is imperative that we address the FS fading scenario. As the signal consumes more bandwidth, more frequency diversity can be exploited. The amount of frequency diversity is equal to the number of independent paths that can be resolved from the channel at the receiver. In cooperative relay systems, system designers should be able to exploit both frequency diversity and cooperative diversity, and existing techniques for flat channels need to be adapted, or new techniques need to be designed.

The existing network structure and protocols may need to be redesigned to support cooperative communication. For example, most distributed coding schemes assume almost simultaneous transmission; if the destination is within the radio reception range of multiple relays, the simultaneous transmission of the multiple relays can cause collision at the destination. This collision may not be allowed

in certain systems, e.g. systems which use carrier sense multiple access (CSMA) mechanism. Furthermore, traditional layered implementations of a communication entity with reference to the Open Systems Interconnection (OSI) model need to be changed to improve communication performance. The layered implementation requires clear specifications and interoperability between the upper layers and the lower layers. The benefit of this layered implementation is easy portability. However, with an increasing need for ubiquitous wireless data service, the limitation of such layered implementations becomes more prominent. For example, the congestion control of transmission control protocol (TCP) in WLANs cannot differentiate between loss due to fading and congestion-related loss, resulting in reduced network throughput. A new paradigm called cross-layer design [11] has emerged to improve network performance. Cross-layer design in wireless networks focuses on passing knowledge such as channel conditions of the physical layer and the medium access control (MAC) layer to higher layers for efficient resource allocation. This practice has been taken into account in CDMA2000, the enhancement High Speed Downlink Packet Access (HSDPA), and other systems.

This dissertation focuses on a particular diversity technique for cooperative networks with FS fading, namely relay selection, which can be considered to be a form of cross-layer design. The first relay selection scheme for cooperative networks was proposed in [12] where in the presence of multiple relays, only a single relay is selected as the forwarding relay and the selection criteria are based on the various forms of physical layer channel gains. It is as spectrally efficient as schemes based on distributed space-time codes (DSTC) but avoids high decoding complexity. In addition, it can achieve the same diversity-multiplexing tradeoff (DMT) [13] as DSTC. Such merits in relay selection have led to an increase in research attention.

In this dissertation, we develop relay selection schemes for a two-hop relay model with FS fading, and we extend the results to multi-hop relay networks. In addition to the study on relay selection, this dissertation also addresses new channel estimation problems that arise in relay channels as it is well recognized that channel state information at the receiver (CSIR) is essential to exploiting diversity.

1.2 Thesis Overview

The main objective of this dissertation is to exploit both frequency diversity and cooperative diversity in broadband wireless relay networks, with consideration to practical issues such as channel estimation and complexity-performance tradeoffs. We focus on system design which can exploit diversity in an efficient manner since diversity has a close connection to the bit-error rate (BER) performance. For fixed rate transmission, diversity can be interpreted as the SNR exponent which describes how fast the error probability can be decreased with SNR, as shown in Fig. 1.8. Hence, the larger the diversity gain, the better the BER performance in the high SNR region. It should be noted that the diversity analysis only accurately predicts behavior in the high SNR region. In evaluating performance over finite SNRs, the diversity measured as the negative slope of each outage curve often does not coincide exactly with the predicted maximal diversity [14,15]. In addition, different ways of system design may result in different power gains which determine what SNR is needed to achieve a specific BER level. However, in general, schemes with larger diversity order tend to achieve larger power gain. Also, the BER of systems designed with larger diversity orders can eventually be lower than those designed with smaller diversity orders if the SNR keeps increasing. Therefore,

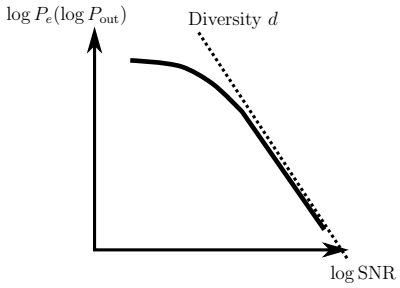

Figure 1.8: Diversity illustrated as the order that the error probability decreases exponentially with the SNR.

in this dissertation, we assume high SNR and focus on diversity to assist in the analysis, but use BER or outage probability as the performance metric.

The main body of this dissertation consists of three major parts:

- Relay selection in two-hop cooperative networks with FS fading (Chapter 2, Chapter 3)
- Routing in multi-hop clustered-based cooperative networks with flat fading and with FS fading (Chapter 4)
- Adaptive channel estimation for decode-and-forward (DF) relay channels (Chapter 5)

and is followed by a conclusion and discussions of future research.

For any system model, it is crucial to understand the maximal diversity present in the system and all the possible diversity techniques that can be used. Given a fixed amount of additional power, we have a choice in that we can either allocate the additional power to extra symbols to increase the rate, or we can allocate

the power to the existent symbols to decrease the error probability. The choice between increasing the rate and decreasing the error probability is called DMT, which is an effective tool to characterize the maximal diversity. As shown in Fig. 1.9, sending the same information twice reduces the rate by half but doubles the diversity. We first use this tool to find the maximal diversity in a single-source, single-destination, multi-relay system with correlated FS fading. In Chapter 2, we study the relay selection when the relays employ the DF protocol. The objective of exploiting both frequency diversity and cooperative diversity is achieved through two stages. In the first stage, full frequency diversity is assumed to be achieved in each point-to-point channel as the matched-filter bound (MFB) is used. Based on this assumption, we derive the DMT for several relaying strategies: best relay selection, random relay selection, and the case when all decoding relays participate. In the second stage, we devote special effort to exploiting frequency diversity and present two transceiver designs which are proven to asymptotically achieve the optimal DMT with best relay selection. In Chapter 3, we study the relay selection when the relays employ the amplify-and-forward (AF) protocol. We find that to achieve full cooperative diversity, the relay selection method is closely connected to the equalization method the destination uses. Accordingly, we employ the MFB to develop a relay selection method for maximum-likelihood sequential estimation (MLSE) and develop another relay selection for linear zero-forcing equalization (ZFE).

While best relay selection can achieve the maximal diversity, it requires channel estimation of each decode-relay-to-destination channel and thus causes delay in information delivery due to channel estimation. On the other hand, random relay selection randomly selects any decoding relay for forwarding and therefore results

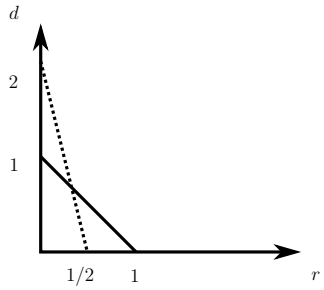

Figure 1.9: Diversity-multiplexing tradeoff curves for a single antenna slow fading Rayleigh channel: repetition coding increases diversity but reduces rate.

in much less delay than best relay selection. In multi-hop relay networks with DF relays, random relay selection might be a significantly better choice than best relay selection as the delay at relays accumulates through hops and may limit the usage of certain applications. This idea is verified in Chapter 4 with our proposed algorithm for routing in clustered multi-hop networks where geographically close nodes at each hop are considered as a cooperation group. Our proposed algorithm uses best relay selection at the last hop and random relay selection at the rest of the hops to help meet additional routing objectives (e.g. delay) without sacrificing too much diversity. We also present a comparison of several routing algorithms (including the one which achieves full diversity) on achievable diversity and complexity. We first analyze the routing algorithms for such multi-hop networks by assuming flat fading, then extend the analysis to FS fading.

Channel state information at the receiver (CSIR) is generally needed to exploit diversity [2] and plays an important role in transceiver design. Even in the proposed algorithm in Chapter 4, without the channel state information for best relay selection at the last hop, the last hop would be the diversity bottleneck. Hence accurate channel knowledge at the receiver is needed to avoid serious degradation in outage

performance. The majority of the current research of channel estimation in cooperative channels focuses on block fading. With the block fading assumption, the training in each block is assumed long enough for channel estimation and the DF-relay-to-destination channel estimation problem is degraded to the point-to-point channel estimation problem. In practice, assuming the BER at the decoding relay is fixed, the longer the block length, the lower the decoding probability of the DF relay. In addition, a longer block length may result in larger processing delay and also cause larger transmission delay which limits its usage in certain time-sensitive applications. On the other hand, due to zero-padded transmission, longer block length can achieve higher throughput efficiency. Hence, the system designer needs to carefully choose the block length to meet the system requirement. In Chapter 5, we study the channel estimation problem for the DF-relay-to-destination channel when the block length is short, and the training data is spread across blocks.

1.3 Thesis Contribution

The main contributions of this dissertation are as follows.

- Relay selection in two-hop cooperative networks with FS fading (Chapter 2 and Chapter 3)

  For a single-source, single-destination, multi-relay network, we derived the upper bound of DMT or the optimal DMT in the presence of correlated FS fading. Under the assumptions that relays work under a half-duplex constraint and orthogonal channel usage between source and relays, we consider the relay selection problem. If multiple relays are selected, we constrain the

transmission power to be the same as when only one relay is selected. For relays employing DF protocol, we have the following results (Chapter 2):

- The characterization and comparison of DMT based on MFB for several relaying strategies: best relay selection, random relay selection, and the case when all decoding relays participate. This leads to the guidance of system design on the tradeoff of performance and complexity. While in this dissertation we primarily studied these three relay selection methods, these methods can be considered as examples of using all decoding relays with certain power allocation strategies and delay variations. Better performance can be achieved with more complicated power allocation schemes which require channel state information at the transmitter (CSIT).
- Two transceiver designs, both of which are proven to asymptotically achieve the optimal DMT if combined with best relay selection method. One design is based on single-carrier (SC) linear ZFE, and the other is based SC infinite-length ZF-DFE.
- Simulation studies on the performance of best relay selection with transceiver designs based on linear ZFE, MMSE-DFE and MLSE.
- Performance comparison of two multi-DF-relay systems where one system uses best relay selection and SC MLSE, and the other uses orthogonal frequency-division multiplexing (OFDM), distributed space-frequency coding (DSFC) and maximum-likelihood estimation. Simulation results show that the performance of relay selection is better than that of DSFC (we acknowledge that the DSFC scheme used for com-

parison requires only knowledge of the number of decoding relays at the transmitters while our best relay selection requires the result of comparing multiple channel state information at the transmitter). While SC has lower peak-to-average power ratio, and is more robust to spectral nulls, less sensitivity to carrier frequency offset, with CSIT, OFDM can employ channel-adaptive subcarrier bit and power loading and power loading to achieve higher throughput and better energy efficiency. To our best knowledge, this is the first comparison between DSFC and relay selection in the context of FS fading.

In Chapter 3, we study the relay selection problem when the relays use the AF protocol. To simplify the analysis, we assume i.i.d. FS fading and only consider the case when a single relay is selected. The summary of the results in this part is as follows:

  - Analysis of a new relay selection method that we show achieves full diversity with MLSE at the destination.
  - Analysis of a new relay selection method that we show achieves full diversity with linear ZFE at the destination.
  - Performance comparison based on simulation for the multi-DF-relay system and the multi-AF-relay system where both use the relay selection to achieve the optimal DMT. In the high SNR region, relay selection with DF protocol performs better than relay selection with AF protocol.

- Routing in multi-hop clustered-based cooperative networks with and without FS fading (Chapter 4)

We consider the routing problem in a multi-hop network where immediate nodes at each hop are clustered together and employ the DF protocol. This hierarchical structure based on clustering has risen to attention for its ability of providing scalable routing, supporting quality-of-service requirements, and easy mobility management. The results are summarized as follows:

  - A low-complexity routing algorithm for clustered-based relay networks which has the flexibility to simultaneously satisfy an additional routing objective such as maximization of network lifetime. By performing opportunistic routing rather than pre-selecting the routing, the proposed algorithm reduces the knowledge of CSIT without drastically degrading attainable diversity.
  - The analytical comparison on achievable diversity in three routing algorithms with different level of CSIT in the clustered multi-hop network with flat fading and FS fading. Our analysis shows that full diversity can be achieved without full CSIT.

- Adaptive channel estimation for decode-and-forward (DF) relay channels (Chapter 5)

  We consider the channel estimation problem for the relay-to-destination channel when the relay uses the DF protocol. The probabilistic presence of training data for the relay-to-destination channel poses a challenge on this estimation problem. By assuming quasi-static fading and short block length to meet the short-delay constraint, we have a channel estimation problem where the training is spread across multiple blocks. We apply the least mean square (LMS) algorithm to adaptively estimate the channel. Our contribu-

tions are:

- A novel algorithm which combines detection and LMS-style adaptation. We analyze the algorithm and give exact analytical results on average time constant and misadjustment, which are functions of the probability of detection and probability of false alarm of the detector.
- A heuristic method for setting the threshold of the detector to achieve a faster convergence speed. We develop an intuitive objective function, which leads to a good threshold to achieve a satisfactory tradeoff between convergence speed and error performance on the channel estimate. We consider practical issues and use empirical average rather than assume that statistics are known.

Chapter 2

Relay Selection in Decode-and-Forward Cooperative Networks with Frequency Selective Fading

This chapter considers the relay selection problem in a two-hop relay network when FS fading is present in the system. The system model with correlated frequency selective (FS) fading is first introduced. An upper bound of the diversity-multiplexing tradeoff (DMT) of such a system is derived without a specific relay protocol or a relay selection method. Then, we apply the decode-and-forward (DF) relay protocol constraint and present the outage probability analysis of three different relay selection schemes, namely, best relay selection, random relay selection and all-decoding-relay participation. Among the three methods, we see that only best relay selection method can achieve the upper bound on DMT of the system. The outage probability analysis is based on the matched filter bound (MFB) which assumes only one symbol is transmitted. Hence, we further analyze the relay selection methods with practical transceiver designs where the information symbols are grouped into blocks before transmission.

2.1 Introduction

Cooperative relay networks have emerged as a powerful technique to combat multipath fading and increase energy efficiency [16, 17]. To exploit spatial diversity in the absence of multiple antennas, several spatially separated single-antenna nodes can cooperate to form a virtual antenna array. Such systems usually employ half-duplex relays and come in two flavors [4, 6, 18, 19]: those where the relays transmit on *orthogonal* channels so that transmission from the source and each relay is received separately at the destination, or those where a single *non-orthogonal* channel is shared between the source and relays so that all nodes may transmit on the same common channel at the same time. Here, we focus on the former class of systems which employ *orthogonal* relay channels, where the orthogonality is often accomplished through time-division.

Cooperative relay systems with orthogonal channels typically either employ multiple orthogonal relay subchannels in conjunction with repetition coding, or all relays use a single orthogonal relay channel along with distributed space-time coding (DSTC) [7]. While the use of repetition codes is attractive for its simplicity, this approach requires relay scheduling and dedicated orthogonal channels for each relay which uses up precious system resources. On the other hand, when using a single orthogonal relay channel with DSTC, the scheduling of relays is of no concern, but DSTC requires synchronization between relays which is very difficult in distributed networks. Asynchronous forms of space-time coding have been proposed (e.g. [8]), but the decoding complexity may still be prohibitively complex to permit their use in low-cost wireless ad hoc networks. Furthermore, the non-linearity of most existing RF front-ends poses additional implementation

challenges for DSTC-based approaches [20].

More recently, relay selection schemes have been proposed [12, 21] which use simple repetition coding, very simple scheduling, and a single relay channel. Remarkably, these schemes can achieve the same diversity-multiplexing tradeoff (DMT) [13] as DSTC relaying, and can even outperform DSTC systems in terms of outage probability [21, 22]. Using relay selection is an attractive alternative to avoid the spectral inefficiency of repetition coding and the increased decoding complexity required for DSTC.

Most existing cooperative diversity research assumes that the fading channels have flat frequency responses. In high data-rate wireless applications, however, the coherence bandwidth of the channels tends to be smaller than the bandwidth of the signal, resulting in frequency selective fading [2]. For such high rate communication in cooperative relay networks, existing techniques for flat fading channels need to be adapted, or new techniques need to be designed for frequency selective fading channels. In [23], the authors considered a system with a single amplify-and-forward (AF) relay over frequency selective channels, and proposed three DSTCs. In [24], the authors consider a multiple-AF-relay OFDM system and proposed a distributed space-frequency code. The three DSTCs in [23] and the distributed space-frequency code in [24] can achieve both cooperative diversity and frequency diversity where the frequency diversity through a relay is up to the minimum of the source-relay channel length and the relay-destination channel length. Simpler, non-DSTC approaches that employ relay selection have been proposed for communication through frequency-selective fading channels. For example, in [25, 26], uncoded OFDM is studied, and it was shown that if relay selection is done on

a per-subcarrier basis, full spatial diversity can be achieved. However, neither of these OFDM-based relay selection methods were able to exploit the frequency diversity of the ISI channel [27]. A linearly precoded OFDM system was proposed in [28] which uses multiple amplify-forward relays with linear transmit precoding; a simulation-based study showed that two relay selection schemes exhibited a coding gain improvement compared to an orthogonal round-robbin relaying scheme.

This paper investigates the performance limits of relay selection with FS fading and focuses on the DMT for single-carrier (SC) systems without CSIT and transmit precoding. We analyze three different relay selection methods, including best relay selection, random relay selection, and all-decoding-relay participation. The relays in these three methods use a single orthogonal subchannel with repetition coding. We derive the DMT for the relay selection methods and then propose two transceiver designs both of which asymptotically attain the optimal DMT. Both transceivers uses uncoded quadrature amplitude modulation (QAM) with guard intervals between blocks along with linear zero-forcing equalization (ZFE) or zero-forcing decision-feedback equalization (ZF-DFE) respectively.

2.2 System Model

2.2.1 Channel Model

We consider a system as in Fig. 2.1, which consists of a single source node ($\mathbf{S}$), K relay nodes ($\mathbf{R}_{1,2,\ldots,K}$), and a single destination node ($\mathbf{D}$). We assume that all nodes have the same average power constraint P watts and transmission bandwidth W

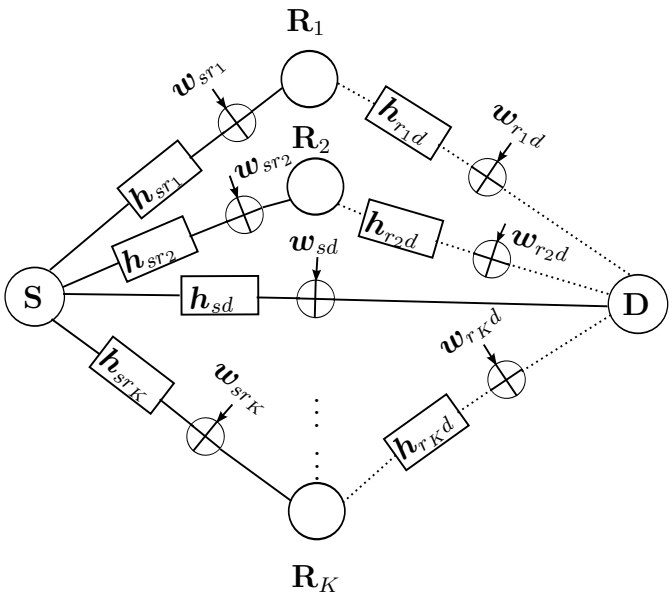

Figure 2.1: System model.

Hz. While this model has been well-studied in the case of static flat channels [29], here the links between the nodes are assumed to be frequency selective quasi-static fading channels, modeled as complex FIR filters. In the subscript, we denote s as source node, r_i as ith relay, and d as destination. Thus the source to destination channel coefficients are contained in the vector $\boldsymbol{h}_{sd}$. Similarly, for $i \in 1, 2, \ldots, K$, the source to relay $\mathbf{R}_i$ channels are contained in $\boldsymbol{h}_{sr_i}$ and the relay $\mathbf{R}_i$ to destination channels are contained in $\boldsymbol{h}_{r_id}$. Most analyses of diversity through frequency selective channels focus on the case where the channel taps are i.i.d. [30,31]. Even when multiple paths in the continuous time channel experience independent fading, however, the channel taps themselves can be highly correlated due to pulse shaping [2]. In addition, pulse shaping typically causes the number of discrete time channel taps to be quite a bit larger than the number of (possibly independent) fading paths. To incorporate correlated fading – as well as the effects of path loss, shadowing and imperfect timing synchronization – we assume that the channel

taps arise as $\boldsymbol{h}_{jk} = \boldsymbol{\Gamma}_{jk}\boldsymbol{\delta}_{jk}$ where jk could be sd, sr_i or r_id, $\boldsymbol{\delta}_{jk} \sim \mathcal{CN}(\mathbf{0}, \boldsymbol{I}_{L_{jk}})$ represents the L_{jk} independent fading paths. The autocovariance of the M_{jk} channel taps can then be specified by appropriate choice of $\boldsymbol{\Gamma}_{jk} \in \mathbb{R}^{M_{jk}\times L_{jk}}$ whose maximum singular value and minimum singular value are denoted as $\xi_{jk,\max}$ and $\xi_{jk,\min}$ respectively. Without loss of generality, we assume that $\boldsymbol{\Gamma}_{jk}$ is full column rank and $M_{jk} \geq L_{jk}$ so that the number of coefficients in the effective channel impulse response may be greater than the number of fading paths in the physical channel.

The channel coefficients are assumed to be constant over a block, and are independent from one block to the next. We assume perfect channel state information (CSI) at the destination and no CSI at the source. Furthermore, the transmission is presumed to be perfectly synchronized at the block level. In addition, all links have additive noise which is assumed to be mutually independent, zero-mean circularly symmetric complex Gaussian with variance N_0 and the discrete-time signal-to-noise ratio is defined as

$$\rho \triangleq \frac{P}{WN_0}.$$

While the assumption of equal node powers and equal noise variances may seem impractical, the case of unequal powers and variances does not change the asymptotic high-SNR analysis which follows since these constants disappear in the derivation; consequently, we make this simplifying assumption to aid the clarity of the exposition.

2.2.2 Diversity-Multiplexing Tradeoff

The DMT has proven to be a useful theoretical tool that has considerably advanced the design of codes in the MIMO context. By restricting attention to system behavior in the high-SNR regime, DMT analysis permits a mathematically tractable comparison of various transmission and relaying schemes.

We define the outage probability as the probability that the mutual information I between source and destination falls below rate R, and this is denoted as $\Pr[I < R(\rho)]$. The multiplexing gain and the diversity gain are then defined as [2]

$$r \triangleq \lim_{\rho\to\infty} \frac{R(\rho)}{\log \rho}, \qquad d(r) \triangleq -\lim_{\rho\to\infty} \frac{\log(\Pr[I < R(\rho)])}{\log \rho}$$

respectively, where I is the mutual information between the source and destination, and $R(\rho)$ denotes the source data rate which is assumed to scale as $R(\rho) = r \log \rho$. The notation $\doteq$ denotes asymptotic equality in the large ρ limit with $A \doteq B$ meaning

$$\lim_{\rho\to\infty} \frac{\log A}{\log \rho} = \lim_{\rho\to\infty} \frac{\log B}{\log \rho}.$$

2.2.3 Upper Bound on the DMT

The MFB assumes that the source only sends a single symbol $x[0]$ and the relay $\mathbf{R}_i$ only sends a single symbol $x_{r_i}[0]$ where $E[|x[0]|^2] = E[|x_{r_i}[0]|^2] = P/W$. For each source-to-relay link, the received signal at the relay is $\boldsymbol{y}_{r_i} = \boldsymbol{h}_{sr_i} x[0] + \boldsymbol{w}_{r_i}$ where $\boldsymbol{w}_{r_i}$ is the noise at $\mathbf{R}_i$, and for each relay-to-destination link, the received signal at the destination can be expressed as $\boldsymbol{y}_{r_i d} = \boldsymbol{h}_{r_i d} x_{r_i}[0] + \boldsymbol{w}_{d_i}$ where $\boldsymbol{w}_{d_i}$ is the noise at the destination $\mathbf{D}$ when $\mathbf{R}_i$ is transmitting. For the source-to-

destination link, the received signal can be written as $\boldsymbol{y}_{sd} = \boldsymbol{h}_{sd}x[0] + \boldsymbol{w}_{d_s}$ where $\boldsymbol{w}_{d_s}$ is the noise at the destination $\mathbf{D}$ when the source $\mathbf{S}$ is transmitting. Thus the mutual information between source and destination can be written as $I_{sd} = \log(1 + \|\boldsymbol{h}_{sd}\|^2\rho)$. Similarly, we can find the mutual information between source and ith relay as $I_{sr_i} = \log(1 + \|\boldsymbol{h}_{sr_i}\|^2\rho)$ and the mutual information between ith relay to destination as $I_{r_id} = \log(1 + \|\boldsymbol{h}_{r_id}\|^2\rho)$. Define set $\mathcal{R}$ consisting of all K relay nodes, and define a partition of $\mathcal{R}$ as $(\mathcal{V}, \mathcal{R}\backslash\mathcal{V})$. For the network as presented in the channel model with a single source $\mathbf{S}$ and a single sink $\mathbf{D}$, a cut $(\mathcal{S}, \mathcal{T})$ is defined as $\mathcal{S} = \{\mathbf{S}\} \cup \mathcal{V}$ and $\mathcal{T} = \{\mathbf{D}\} \cup (\mathcal{R}\backslash\mathcal{V})$. The capacity of a minimum cut of such a network can be upper bounded as [32]

$$I_{\text{cut}} = \min_{\mathcal{V}}(I_{sd} + \sum_{\mathbf{R}_i \in (\mathcal{R}\backslash\mathcal{V})} I_{sr_i} + \sum_{\mathbf{R}_i \in \mathcal{V}} I_{r_id}). \tag{2.1}$$

The outage probability is lower bounded as

$$\begin{aligned} \mathrm{P}_{\text{out}} &\geq \Pr[I_{\text{cut}} < r\log\rho] \\ &= \Pr[\min_{\mathcal{V}}(I_{sd} + \sum_{\mathbf{R}_i \in (\mathcal{R}\backslash\mathcal{V})} I_{sr_i} + \sum_{\mathbf{R}_i \in \mathcal{V}} I_{r_id}) < r\log\rho] \\ &= \max_{\mathcal{V}} \Pr[(I_{sd} + \sum_{\mathbf{R}_i \in (\mathcal{R}\backslash\mathcal{V})} I_{sr_i} + \sum_{\mathbf{R}_i \in \mathcal{V}} I_{r_id}) < r\log\rho]. \end{aligned} \tag{2.2}$$

For a particular partition of relay nodes $\mathcal{V}$, we have the outage probability

$$\begin{aligned}
& \Pr[I_{sd} + \sum_{\mathbf{R}_i \in (\mathcal{R}\setminus\mathcal{V})} I_{sr_i} + \sum_{\mathbf{R}_i \in \mathcal{V}} I_{r_i d} < r \log \rho] \\
= \; & \Pr[\log(1 + \|\boldsymbol{h}_{sd}\|^2 \rho) + \sum_{\mathbf{R}_i \in (\mathcal{R}\setminus\mathcal{V})} \log(1 + \|\boldsymbol{h}_{sr_i}\|^2 \rho) + \sum_{\mathbf{R}_i \in \mathcal{V}} \log(1 + \|\boldsymbol{h}_{r_i d}\|^2 \rho) < r \log \rho] \\
= \; & \Pr[\log((1 + \|\boldsymbol{h}_{sd}\|^2 \rho) \cdot \prod_{\mathbf{R}_i \in (\mathcal{R}\setminus\mathcal{V})} (1 + \|\boldsymbol{h}_{sr_i}\|^2 \rho) \cdot \prod_{\mathbf{R}_i \in \mathcal{V}} (1 + \|\boldsymbol{h}_{r_i d}\|^2 \rho)) < r \log \rho] \quad (2.3) \\
\dot{\leq} \; & \Pr\left[\|\boldsymbol{h}_{sd}\|^2 \rho + \sum_{\mathbf{R}_i \in (\mathcal{R}\setminus\mathcal{V})} \|\boldsymbol{h}_{sr_i}\|^2 \rho + \sum_{\mathbf{R}_i \in \mathcal{V}} \|\boldsymbol{h}_{r_i d}\|^2 \rho < \rho^r \right] \quad (2.4) \\
\doteq \; & \Pr\left[\|\boldsymbol{\delta}_{sd}\|^2 \rho + \sum_{\mathbf{R}_i \in (\mathcal{R}\setminus\mathcal{V})} \|\boldsymbol{\delta}_{sr_i}\|^2 \rho + \sum_{\mathbf{R}_i \in \mathcal{V}} \|\boldsymbol{\delta}_{r_i d}\|^2 \rho < \rho^r \right] \quad (2.5) \\
\doteq \; & \rho^{-(L_{sd} + \sum_{\mathbf{R}_i \in (\mathcal{R}\setminus\mathcal{V})} L_{sr_i} + \sum_{\mathbf{R}_i \in \mathcal{V}} L_{r_i d})(1-r)}. \quad (2.6)
\end{aligned}$$

where (2.3) follows from $\log A + \log B = \log(AB)$, (2.4) follows from the fact that $\Pr(a + b < c) \leq \Pr(a < c)$ for any $a, b, c \geq 0$, (2.5) follows from the fact that $\xi^2_{jk,\min} \|\boldsymbol{\delta}_{jk}\|^2 \leq \|\boldsymbol{h}_{jk}\|^2 \leq \xi^2_{jk,\max} \|\boldsymbol{\delta}_{jk}\|^2$, and (2.6) holds as $\|\boldsymbol{\delta}_{sd}\|^2 + \sum_{\mathbf{R}_i \in (\mathcal{R}\setminus\mathcal{V})} \|\boldsymbol{\delta}_{sr_i}\|^2 + \sum_{\mathbf{R}_i \in \mathcal{V}} \|\boldsymbol{\delta}_{r_i d}\|^2$ is chi-squared distributed with $L_{sd} + \sum_{\mathbf{R}_i \in (\mathcal{R}\setminus\mathcal{V})} L_{sr_i} + \sum_{\mathbf{R}_i \in \mathcal{V}} L_{r_i d}$ degrees of freedom.

Substituting (2.6) into (2.2), the outage probability is lower bounded as

$$\mathrm{P}_{\text{out}} \;\dot{\geq}\; \rho^{-\min_{\mathcal{V}}(L_{sd} + \sum_{\mathbf{R}_i \in (\mathcal{R}\setminus\mathcal{V})} L_{sr_i} + \sum_{\mathbf{R}_i \in \mathcal{V}} L_{r_i d})(1-r)}. \quad (2.7)$$

Thus the DMT is upper bounded as

$$\begin{aligned}
d(r) \; & \leq \; \min_{\mathcal{V}} (L_{sd} + \sum_{\mathbf{R}_i \in (\mathcal{R}\setminus\mathcal{V})} L_{sr_i} + \sum_{\mathbf{R}_i \in \mathcal{V}} L_{r_i d})(1-r) \\
& = \; (L_{sd} + \sum_{i=1}^{K} \min(L_{sr_i}, L_{r_i d}))(1-r) \quad (2.8)
\end{aligned}$$

as the minimum is attained when relay $\mathbf{R}_i$ is in $\mathcal{V}$ if $L_{r_i d} < L_{sr_i}$ and is not in $\mathcal{V}$ otherwise.

For half-duplex orthogonal relays, the multiplexing gain is halved [33] and the upper bound on the DMT for the same channel model but with half-duplex relaying becomes

$$d(r) \leq (L_{sd} + \sum_{i=1}^{K} \min(L_{sr_i}, L_{r_i d}))(1 - 2r). \tag{2.9}$$

2.3 Outage Probability Analysis

We now focus on the decode-and-forward relay system and derive its outage probability and diversity-multiplexing tradeoff under several different relaying strategies. We assume the message sent by the source node is encoded to a block of N source symbols. The relays operate in half-duplex mode, and thus do not transmit and receive at the same time. In addition, the relay nodes and the source use the same transmission bandwidth but employ time division so that the relays transmit on a channel orthogonal to the source. The transmission of a complete message is divided into two phases:

1. In phase one, the source broadcasts the message to the destination and the relays, and each relay attempts to decode the message.

2. In phase two, the source is silent. Depending on the relay selection strategy, some or all of the relays that successfully decoded the message (if any) forward the message to the destination.

The source and relays then alternate between these two phases; this is shown in Fig. 5.2 for the case where two relays $\mathbf{R}_1$ and $\mathbf{R}_K$ participate in the second

phase, and we note that the destination receives the composite signal corrupted by intersymbol interference, interblock interference, and additive noise. Only the relays which can correctly decode the message from the source can participate in forwarding the decoded message to the destination. We define such relays as *decoding relays* and they form a *decoding set*. In practice, the decision of whether the message is decoded successfully can be made with the help of a checksum (e.g. CRC) and we assume the relays which pass this checksum do not contain any errors in the decoded message. We consider several relaying strategies in this chapter, including a best selection scheme, a random selection scheme, and a scheme where all decoding relays participate. We continue to use the MFB to derive the upper

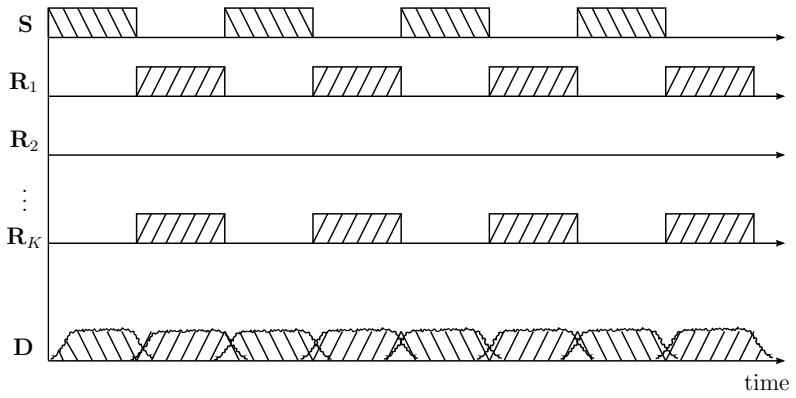

Figure 2.2: Transmission process.

bound on outage probability for the three relaying strategies and assume that a single symbol $x[0]$ is sent by the source.

In the first phase of transmission, the received signals at the destination and at each relay are given by

$$\boldsymbol{y}_{sd} = \boldsymbol{h}_{sd}x[0] + \boldsymbol{w}_{sd}, \tag{2.10}$$

$$\boldsymbol{y}_{r_i} = \boldsymbol{h}_{sr_i}x[0] + \boldsymbol{w}_{sr_i}. \tag{2.11}$$

For classical direct transmission where the source transmits continuously without help from the relays, the mutual information between the source and $\mathbf{R}_i$ [2] would be $\log(1 + \|\boldsymbol{h}_{sr_i}\|^2\rho)$ bits/s/Hz. In our system model, however, the use of time-division constrains the source to be silent half of the time which halves the mutual information but doubles the power, giving the mutual information between source and $\mathbf{R}_i$ in the first phase as

$$I_{sr_i} = \frac{1}{2}\log(1 + 2\|\boldsymbol{h}_{sr_i}\|^2\rho).$$

Next, in phase two, each relay attempts to decode the message. Those relays which are able to successfully decode the message comprise the decoding set $\mathcal{D}$ where $\mathcal{D} \subseteq \{\mathbf{R}_1, \ldots, \mathbf{R}_K\}$. Depending on the relay selection strategy that is employed, some nodes in the decoding set will participate in the relaying.

To calculate the outage probability, we seek the overall mutual information I between the source and destination. Conditioning on the random set $\mathcal{D}$, the total probability theorem gives the outage probability as

$$\Pr[I < R] = \sum_{\mathcal{D}} \Pr[\mathcal{D}]\Pr[I < R|\mathcal{D}] \tag{2.12}$$

with the summation over all possible decoding sets. To calculate the probability of a given decoding set $\Pr[\mathcal{D}]$, first let

$$b \triangleq \frac{2^{2R} - 1}{2\rho}$$

where we note that $b \doteq \rho^{2r-1}$ and $0 \leq r \leq 1/2$. The probability that a relay node is in the decoding set is

$$\begin{aligned} \Pr[\mathbf{R}_i \in \mathcal{D}] &= \Pr[I_{sr_i} > R] \\ &= \Pr[\|\boldsymbol{h}_{sr_i}\|^2 > b] \\ &\doteq \Pr[\|\boldsymbol{\delta}_{sr_i}\|^2 > b] \\ &\doteq e^{-b} \sum_{k=0}^{L_{sr_i}-1} \frac{b^k}{k!} \end{aligned}$$

where the penultimate asymptotic equality follows from $\xi^2_{sr_i,\min}\|\boldsymbol{\delta}_{sr_i}\|^2 \leq \|\boldsymbol{h}_{sr_i}\|^2 \leq \xi^2_{sr_i,\max}\|\boldsymbol{\delta}_{sr_i}\|^2$ and the last asymptotic equality follows as $\|\boldsymbol{\delta}_{sr_i}\|^2$ is chi-squared distributed with L_{sr_i} degrees of freedom. Since each relay independently decodes the message, and since the channels from source to each relay are independent, the probability of the decoding set is

$$\begin{aligned} \Pr[\mathcal{D}] &\doteq \prod_{\mathbf{R}_i \notin \mathcal{D}} (1 - e^{-b} \sum_{k=0}^{L_{sr_i}-1} \frac{b^k}{k!}) \prod_{\mathbf{R}_i \in \mathcal{D}} e^{-b} \sum_{k=0}^{L_{sr_i}-1} \frac{b^k}{k!} \\ &\doteq b^{\sum_{\mathbf{R}_i \notin \mathcal{D}} L_{sr_i}}. \end{aligned} \tag{2.13}$$

Referring back to (2.12), we now need to calculate $\Pr[I < R|\mathcal{D}]$, which depends on the particular choice of relay selection strategy. Next, we complete the outage probability and DMT derivation for each of the three selection strategies.

2.3.1 Best Relay Selection DMT

We first analyze the outage of the best relay selection scheme, where the "best" relay is defined as the one with the largest sum-squared relay-to-destination channel coefficients. The chosen relay uses repetition coding, and simply forwards the decoded signal to the destination in phase two. The best relay selection process

can be completed either centrally at the destination or in a distributed fashion by relays, as follows:

- *Centralized selection:* In turn, each decoding relay transmits some known information to the destination, and the destination estimates each relay-to-destination channel. The destination chooses the relay with the largest sum-squared relay-to-destination channel coefficients, and feeds back this decision to the relays. The feedback requires $|\mathcal{D}|$ bits, and is assumed to be fed back reliably.

- *Distributed selection:* The relay-to-destination channel and the destination-to-relay channel are assumed to be the same due to reciprocity. The destination broadcasts some known information to all the relays, each of which individually estimate its relay-to-destination channel. Each relay waits for a time duration which is inversely proportional to its sum-squared relay-destination channel coefficients before sending its signal to the destination, so the relay with the largest sum-squared relay-to-destination channel will be the first to send its signal to the destination. Other relays do not start transmission if they overhear any signal from the best relay. The detailed process for this distributed relay selection is discussed in [12].

The system designer may choose which of these two approaches to adopt depending on the application. The centralized selection might consume more time since the channels between relays and destination would need to be estimated sequentially. Centralized selection also puts more estimation load on the destination. Distributed selection, on the other hand, is more spectrally efficiently since relays

concurrently estimate the channels; however, the relays need to resolve collisions which may complicate the implementation. The practical details of the selection process itself – such as the overhead in performing the selection, as well as the possibility of poor channel estimates that result in a sub-optimal relay selection – are beyond the scope of the present work. Throughout our analysis, we assume that the best relay is always selected with negligible overhead.

Again, transmission takes place in two alternating phases, where the received signals in the first phase are given by (3.1) and (3.2). Here, however, only the selected relay participates in the second phase. Let the selected relay index be m and denote its relay-destination channel coefficients as $\boldsymbol{h}_{r_* d}$ so that

$$\|\boldsymbol{h}_{r_* d}\|^2 \triangleq \max_{\mathbf{R}_i \in \mathcal{D}} \|\boldsymbol{h}_{r_i d}\|^2. \tag{2.14}$$

The received signal at the destination becomes

$$\boldsymbol{y}_{rd} = \boldsymbol{h}_{r_* d} x[0] + \boldsymbol{w}_{rd}. \tag{2.15}$$

Due to the use of repetition coding by the selected relay and the orthogonality of the source-destination and source-relay channels, the conditional mutual information of the best relay selection scheme can be written as

$$I_{\text{best}} = \frac{1}{2} \log(1 + 2\rho(\max_{\mathbf{R}_i \in \mathcal{D}} \|\boldsymbol{h}_{r_i d}\|^2 + \|\boldsymbol{h}_{sd}\|^2)). \tag{2.16}$$

Denote $\xi_{\max} = \max(\max_{\mathbf{R}_i \in \mathcal{D}} \xi_{r_i d,\max}, \xi_{sd,\max})$, $\xi_{\min} = \min(\min_{\mathbf{R}_i \in \mathcal{D}} \xi_{r_i d,\min}, \xi_{sd,\min})$, we have the following upper bound and lower bound on I_{best} as

$$\begin{aligned} &\frac{1}{2} \log(1 + 2\rho\xi_{\min}^2(\max_{\mathbf{R}_i \in \mathcal{D}} \|\boldsymbol{\delta}_{r_i d}\|^2 + \|\boldsymbol{\delta}_{sd}\|^2)) \leq I_{\text{best}} \\ &\leq \frac{1}{2} \log(1 + 2\rho\xi_{\max}^2(\max_{\mathbf{R}_i \in \mathcal{D}} \|\boldsymbol{\delta}_{r_i d}\|^2 + \|\boldsymbol{\delta}_{sd}\|^2)). \end{aligned} \tag{2.17}$$

Let $Y \triangleq \|\boldsymbol{\delta}_{sd}\|^2$ and $f_Y(y)$ be the probability density function (pdf) of Y which is chi-squared distributed with L_{sd} degrees of freedom. The conditional outage probability for best relay selection is then

$$\begin{aligned}
\Pr[I_{\text{best}} < R|\mathcal{D}] &= \Pr[(\max_{\mathbf{R}_i \in \mathcal{D}} \|\boldsymbol{h}_{r_i d}\|^2 + \|\boldsymbol{h}_{sd}\|^2) < b] && (2.18)\\
&\doteq \Pr[(\max_{\mathbf{R}_i \in \mathcal{D}} \|\boldsymbol{\delta}_{r_i d}\|^2 + Y) < b] && (2.19)\\
&= \int_0^b \Pr[\max_{\mathbf{R}_i \in \mathcal{D}} \|\boldsymbol{\delta}_{r_i d}\|^2 < b - y] f_Y(y) dy \\
&= \int_0^b \left(\prod_{\mathbf{R}_i \in \mathcal{D}} \Pr[\|\boldsymbol{\delta}_{r_i d}\|^2 < b - y] \right) \frac{1}{(L_{sd}-1)!} y^{L_{sd}-1} e^{-y} dy \\
&= \int_0^b \left[\prod_{\mathbf{R}_i \in \mathcal{D}} e^{-(b-y)} \left(\sum_{k=L_{r_i d}}^{+\infty} \frac{(b-y)^k}{k!} \right) \right] \cdot \\
&\quad \frac{1}{(L_{sd}-1)!} y^{L_{sd}-1} e^{-y} dy && (2.20)\\
&= \int_0^1 e^{-b} \left[\prod_{\mathbf{R}_i \in \mathcal{D}} \left(\sum_{k=L_{r_i d}}^{+\infty} b^k \frac{(1-\alpha)^k}{k!} \right) \right] \cdot \\
&\quad \frac{1}{(L_{sd}-1)!} (b\alpha)^{L_{sd}-1} b d\alpha && (2.21)\\
&\doteq b^{L_{sd} + \sum_{\mathbf{R}_i \in \mathcal{D}} L_{r_i d}} \int_0^1 \frac{(1-\alpha)^{\sum_{\mathbf{R}_i \in \mathcal{D}} L_{r_i d}} \alpha^{L_{sd}-1}}{(\prod_{\mathbf{R}_i \in \mathcal{D}} L_{r_i d}!)(L_{sd}-1)!} d\alpha && (2.22)\\
&\doteq b^{L_{sd} + \sum_{\mathbf{R}_i \in \mathcal{D}} L_{r_i d}} && (2.23)
\end{aligned}$$

where (2.19) follows by applying (2.17), (2.20) follows from [34, equation 2.321], (2.21) follows from the change of variable $y = \alpha b$ with $0 \leq \alpha \leq 1$, (2.22) comes by dropping terms in the polynomial of b with order higher than $L_{r_i d}$, and (2.23) follows from the fact that the integration in (2.22) is not a function of b.

Substituting (2.13) and (2.23) into (2.12), the outage of best relay selection is then

$$\begin{aligned}
\Pr[I_{\text{best}} < R] &= \sum_{\mathcal{D}} \Pr[I_{\text{best}} < R|\mathcal{D}]\Pr[\mathcal{D}] \\
&\doteq \sum_{\mathcal{D}} b^{L_{sd}+\sum_{\mathbf{R}_i\in\mathcal{D}} L_{r_i d}+\sum_{\mathbf{R}_i\notin\mathcal{D}} L_{sr_i}} \\
&\doteq b^{L_{sd}+\min_{\mathcal{D}}\left\{\left(\sum_{\mathbf{R}_i\in\mathcal{D}} L_{r_i d}\right)+\left(\sum_{\mathbf{R}_i\notin\mathcal{D}} L_{sr_i}\right)\right\}} \\
&\doteq \rho^{(2r-1)\left(L_{sd}+\min_{\mathcal{D}}\left\{\left(\sum_{\mathbf{R}_i\in\mathcal{D}} L_{r_i d}\right)+\left(\sum_{\mathbf{R}_i\notin\mathcal{D}} L_{sr_i}\right)\right\}\right)} \qquad (2.24) \\
&\doteq \rho^{(2r-1)(L_{sd}+\sum_{i=1}^{K}\min(L_{r_i d},L_{sr_i}))} \qquad (2.25)
\end{aligned}$$

where (2.25) follows as the minimum in (2.24) is attained when relay $\mathbf{R}_i$ is in decoding set if $L_{r_i d} < L_{sr_i}$ and is not in decoding set otherwise. We see that full spatial diversity is achieved by this relay selection method since there are $K+1$ terms in (2.25), but the achieved frequency diversity through each relay is the minimum of the length of the source-to-relay and relay-to-destination channels.

2.3.2 Random Relay Selection DMT

In this subsection, we analyze the outage of a random relay selection scheme, where a random relay in the decoding set handles the forwarding. While this strategy would appear to be suboptimal compared to the best relay selection scheme, random selection is attractive for its simplicity and the fact that it requires no feedback nor CSI. In random selection, the probability of a decoding relay being selected as the forwarding relay is $1/|\mathcal{D}|$. The chosen relay employs repetition coding for the second phase of transmission. Similar to Section 2.3.1, this relay selection method can also be operated in a centralized mode or a distributed mode. Under centralized mode, there is no need to estimate the relay-to-destination channel,

and the destination broadcasts the index number of a randomly selected relay in the decoding set; in distributed mode, each decoding relay waits for a random time which is uniformly distributed within a range with the maximum predefined by the system, and the first to transmit becomes the chosen relay. The mutual information conditioned on selecting relay $\mathbf{R}_i \in \mathcal{D}$ can be written as

$$I_{\text{random}} = \frac{1}{2}\log(1 + 2\rho(\|\boldsymbol{h}_{r_i d}\|^2 + \|\boldsymbol{h}_{sd}\|^2)). \tag{2.26}$$

We have

$$\begin{aligned} &\frac{1}{2}\log(1 + 2\rho \min\{\xi^2_{r_i d,\min}, \xi^2_{sd,\min}\}(\|\boldsymbol{\delta}_{r_i d}\|^2 + \|\boldsymbol{\delta}_{sd}\|^2)) \leq I_{\text{random}} \\ &\leq \frac{1}{2}\log(1 + 2\rho \max\{\xi^2_{r_i d,\max}, \xi^2_{sd,\max}\}(\|\boldsymbol{\delta}_{r_i d}\|^2 + \|\boldsymbol{\delta}_{sd}\|^2)). \end{aligned} \tag{2.27}$$

Let $Y \triangleq \|\boldsymbol{\delta}_{sd}\|^2$ and $f_Y(y)$ be the pdf of Y which is chi-squared distributed with L_{sd} degrees of freedom. The conditional outage probability for the random relay selection method is

$$\begin{aligned} \Pr[I_{\text{random}} < R|\mathcal{D}] &= \sum_{\mathbf{R}_i \in \mathcal{D}} \frac{1}{|\mathcal{D}|} \Pr[I_{\text{random}} < R|\mathbf{R}_i, \mathcal{D}] \\ &= \sum_{\mathbf{R}_i \in \mathcal{D}} \frac{1}{|\mathcal{D}|} \Pr[\|\boldsymbol{h}_{r_i d}\|^2 + \|\boldsymbol{h}_{sd}\|^2 < b] \\ &\doteq \sum_{\mathbf{R}_i \in \mathcal{D}} \frac{1}{|\mathcal{D}|} b^{L_{sd} + L_{r_i d}} \qquad (2.28) \\ &\doteq b^{L_{sd} + \min_{\mathbf{R}_i \in \mathcal{D}} L_{r_i d}} \qquad (2.29) \end{aligned}$$

where (2.28) follows from the same steps used in going from (2.18) to (2.23), but with only one relay in the decoding set. From (2.29), we see that within the decoding set, random relaying offers no spatial diversity but only frequency diversity, where the diversity order equals the shortest channel length. Substituting

(2.13) and (2.29) into (2.12), the outage of the random relay selection is

$$\begin{aligned}
\Pr[I_{\text{random}} < R] &= \sum_{\mathcal{D}} \Pr[I_{\text{random}} < R|\mathcal{D}]\Pr[\mathcal{D}] \\
&\doteq \sum_{\mathcal{D}} b^{L_{sd}+\min_{\mathbf{R}_i\in\mathcal{D}} L_{r_id}+\sum_{\mathbf{R}_i\notin\mathcal{D}} L_{sr_i}} \\
&\doteq \rho^{(2r-1)(L_{sd}+\min_{\mathcal{D}}\left\{\left(\min_{\mathbf{R}_i\in\mathcal{D}} L_{r_id}\right)+\left(\sum_{\mathbf{R}_i\notin\mathcal{D}} L_{sr_i}\right)\right\})} \qquad (2.30) \\
&\doteq \rho^{(2r-1)\left(L_{sd}+\min\left\{\left(\min_{i\in1,\cdots,K} L_{r_id}\right),\left(\sum_{i=1}^{K} L_{sr_i}\right)\right\}\right)} \qquad (2.31)
\end{aligned}$$

where the last line follows from the fact that $\min_{\mathbf{R}_i\in\mathcal{D}} L_{r_id} \geq \min_{i\in1,\cdots,K} L_{r_id}$ for any decoding set $\mathcal{D}$. A detailed explanation for the last step in the above derivation follows. Denote

$$Z(\mathcal{D}) \triangleq \min_{\mathbf{R}_i\in\mathcal{D}} L_{r_id} + \sum_{\mathbf{R}_i\notin\mathcal{D}} L_{sr_i}.$$

Let $\mathcal{D}_n$ be a set with n decoding relays so that $|\mathcal{D}_n| = n$. Then $Z(\mathcal{D}_K) = \min_{i\in1,\cdots,K} L_{r_id}$ when all the relays are in the decoding set and $Z(\mathcal{D}_0) = \sum_{i\in1,\cdots,K} L_{sr_i}$ when no relay is in the decoding set. For $1 \leq n < K$,

$$\begin{aligned}
Z(\mathcal{D}_n) &= \min_{\mathbf{R}_i\in\mathcal{D}_n} L_{r_id} + \sum_{\mathbf{R}_i\notin\mathcal{D}_n} L_{sr_i} \\
&\geq \min_{\mathbf{R}_i\in\mathcal{D}_K} L_{r_id} + \sum_{\mathbf{R}_i\notin\mathcal{D}_n} L_{sr_i} \\
&\geq \min_{\mathbf{R}_i\in\mathcal{D}_K} L_{r_id} = Z(\mathcal{D}_K).
\end{aligned}$$

Thus the minimum of $Z(\mathcal{D})$ over all possible decoding sets happens either when $|\mathcal{D}| = K$ or $|\mathcal{D}| = 0$. We can write

$$\min_{\mathcal{D}} Z(\mathcal{D}) = \min\left(Z(\mathcal{D}_K), Z(\mathcal{D}_0)\right) = \min\left(\min_{i\in1,\cdots,K} L_{r_id}, \sum_{i\in1,\cdots,K} L_{sr_i}\right).$$

Comparing (2.30) with (2.24), we find that the DMT offered by the random selection method is dominated by the best relay selection method. The random selection method cannot always fully exploit the spatial diversity due to the presence of the min in (2.30) which results in a diversity bottleneck, though we will

consider some cases in Section 2.3.4 where random selection *can* exploit full spatial diversity.

2.3.3 All-Decoding-Relay DMT

Next, we analyze the outage of a scheme where all relays in the decoding set participate. Since all decoding relays participate in the forwarding, no overhead, no feedback, and no CSI is needed to perform selection. We assume perfect symbol synchronization now and will comment on this later.

As the decoding relays participate in the second phase of transmission and employ repetition coding, the effective channel from the relays to the destination becomes

$$\boldsymbol{h}_{rd} = \sum_{\mathbf{R}_i \in \mathcal{D}} \boldsymbol{h}_{r_i d}.$$

For a fair comparison, we assume each relay transmits at the power of $2P/|\mathcal{D}|$ where 2 is due to half-duplex relaying. We can write the conditional mutual information between the source and the destination through the decoding set as

$$I_{\text{all}} = \frac{1}{2}\log(1 + 2\rho(\frac{\|\boldsymbol{h}_{rd}\|^2}{|\mathcal{D}|} + \|\boldsymbol{h}_{sd}\|^2)). \tag{2.32}$$

We denote $\xi_{\max} = \max\{\max_{\mathbf{R}_i \in \mathcal{D}} \xi_{r_i d,\max}, \xi_{sd,\max}\}$, $\xi_{\min} = \min\{\min_{\mathbf{R}_i \in \mathcal{D}} \xi_{r_i d,\min}, \xi_{sd,\min}\}$, and we can bound I_{all} as

$$\begin{aligned} &\frac{1}{2}\log(1 + 2\rho\xi_{\min}^2(\frac{\|\boldsymbol{\delta}_{rd}\|^2}{|\mathcal{D}|} + \|\boldsymbol{\delta}_{sd}\|^2)) \leq I_{\text{all}} \leq \\ &\frac{1}{2}\log(1 + 2\rho\xi_{\max}^2(\frac{\|\boldsymbol{\delta}_{rd}\|^2}{|\mathcal{D}|} + \|\boldsymbol{\delta}_{sd}\|^2)) \end{aligned} \tag{2.33}$$

where $\boldsymbol{\delta}_{rd} = \sum_{\mathbf{R}_i \in \mathcal{D}} \boldsymbol{\delta}_{r_i d}$ with length $L_{rd} \triangleq \max_{\mathbf{R}_i \in \mathcal{D}} L_{r_i d}$. Denote the covariance matrix of $\boldsymbol{\delta}_{rd}$ as $\boldsymbol{C} \in \mathbb{R}^{L_{rd} \times L_{rd}}$. We note that $\boldsymbol{C}$ is a diagonal matrix with the

largest element $|\mathcal{D}|$ and the smallest element greater than or equal to 1. Define

$$\bar{\boldsymbol{\delta}}_{rd} \triangleq \boldsymbol{C}^{-1/2}\boldsymbol{\delta}_{rd}.$$

Each element of $\bar{\boldsymbol{\delta}}_{rd}$ is then Gaussian distributed with variance 1, $\|\bar{\boldsymbol{\delta}}_{rd}\|^2$ is chi-squared distributed with L_{rd} degrees of freedom, and

$$\|\bar{\boldsymbol{\delta}}_{rd}\|^2 \leq \|\boldsymbol{\delta}_{rd}\|^2 \leq |\mathcal{D}|\|\bar{\boldsymbol{\delta}}_{rd}\|^2. \tag{2.34}$$

Let $Y \triangleq \|\boldsymbol{\delta}_{sd}\|^2$ and $f_Y(y)$ be the pdf of Y which is chi-squared distributed with L_{sd} degrees of freedom. We develop the conditional outage probability for the all-decoding-relay method as

$$\begin{aligned}
\Pr[I_{all} < R|\mathcal{D}] &= \Pr[\frac{\|\boldsymbol{h}_{rd}\|^2}{|\mathcal{D}|} + Y < b] \\
&\doteq \Pr[\frac{\|\boldsymbol{\delta}_{rd}\|^2}{|\mathcal{D}|} + Y < b] && (2.35) \\
&\doteq \Pr[\|\bar{\boldsymbol{\delta}}_{rd}\|^2 + Y < b] && (2.36) \\
&\doteq b^{L_{sd}+L_{rd}} && (2.37)
\end{aligned}$$

where (2.35) follows by applying (2.33), (2.36) follows by applying (2.34), and (2.37) follows as $\|\bar{\boldsymbol{\delta}}_{rd}\|^2 + Y$ is chi-squared distributed with $L_{sd} + L_{rd}$ degrees of freedom. From (2.37), we see that within the decoding set, dividing power among transmit antennas without phase alignment does not offer spatial diversity and only offers frequency diversity where the diversity order equals the longest delay length.

Substituting (2.13) and (2.37) into (2.12), the outage probability of the all-

decoding-relay method is

$$\begin{aligned}\Pr[I_{all} < R] &= \sum_{\mathcal{D}} \Pr[I_{all} < R|\mathcal{D}]\Pr[\mathcal{D}] \\ &\doteq \sum_{\mathcal{D}} b^{L_{sd}+\max_{\mathbf{R}_i\in\mathcal{D}} L_{r_i d}+\sum_{\mathbf{R}_i\notin\mathcal{D}} L_{sr_i}} \\ &\doteq \rho^{(2r-1)\left(L_{sd}+\min_{\mathcal{D}}\left\{\left(\max_{\mathbf{R}_i\in\mathcal{D}} L_{r_i d}\right)+\left(\sum_{\mathbf{R}_i\notin\mathcal{D}} L_{sr_i}\right)\right\}\right)}. \qquad (2.38)\end{aligned}$$

While we assume perfect symbol synchronization, we note that imperfect symbol synchronization has the effect of artificially increasing the channel lengths by adding zeros (or delays) to the front of the impulse responses. The use of intentional asynchronization to induce delay diversity was studied in [35] for the case of flat fading channels. A similar approach could be used in ISI channels; by artificially adding zeros to the front of each component relay-to-destination channel, the effective sum channel from all relays to the destination can be made to have $L_{rd} = \sum_{\mathbf{R}_i\in\mathcal{D}} L_{r_i d}$ independent paths so that the all-decoding-relay scheme can attain performance equal to the best relay selection if the symbol-level asynchronization is chosen appropriately.

2.3.4 Summary

Collecting the expressions in (2.25), (2.30), and (2.38), we arrive at the DMT expressions for each scheme shown in Table 2.1.

By comparing the original outage expressions, it is apparent that

$$d_{\text{best}}(r) \geq d_{\text{all}}(r) \geq d_{\text{random}}(r).$$

Comparing each of these expressions with the DMT upper bound in (2.9), we see that the best relay selection method is the only one which can always achieve

Table 2.1: DMT of each selection scheme for $r \in [0, 1/2]$.

Selection	$d(r)$	$d(r)$ when $\forall i$, $L_{r_i d} = L_{rd}$, $L_{sr_i} = L_{sr}$
Best	$(1-2r)(L_{sd} + \sum_{i=1}^{K} \min\{L_{r_i d}, L_{sr_i}\})$	$(1-2r)(L_{sd} + \min\{KL_{rd}, KL_{sr}\})$
Random	$(1-2r)(L_{sd} + \min_{\mathcal{D}}\{\left(\min_{\mathbf{R}_i \in \mathcal{D}} L_{r_i d}\right) + (\sum_{\mathbf{R}_i \notin \mathcal{D}} L_{sr_i})\})$	$(1-2r)(L_{sd} + \min\{L_{rd}, KL_{sr}\})$
All	$(1-2r)(L_{sd} + \min_{\mathcal{D}}\{\left(\max_{\mathbf{R}_i \in \mathcal{D}} L_{r_i d}\right) + (\sum_{\mathbf{R}_i \notin \mathcal{D}} L_{sr_i})\})$	$(1-2r)(L_{sd} + \min\{L_{rd}, KL_{sr}\})$

the DMT bound. Table 2.1 also includes the special case when all source-to-relay channels have identical length L_{sr}, and all relay-to-destination channels have identical length L_{rd}. We note that our theoretical diversity expressions agree with results reported in elsewhere in the literature. For example, in the special case of flat-fading, our results coincide with those of [12, 21] which showed that the best relay selection protocol can achieve diversity equal to $K + 1$. Another example is that in [23], with a single relay $K = 1$, a system employing STBC can achieve diversity equal to the expression we found for all the three relaying schemes. Additionally, the diversity achieved when using multiple orthogonal relay subchannels in an OFDM system with precoding [28] is identical to the one achieved here by the best relay selection scheme.

It is interesting to note that even random relay selection can achieve the same diversity as best relay selection in some cases. For example, looking at the last column of Table 2.1, we see that all schemes have an equivalent DMT when $L_{rd} \geq KL_{sr}$. This situation could arise when there is significant scattering and dispersion in the relay-to-destination channel (due to a high density of large buildings, for example) when compared with the source-to-relay channel (which may have a lower density of reflecting structures and terrain). Thus, when the relay-to-destination channel is sufficiently rich, the lower overhead of random relay selection is attractive. This is different from the situation in flat fading channels,

since with $L_{sr} = L_{rd} = 1$, best relay selection is the only scheme which can exploit spatial diversity.

The outage probability and DMT bounds derived here are based on the MFB. As the MFB effectively ignores the intersymbol interference, these results provide an optimistic bound on the attainable outage probability and DMT. We now consider transceiver designs for attaining the bound for best relay selection.

2.4 Transceiver Design

In the previous section, we proved that best relay selection can achieve the optimal DMT, as derived in Section 2.2. We next propose two specific transmission-and-reception schemes for best relay selection. One is based on linear ZFE, and the other is based on infinite-length ZF-DFE. We will prove that both schemes can asymptotically achieve the optimal DMT. In addition, we give the structure of the finite-length MMSE-DFE receiver at the destination, which can achieve full diversity as shown in simulation results.

2.4.1 Transmission Scheme

In all the following transceiver designs, we use the same transmission scheme. In this scheme, the source sends N QAM-symbols, denoted as $\boldsymbol{x}$, which are drawn from a constellation of $Q = \rho^{2r'}$ points where [36, Equation (2)]

$$r' = \frac{r}{1 - \frac{M_{\max}-1}{N+M_{\max}-1}} \tag{2.39}$$

and

$$M_{\max} \geq \max_{i \in 1,\ldots,K} \{M_{sr_i}, M_{r_i d}, M_{sd}\}.$$

After transmission of N symbols, a guard interval of length $M_{\max} - 1$ zeros follows. The choice of Q or r' here is to make sure the total transmission rate is still $R = r \log \rho$ with the guard interval. $M_{\max}$ is essentially an upper bound on the length of all channels in the system. In practice, it is unrealistic for the source node to have knowledge of the lengths of all channels in the system. The system designer needs only choose the parameter $M_{\max}$ to be greater than or equal to the largest channel length expected in the transmission environment. The insertion of guard time eliminates the possibility of interblock interference, but intersymbol interference is still present. Due to the insertion of guard time between alternating phases of source/relay transmission, we see from (3.12) that the system incurs a rate penalty that can be made arbitrarily small by increasing the block length N. Such scheme is also extended for the transmission at the selected forwarding relay.

We assume channel state information at the receiver (CSIR) is perfect, but that no channel state information at the transmitter (CSIT) is needed. We also assume perfect frame synchronization though in practice the system can accommodate modest symbol-level synchronization errors since they can be lumped into the FIR channel model.

2.4.2 Optimal-DMT-Achieving Receiver Based on Linear ZFE

In this scheme, the transmission at the source and the selected relay use the scheme as described in Section 2.4.1. Each relay and the destination uses a zero-forcing (ZF) equalizer prior to detection to compensate for the intersymbol interference.

In the first phase, the received signal at each relay is

$$\boldsymbol{y}_{r_i} = \boldsymbol{H}_{sr_i}\boldsymbol{x} + \boldsymbol{w}_{sr_i} \tag{2.40}$$

where the $\boldsymbol{H}_{sr_i} \in \mathbb{C}^{(M_{\max}+N-1)\times N}$ are the Tœplitz channel convolution matrices corresponding to $\boldsymbol{h}_{sr_i}$, i.e. $[\boldsymbol{H}_{sr_i}]_{j,k} = h_{sr_i}[j-k]$. Since $\|\boldsymbol{h}_{sr_i}\| \neq 0$ with probability 1, and the minimum eigenvalue of $\boldsymbol{H}_{sr_i}^H\boldsymbol{H}_{sr_i}$ is greater than zero due to [36, Lemma IV.1], $\boldsymbol{H}_{sr_i}^H\boldsymbol{H}_{sr_i}$ is invertible and the ZF equalizer coefficients used at the ith relay are

$$\boldsymbol{G}_{r_i} = (\boldsymbol{H}_{sr_i}^H\boldsymbol{H}_{sr_i})^{-1}\boldsymbol{H}_{sr_i}^H.$$

The filtered estimate of $\boldsymbol{x}$ at each relay is

$$\begin{aligned}\tilde{\boldsymbol{y}}_{r_i} &= \boldsymbol{G}_{r_i}\boldsymbol{y}_{r_i} \\ &= \boldsymbol{x} + (\boldsymbol{H}_{sr_i}^H\boldsymbol{H}_{sr_i})^{-1}\boldsymbol{H}_{sr_i}^H\boldsymbol{w}_{sr_i}.\end{aligned}$$

A given relay is declared to have successfully decoded the message only when each symbol in the block is decoded correctly. The best relay selection scheme described in the previous section is employed, which selects the relay in the decoding set with the largest sum-squared relay-to-destination channel. After the completion of relay selection, in the second phase, the selected relay forwards the

length N decoded message to the destination and another guard interval of length $M_{\max} - 1$ follows the relayed signal. This process continues and the source sends another block of N symbols. Let r_* be the subscript of the selected relay and denote its relay-destination channel coefficients as $\boldsymbol{h}_{r_*d}$ so that

$$\|\boldsymbol{h}_{r_*d}\|^2 \triangleq \max_{\mathbf{R}_i \in \mathcal{D}} \|\boldsymbol{h}_{r_i d}\|^2. \tag{2.41}$$

Let $\boldsymbol{H}_{sd} \in \mathbb{C}^{(M_{\max}+N-1)\times N}$, $\boldsymbol{H}_{r_*d} \in \mathbb{C}^{(M_{\max}+N-1)\times N}$ be the Tœplitz channel convolution matrices corresponding to $\boldsymbol{h}_{sd}$ and $\boldsymbol{h}_{r_*d}$ respectively. Define

$$\boldsymbol{H}_{\text{eff}} = \begin{bmatrix} \boldsymbol{H}_{sd} \\ \boldsymbol{H}_{r_*d} \end{bmatrix}, \quad \boldsymbol{w}_{\text{eff}} = \begin{bmatrix} \boldsymbol{w}_{sd} \\ \boldsymbol{w}_{rd} \end{bmatrix}.$$

Then the received signal to be equalized at the destination is then given by

$$\boldsymbol{y} = \boldsymbol{H}_{\text{eff}}\boldsymbol{x} + \boldsymbol{w}_{\text{eff}}. \tag{2.42}$$

We note that this model includes the guard intervals inserted between the two transmission phases as can be seen by the dimensions of $\boldsymbol{H}_{sr_i}$, $\boldsymbol{H}_{sd}$, and $\boldsymbol{H}_{r_*d}$. We note

$$\boldsymbol{H}_{\text{eff}}^H \boldsymbol{H}_{\text{eff}} = \boldsymbol{H}_{sd}^H \boldsymbol{H}_{sd} + \boldsymbol{H}_{r_*d}^H \boldsymbol{H}_{r_*d}. \tag{2.43}$$

Denote the minimum eigenvalue of $\boldsymbol{H}_{r_*d}^H \boldsymbol{H}_{r_*d}$ as $\lambda_{r_*d,\min}$, the minimum eigenvalue of $\boldsymbol{H}_{sd}^H \boldsymbol{H}_{sd}$ as $\lambda_{sd,\min}$, and the minimum eigenvalue of $\boldsymbol{H}_{\text{eff}}^H \boldsymbol{H}_{\text{eff}}$ as $\lambda_{\text{eff},\min}$. From (3.14) and the fact that these three matrices are Hermitian, Weyl's Inequality [37, Theorem 4.3.1] gives

$$\lambda_{\text{eff},\min} \geq \lambda_{sd,\min} + \lambda_{r_*d,\min}. \tag{2.44}$$

Since $\lambda_{sd,\min} > 0$ and $\lambda_{r_*d,\min} > 0$ again due to [36, Lemma IV.1], we have $\lambda_{\text{eff},\min} > 0$ and thus $\boldsymbol{H}_{\text{eff}}^H \boldsymbol{H}_{\text{eff}}$ is invertible. The destination processes the received signal with a ZF equalizer

$$\boldsymbol{G} = (\boldsymbol{H}_{\text{eff}}^H \boldsymbol{H}_{\text{eff}})^{-1} \boldsymbol{H}_{\text{eff}}^H.$$

The filtered estimate of $\boldsymbol{x}$ at the destination is then

$$\begin{aligned}\tilde{\boldsymbol{y}} &= \boldsymbol{G}\boldsymbol{y} \\ &= \boldsymbol{x} + (\boldsymbol{H}_{\text{eff}}^H \boldsymbol{H}_{\text{eff}})^{-1} \boldsymbol{H}_{\text{eff}}^H \boldsymbol{w}_{\text{eff}}.\end{aligned}$$

The filtered noise $\boldsymbol{z} = (\boldsymbol{H}_{\text{eff}}^H \boldsymbol{H}_{\text{eff}})^{-1} \boldsymbol{H}_{\text{eff}}^H \boldsymbol{w}_{\text{eff}}$ has total variance

$$\begin{aligned}E\left[\|\boldsymbol{z}\|^2\right] &= E[\boldsymbol{z}^H \boldsymbol{z}] &(2.45)\\ &= \text{tr}[(\boldsymbol{H}_{\text{eff}}^H \boldsymbol{H}_{\text{eff}})^{-1}] N_0. &(2.46)\end{aligned}$$

We first analyze the probability of decoding set of this scheme. Define the error probability at the ith relay after ZF equalization as $P_{e,i}$ and denote the minimum eigenvalue of $\boldsymbol{H}_{sr_i}^H \boldsymbol{H}_{sr_i}$ as $\lambda_{sr_i,\min}$. Following the steps in Theorem III.6 of [36], we have

$$\begin{aligned}P_{e,i} &\doteq \Pr(\|\boldsymbol{h}_{sr_i}\|^2 < N \bar{\lambda}_{sr_i}^{-1} \rho^{2r'-1}) \\ &\leq \Pr(\xi_{sr_i,\min}^2 \|\boldsymbol{\delta}_{sr_i}\|^2 < N \bar{\lambda}_{sr_i}^{-1} \rho^{2r'-1}) \\ &\doteq \rho^{-L_{sr_i}(1-2r')} &(2.47)\end{aligned}$$

where $\xi_{sr_i,\min}$ is the smallest singular value of $\boldsymbol{\Gamma}_{sr_i}$, and

$$\bar{\lambda}_{sr_i} = \inf_{\boldsymbol{h}_{sr_i} \in \mathbb{C}^{M_{sr_i}}} \lambda_{sr_i,\min}(\bar{\boldsymbol{H}}_{sr_i}^H \bar{\boldsymbol{H}}_{sr_i}).$$

Following the steps in Theorem VII.7 of [36], we have

$$\begin{aligned}P_{e,i} \geq P_{\text{out,i}} &\doteq \Pr(\|\boldsymbol{h}_{sr_i}\|^2 < \rho^{2r'-1}) \\ &\geq \Pr(\xi_{sr_i,\max}^2 \|\boldsymbol{\delta}_{sr_i}\|^2 < \rho^{2r'-1}) \\ &\doteq \rho^{-L_{sr_i}(1-2r')} &(2.48)\end{aligned}$$

where $\xi_{sr_i,\max}$ is the largest singular value of $\boldsymbol{\Gamma}_{sr_i}$. Thus we can conclude

$$P_{e,i} \doteq \rho^{-L_{sr_i}(1-2r')}.$$

As a relay is in the decoding set only when all N symbols are decoded correctly,

$$\Pr[\mathbf{R}_i \in \mathcal{D}] = (1 - P_{e,i})^N.$$

Thus the probability of the decoding set is

$$\begin{aligned} \Pr[\mathcal{D}] &= \prod_{\mathbf{R}_i \notin \mathcal{D}} (1 - (1 - P_{e,i})^N)) \prod_{\mathbf{R}_i \in \mathcal{D}} (1 - P_{e,i})^N \\ &\doteq \rho^{-(1-2r')\sum_{\mathbf{R}_i \notin \mathcal{D}} L_{sr_i}} \end{aligned} \tag{2.49}$$

where asymptotic equality in (2.54) follows from the binomial theorem. We next analyze the error probability at the destination conditioned on the decoding set. Denote $\lambda_{\text{eff},k}$ as the kth eigenvalue for $\boldsymbol{H}_{\text{eff}}^H \boldsymbol{H}_{\text{eff}}$ with $k \in \{0, 1, \ldots, N-1\}$. Assume we estimate each symbol in the block separately, then the effective ρ for decoding the kth symbol is

$$\begin{aligned} \rho_{\text{eff}}(k) &= \frac{P}{WE[|z_k|^2]} \\ &\geq \frac{P}{WE\left[\|\boldsymbol{z}\|^2\right]} \\ &= \frac{\rho}{\text{tr}[(\boldsymbol{H}_{\text{eff}}^H \boldsymbol{H}_{\text{eff}})^{-1}]} \\ &= \frac{\rho}{\sum_{k=0}^{N-1} \lambda_{\text{eff},k}^{-1}} \\ &\geq \frac{\rho}{N\lambda_{\text{eff,min}}^{-1}} \\ &\geq \frac{1}{N}\rho(\lambda_{sd,\min} + \lambda_{r_*d,\min}) \\ &\geq \frac{1}{N}\rho(\bar{\lambda}_{sd,\min}\|\boldsymbol{h}_{sd}\|^2 + \bar{\lambda}_{r_*d,\min}\|\boldsymbol{h}_{r_*d}\|^2) \\ &\geq \frac{1}{N}\rho\bar{\lambda}(\|\boldsymbol{h}_{sd}\|^2 + \|\boldsymbol{h}_{r_*d}\|^2) \end{aligned}$$

where $\bar{\lambda} = \min(\bar{\lambda}_{sd}, \bar{\lambda}_{r_*d})$ with

$$\bar{\lambda}_{sd} = \inf_{\boldsymbol{h}_{sd} \in \mathbb{C}^{M_{sd}}} \lambda_{sd,\min}(\bar{\boldsymbol{H}}_{sd}^H \bar{\boldsymbol{H}}_{sd}),$$

$$\bar{\lambda}_{r_*d} \;=\; \inf_{\boldsymbol{h}_{r_*d}\in\mathbb{C}^{M_{r_*d}}} \lambda_{r_*d,\min}(\bar{\boldsymbol{H}}_{r_*d}^H \bar{\boldsymbol{H}}_{r_*d}),$$

and

$$\bar{\boldsymbol{H}}_{sd} \;\triangleq\; \tfrac{\boldsymbol{H}_{sd}}{\|\boldsymbol{h}_{sd}\|},\quad \bar{\boldsymbol{H}}_{r_*d} \;\triangleq\; \tfrac{\boldsymbol{H}_{r_*d}}{\|\boldsymbol{h}_{r_*d}\|}.$$

Using a proof identical to [36, Lemma IV.1], it can be shown that $\bar{\lambda}_{sd} > 0$ and $\bar{\lambda}_{r_*d} > 0$, therefore $\bar{\lambda} > 0$. The error probability at the destination conditioned on $\mathcal{D}$ [36, Lemma VII.6] is

$$\begin{aligned}
P_{e|\mathcal{D}} &\doteq \Pr[\rho_{\text{eff}}(k) < \rho^{2r'}|\mathcal{D}] \\
&\leq \Pr[(\|\boldsymbol{h}_{sd}\|^2 + \|\boldsymbol{h}_{r_*d}\|^2)\frac{1}{N}\rho\bar{\lambda} < \rho^{2r'}] \\
&= \Pr[(\|\boldsymbol{h}_{sd}\|^2 + \max_{\mathbf{R}_i\in\mathcal{D}} \|\boldsymbol{h}_{r_id}\|^2) < \frac{N}{\bar{\lambda}}\rho^{2r'-1}] \\
&\doteq \Pr[(\|\boldsymbol{\delta}_{sd}\|^2 + \max_{\mathbf{R}_i\in\mathcal{D}} \|\boldsymbol{\delta}_{r_id}\|^2) < \frac{N}{\bar{\lambda}}\rho^{2r'-1}] \qquad (2.50) \\
&\doteq \rho^{(2r'-1)(L_{sd}+\sum_{\mathbf{R}_i\in\mathcal{D}} L_{r_id})} \qquad (2.51)
\end{aligned}$$

where (2.50) follows by applying (2.17), and the last step comes from steps identical to (2.18)-(2.23). Combining (2.54) and (2.57) by the total probability theorem, we conclude that the proposed transmission scheme and equalization method have the following upper bound on the error probability:

$$\begin{aligned}
P_e &\doteq \sum_{\mathcal{D}} P_{e|\mathcal{D}}\Pr[\mathcal{D}] \\
&\dot{\leq} \sum_{\mathcal{D}} \rho^{(2r'-1)(L_{sd}+\sum_{\mathbf{R}_i\in\mathcal{D}} L_{r_id}+\sum_{\mathbf{R}_i\notin\mathcal{D}} L_{sr_i})} \\
&\doteq \rho^{(2r'-1)(L_{sd}+\sum_{i=1}^{K}\min(L_{r_id},L_{sr_i}))}.
\end{aligned}$$

Combining [36, Lemma III.1] and the result in (2.25), we also have

$$P_e \dot{\geq} \rho^{(2r'-1)(L_{sd}+\sum_{i=1}^{K}\min(L_{r_id},L_{sr_i}))}.$$

Thus we can conclude that

$$P_e \doteq \rho^{(2r'-1)(L_{sd}+\sum_{i=1}^{K}\min(L_{r_id},L_{sr_i}))}$$

which shows that the proposed scheme can asymptotically achieve the DMT for best relay selection.

We also point out that since minimum mean squared-error (MMSE) and decision feedback equalizer (DFE) performance dominates ZF equalizers [38], MMSE equalizers and DFEs should attain the same DMT curve. In practice, a system designer may prefer a MMSE or DFE equalizer for their improved BER performance.

2.4.3 Optimal-DMT-Achieving Receiver Based on ZF-DFE

In Section 2.4.2, we prove that with the relay selection method in (2.14), the transmission scheme in Section 2.4.1 and the receiver based on linear ZFE are able to asymptotically achieve the optimal DMT. In this section, we prove that with the same relay selection method and transmission scheme, a receiver based on ZF-DFE can also asymptotically achieve the optimal DMT.

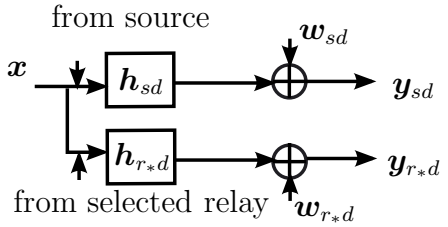

Figure 2.3: Received signal at the destination.

Fig. 2.3 shows the equivalent channel model for the received signal at the destination. The received signal from the source and the received signal from the selected relay are respectively

$$y_{sd}[k] = \sum_{m=-\infty}^{+\infty} h_{sd}[k-m]x[m] + w_{sd}[k], \tag{2.52}$$

$$y_{r_*d}[k] = \sum_{m=-\infty}^{+\infty} h_{r_*d}[k-m]x[m] + w_{rd}[k]. \tag{2.53}$$

for $k = 1, \cdots, \max(L_{sd}, L_{r_*d} + N - 1)$, $x[m] = 0$ for $m \notin \{1, \cdots, N\}$, $\boldsymbol{w}_{sd}$ is the noise at the destination at the first phase, and $\boldsymbol{w}_{rd}$ is the noise at the destination at the second phase.

We assume that the DFE receiver is used at the destination, as well as relays, as relays employ decode-and-forward protocol. After the DFE, the decoding is performed by a simple memoryless slicer. We assume that the receiver either uses the infinite-length ZF-DFE (which we adopt for its simplicity in analysis) or alternatively the receiver uses a finite-length MMSE-DFE (which is used more commonly in practice). If no relay is able to decode the transmitted signal, the receiver at the destination follows the standard DFE design just as the receiver at the relays, since the channel is a single point-to-point channel. In the case where a relay is able to successfully decode, and after one is chosen as described above, the channel is equivalent to a single-input multi-output (SIMO) channel as shown in Fig. 2.3. Fig. 2.4 shows the basic structure of DFE receiver for SIMO channel with the two outputs. The feed forward filters (FFFs) are $F_1(z)$ and $F_2(z)$ and the feedback filter (FBF) is $G(z)$. $\mathcal{Q}$ represents the memoryless decision device with

input $\tilde{\boldsymbol{x}}$ and $\hat{\boldsymbol{x}}$.

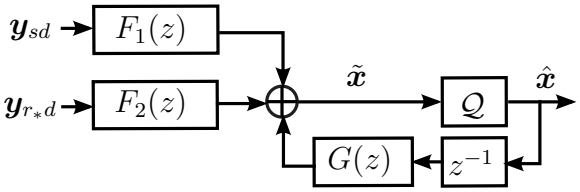

Figure 2.4: DFE receiver.

In the following, we analyze the probability of error of the system with infinite-length ZF-DFE receiver to show that the relay selection method can exploit both frequency diversity and spatial diversity as given by the optimal DMT. We first calculate the probability of a given decoding set, then we present the conditional probability of error at the destination conditioned on a certain decoding set, and finally we combine the above two probabilities by total probability theorem to arrive at the final probability of error.

As each DF relay uses an infinite-length ZF-DFE to decode the received signal from the source, the error probability at each relay is equivalent to that of a ZF-DFE in a point-to-point channel. Using the error probability bound in [36, Theorem III.10] for the case of a point-to-point transmission with an infinite-length ZF-DFE, we have the upper bound on the error probability at each relay as

$$P_{e,i} \dot{\leq} \rho^{-L_{sr_i}(1-r')}.$$

We assume that a relay is in the decoding set only when all N symbols are decoded correctly, so the probability that a relay is in the decoding set becomes

$$\Pr[\mathbf{R}_i \in \mathcal{D}] \dot{\leq} (1 - P_{e,i})^N,$$

and the probability of a given decoding set is bounded

$$\begin{aligned}\Pr[\mathcal{D}] &\dot{\leq} \prod_{\mathbf{R}_i \notin \mathcal{D}} (1-(1-P_{e,i})^N)) \prod_{\mathbf{R}_i \in \mathcal{D}} (1-P_{e,i})^N \\ &\doteq \rho^{-(1-2r')\sum_{\mathbf{R}_i \notin \mathcal{D}} L_{sr_i}} \end{aligned} \tag{2.54}$$

where asymptotic equality in (2.54) follows from the binomial theorem.

We next analyze the error probability at the destination conditioned on the decoding set. When the decoding set is not empty, the forwarding relay is selected according to (2.14). The input-output relation between the original message sent from the source and the received signals at the destination during the two phases are

$$\boldsymbol{y}[k] \triangleq \begin{bmatrix} y_{sd}[k] \\ y_{r_*d}[k] \end{bmatrix} = \sum_{m=-\infty}^{+\infty} \begin{bmatrix} h_{sd}[k-m] \\ h_{r_*d}[k-m] \end{bmatrix} x[m] + \begin{bmatrix} w_{sd}[k] \\ w_{rd}[k] \end{bmatrix} \tag{2.55}$$

for $k = 1, \cdots, \max(L_{sd}, L_{r_*d} + N - 1)$, $x[m] = 0$ for $m \notin \{1, \cdots, N\}$. Thus the transfer function for (2.55)

$$\boldsymbol{H}(z) = \begin{bmatrix} H_{sd}(z) \\ H_{r_*d}(z) \end{bmatrix} = \begin{bmatrix} \sum_{l=0}^{L_{sd}-1} h_{sd}[l] z^{-l} \\ \sum_{l=0}^{L_{r_*d}-1} h_{r_*d}[l] z^{-l} \end{bmatrix}.$$

According to the minimum-phase spectral factorization

$$\boldsymbol{H}^H(1/z^*)\boldsymbol{H}(z) = V^*(1/z^*)\Gamma^2 V(z),$$

the infinite-length ZF-DFE receiver consists of a precursor equalizer is

$$\boldsymbol{F}(z) = \begin{bmatrix} F_1(z) \\ F_2(z) \end{bmatrix} = \boldsymbol{H}^H(1/z^*) \frac{1}{\gamma^2 V^*(1/z^*)}$$

and a postcursor equalizer is $G(z) = (V(z) - 1)z$.

Assuming correct decisions, we find that the effective SNR at the output of this equalizer is

$$\rho_{\text{eff}}^{\text{ZF-DFE}} = e^{\frac{1}{2\pi}\int_0^{2\pi}\log(\rho \boldsymbol{H}^H(\omega)\boldsymbol{H}(\omega))}.$$

Let $X : [0, 2\pi) \to \mathbb{R}$ and define the set

$$\mathcal{U}_\epsilon \triangleq \{\omega \in [0, 2\pi) | X(\omega) \leq \epsilon\}.$$

Define $\bar{H}_{sd}(\omega) \triangleq H_{sd}(\omega)/\|\boldsymbol{h}_{sd}\|^2$ and $\bar{H}_{r_i d}(\omega) \triangleq H_{r_i d}(\omega)/\|\boldsymbol{h}_{r_i d}\|^2$.

The error probability at the destination conditioned on $\mathcal{D}$ [36, Lemma VII.6] is

$$\begin{aligned}
P_{e|\mathcal{D}} &\doteq \Pr[\rho_{\text{eff}}^{\text{DFE-ZF}} < \rho^{2r'}|\mathcal{D}] \\
&\leq \Pr[e^{\frac{1}{2\pi}\int_0^{2\pi}\log(\rho \boldsymbol{H}^H(\omega)\boldsymbol{H}(\omega))} < \rho^{2r'}] \\
&= \Pr[e^{\frac{1}{2\pi}\int_0^{2\pi}\log(\rho(|H_{sd}(\omega)|^2+|H_{r_* d}(\omega)|^2))} < \rho^{2r'}] \\
&< \Pr[e^{\frac{1}{2\pi}\int_0^{2\pi}\max(\log(\rho|H_{sd}(\omega)|^2),\log(\rho|H_{r_* d}(\omega)|^2))} < \rho^{2r'}] \\
&= \Pr[e^{\frac{1}{2\pi}\int_0^{2\pi}\log(\rho|H_{sd}(\omega)|^2)} < \rho^{2r'}] \cdot \\
&\quad \prod_{\mathbf{R}_i \in \mathcal{D}} \Pr[e^{\frac{1}{2\pi}\int_0^{2\pi}\log(\rho|H_{r_i d}(\omega)|^2))} < \rho^{2r'}] \\
&\dot{\leq} \frac{1}{\epsilon^{L_{sd}}}\rho^{-L_{sd}(1-\frac{r'}{1-\sup_{\boldsymbol{h}_{sd}\in\mathbb{C}^{L_{sd}}}|\mathcal{U}_\epsilon(\bar{\boldsymbol{H}}_{sd})|})} \cdot \\
&\quad \prod_{\mathbf{R}_i \in \mathcal{D}} \frac{1}{\epsilon^{L_{r_i d}}}\rho^{-L_{r_i d}(1-\frac{r'}{1-\sup_{\boldsymbol{h}_{r_i d}\in\mathbb{C}^{L_{r_i d}}}|\mathcal{U}_\epsilon(\boldsymbol{H}_{r_i d})|})} \qquad (2.56) \\
&\dot{\leq} \rho^{(2r'-1)(L_{sd}+\sum_{\mathbf{R}_i\in\mathcal{D}} L_{r_i d})} \qquad (2.57)
\end{aligned}$$

where (2.56) and (2.57) follow the very similar argument as that in proof of [36, Theorem III.10].

Combining (2.54) and (2.57) by the total probability theorem, we conclude that the proposed transmission scheme and infinite-length ZF-DFE receiver result

in the following upper bound on the error probability:

$$\begin{aligned} P_e &\doteq \sum_{\mathcal{D}} P_{e|\mathcal{D}} \Pr[\mathcal{D}] \\ &\dot{\leq} \sum_{\mathcal{D}} \rho^{(2r'-1)(L_{sd}+\sum_{\mathbf{R}_i \in \mathcal{D}} L_{r_i d}+\sum_{\mathbf{R}_i \notin \mathcal{D}} L_{sr_i})} \\ &\doteq \rho^{(2r'-1)(L_{sd}+\sum_{i=1}^{K} \min(L_{r_i d}, L_{sr_i}))}. \end{aligned}$$

Combining [36, Lemma III.1] and the result in [39, equation (24)], we can conclude that

$$P_e \doteq \rho^{(2r'-1)(L_{sd}+\sum_{i=1}^{K} \min(L_{r_i d}, L_{sr_i}))}$$

which shows that the proposed scheme can asymptotically achieve the optimal DMT.

2.4.4 Finite-length MMSE-DFE Receiver

In the previous subsection, we proved that by selecting the decoding relay with the largest sum-square of the relay-destination channel, the infinite-length ZF-DFE receiver can asymptotically achieve the optimal DMT. In Section 2.4.2, we proved that with the same relay selection method, linear zero-forcing equalizer (ZFE) can also asymptotically achieve the optimal DMT. While these theoretical results are encouraging, zero-forcing receivers are rarely used in practice for various reasons. For example, the block linear ZF equalizer in Section 2.4.2 requires inversion of a matrix of dimension N-by-N, where N is the block length; thus, the equalizer is effectively a bank of equalizers. In addition, the decoding delay is as large as the block length. The infinite-length equalizer is not realizable, and can only be approximated, not to mention the fact that it has infinite decoding delay. Here we

propose a realizable finite-length MMSE-DFE receiver which results in a decoding delay that can be chosen to be much shorter than the block length. As MMSE-DFE receivers minimize the mean square error (MSE), however, there is not only noise but residual ISI at the input of the decision device. Hence, calculating the exact probability of error is difficult [40] since the symbols are corrupted by residual interference which is not purely Gaussian.

We assume that MMSE-DFE equalization is used at the relays and the destination. We focus on the equalization at the destination for the single-input-multiple-output (SIMO) channel. Different from [41], our receiver structure can have different equalizer length for each individual channel output in the SIMO channel, which is efficient when the lengths of the two individual channels are of large difference.

The MMSE-DFE receiver structure which follows the receiver design in [41] is shown in Fig. 2.4. The feed forward filters (FFFs) can be designed as the finite impulse response filters $\boldsymbol{f}_1 \in \mathbb{C}^{L_{f1}}$ and $\boldsymbol{f}_2 \in \mathbb{C}^{L_{f2}}$ where $F_1(z) = \sum_{l=0}^{L_{f1}} f_1[l]z^{-l}$ and $F_2(z) = \sum_{l=0}^{L_{f2}} f_2[l]z^{-l}$. The feedback filter (FBF) can be specified by $\boldsymbol{g} \in \mathbb{C}^{L_g}$ where $G(z) = \sum_{l=0}^{L_g} g[l]z^{-l}$.

To simplify the derivation, we assume that $L_{f1} + L_{sd} = L_{f2} + L_{r_*d}$. We can write the received signals from the source and from the selected relay as

$$\boldsymbol{y}_{sd}[k] = \boldsymbol{H}_{sd}\boldsymbol{x}[k] + \boldsymbol{w}_{sd}[k]$$

$$\boldsymbol{y}_{r_*d}[k] = \boldsymbol{H}_{r_*d}\boldsymbol{x}[k] + \boldsymbol{w}_{r_*d}[k]$$

where $\boldsymbol{H}_{sd} \in \mathbb{C}^{L_{f1}\times(L_{f1}+L_{sd}-1)}$ and $\boldsymbol{H}_{r_*d} \in \mathbb{C}^{L_{f2}\times(L_{f2}+L_{r_*d}-1)}$ are the Tœplitz channel convolution matrices defined, for example, as $[\boldsymbol{H}_{sd}]_{i,j} = h_{sd}[j-i]$ and

$\boldsymbol{x}[k] = [x[k], x[k-1], \cdots, x[k-L_{f1}-L_{sd}+2]]^T \in \mathbb{C}^{L_{f1}+L_{sd}-1}$. Assume the desired output delay is δ, the coefficients of the FFF $\boldsymbol{f}_1$ and $\boldsymbol{f}_2$ and FBF $\boldsymbol{g}$ can be obtained by assuming correct past decisions and minimizing MSE $= \|x[k-\delta] - \tilde{x}[k]\|_2^2$ where $\tilde{x}[k] = \boldsymbol{u}^T[k]\boldsymbol{c}$ is the equalized output with the filter input $\boldsymbol{u}_k^T$ defined as

$$\boldsymbol{u}^T[k] \triangleq \left[\boldsymbol{y}_{sd}[k]^T, \boldsymbol{y}_{r_*d}[k]^T, \boldsymbol{x}^T[k]\boldsymbol{M}\right]$$

where

$$\boldsymbol{M}^T \triangleq \begin{bmatrix} \boldsymbol{0}_{\delta \times L_g} & \boldsymbol{I}_{L_g \times L_g} & \boldsymbol{0}_{L_g \times (L_{f1}+L_{sd}-L_g-\delta-1)} \end{bmatrix}$$

and the filter coefficient $\boldsymbol{c}$ defined as

$$\boldsymbol{c} \triangleq [\boldsymbol{f}_1^T \ \boldsymbol{f}_2^T \ \boldsymbol{g}^T]^T.$$

By applying the orthogonality principle, the equalizer coefficients are

$$\boldsymbol{c} = (E[\boldsymbol{u}^*[k]\boldsymbol{u}^T[k]])^{-1} E[\boldsymbol{u}^*[k]x[k-\delta]]. \tag{2.58}$$

When the input and noise processes are mutually uncorrelated, we can compute the correlation

$$E[\boldsymbol{u}^*[k]x[k-\delta]] = \begin{bmatrix} (\boldsymbol{H}_{sd}^*\boldsymbol{e}_\delta)^T & (\boldsymbol{H}_{r_*d}^*\boldsymbol{e}_\delta)^T & \boldsymbol{0}_{1\times L_g} \end{bmatrix}^T \tag{2.59}$$

where $e_\delta[i] = 0$ except $e_\delta[\delta] = 1$ with $1 \le i \le L_{f1} + L_{sd} - 1$. To complete the computation of the coefficient $\boldsymbol{c}$ in (2.58), we can further compute the autocorrelation matrix

$$E[\boldsymbol{u}^*[k]\boldsymbol{u}^T[k]] = \begin{bmatrix} \boldsymbol{H}^*\boldsymbol{H}^T + N_0\boldsymbol{I}_{L_{f1}+L_{f2}} & \boldsymbol{H}^*\boldsymbol{M} \\ \boldsymbol{M}^T\boldsymbol{H}^T & \boldsymbol{I}_{L_g} \end{bmatrix} \tag{2.60}$$

where $\boldsymbol{H}^T = \begin{bmatrix} \boldsymbol{H}_{sd}^T & \boldsymbol{H}_{r_*d}^T \end{bmatrix}$ is the composite SIMO channel. Applying the inversion of a block matrix to (2.60) and substituting the results and (2.59) to the cross-

correlation (2.58), we have the feed-forward filter coefficients

$$\boldsymbol{f} = \begin{bmatrix} \boldsymbol{f}_1 \\ \boldsymbol{f}_2 \end{bmatrix} = (\boldsymbol{H}^*(\boldsymbol{I} - \boldsymbol{M}\boldsymbol{M}^T)\boldsymbol{H}^T + N_0\boldsymbol{I})^{-1}\boldsymbol{H}^*\boldsymbol{e}_\delta \tag{2.61}$$

and the feedback filter coefficients

$$\boldsymbol{g} = -\boldsymbol{M}^T\boldsymbol{H}^T\boldsymbol{f}. \tag{2.62}$$

2.5 Numerical Results

This section presents numerical examples of the performance of the proposed relay selection methods developed in Sections 2.3 and 2.4. In evaluating performance over finite SNRs, the diversity measured as the negative slope of each outage curve often does not coincide exactly with the predicted maximal diversity [14, 15]; the predicted diversity assumes that the SNR grows arbitrarily large to permit the analysis to be mathematically tractable. We now compare the performance of the three selection schemes in a variety of scenarios at finite SNR, and show that the schemes follow the general trends predicted by the diversity-multiplexing tradeoff results.

2.5.1 Outage Performance

To illustrate the attainable frequency and spatial diversity, we consider 10 scenarios shown in Table 4.1 where the maximum diversity order is computed from (2.25), (2.31), and (2.38). The first 5 scenarios – which use a single relay and therefore

Table 2.2: Simulation scenarios.

Scenario	K	L_{sd}	L_{sr}	L_{rd}	$d_{\max,\text{best}}$	$d_{\max,\text{random}}$	$d_{\max,\text{all}}$
1	1	2	2	2	4	4	4
2	1	2	2	3	4	4	4
3	1	2	3	2	4	4	4
4	1	2	4	4	6	6	6
5	1	4	2	2	6	6	6
6	2	2	2,2	2,2	6	4	4
7	2	2	2,2	3,3	6	5	5
8	2	2	3,3	2,2	6	4	4
9	2	2	4,4	4,4	10	6	6
10	2	4	2,2	2,2	8	6	6

are unaffected by the choice of selection strategy – are included to illustrate the relative improvement in spatial diversity by adding additional relays.

The outage probability for the best relay selection, random relay selection, and all-decoding-relay methods are plotted in Figs. 2.5, 2.6, and 2.7, respectively, where the rate $R = 2$ bits/s/Hz and each $\mathbf{\Gamma}_{jk}$ is a square identity matrix, i.e. each fading tap of $\boldsymbol{h}_{jk}$ is i.i.d. Rayleigh fading with variance 1. For the best relay selection performance shown in Fig. 2.5, the outage curves for Scenarios 1 through 3 have roughly the same slope which agrees with the trend predicted by Table 4.1. Scenario 4 has a higher diversity order since the minimum length of the source-to-relay and relay-to-destination channels increases, and Scenario 5 has an increased diversity order due to the increased length of the source-to-destination channel. Similar

behavior is observed for Scenarios 6 through 10, which have correspondingly larger diversity orders than Scenarios 1 through 5 because of the spatial diversity offered by the additional relay. We also notice that increasing the frequency diversity in the source-to-relay channel results in a more pronounced coding gain than increasing the frequency diversity in the relay-to-destination channel, as Scenario 3 has a larger coding gain than Scenario 2 in Fig. 2.5. As shown by Figs. 2.6 and 2.7, the random relay selection and all-decoding-relay methods have nearly the same outage performance as each other for the considered scenarios; this is another trend predicted by the maximum diversity order in Table 4.1. Furthermore, both of these schemes have outage performance dominated by the best relay selection method as expected.

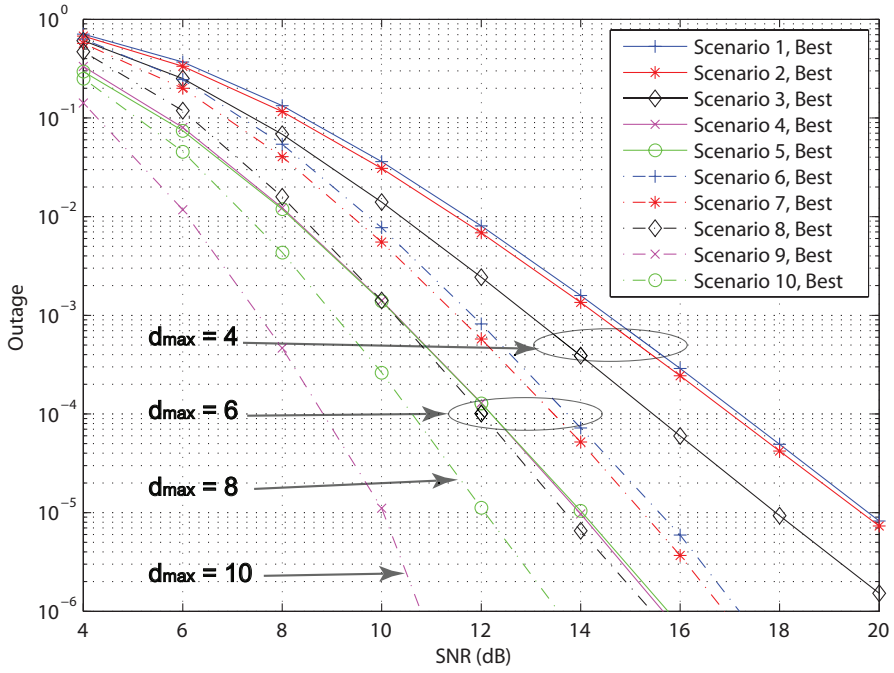

Figure 2.5: Simulated outage probability for best relay selection method, $R = 2$ bits/s/Hz.

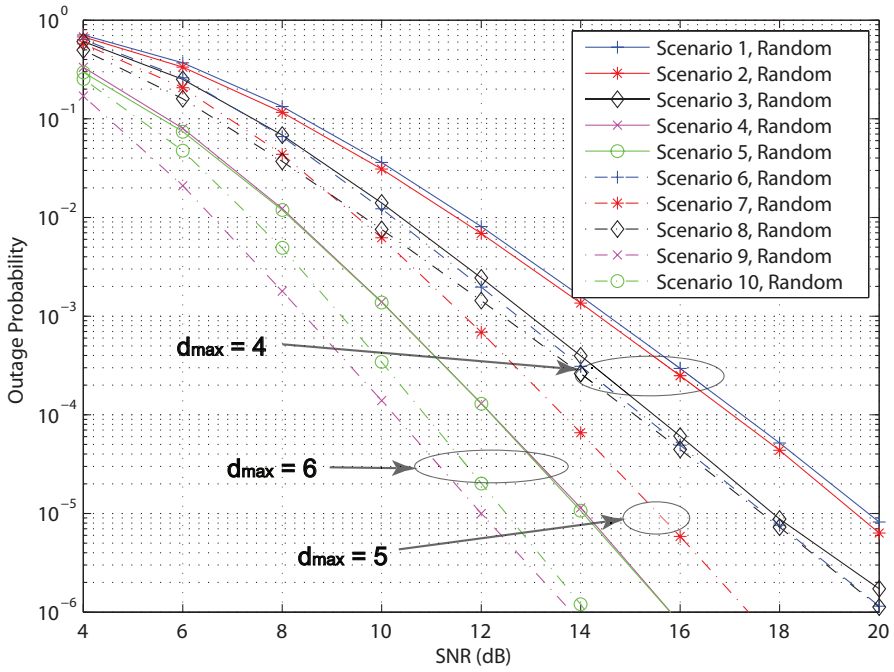

Figure 2.6: Simulated outage probability for random relay selection method, $R = 2$ bits/s/Hz.

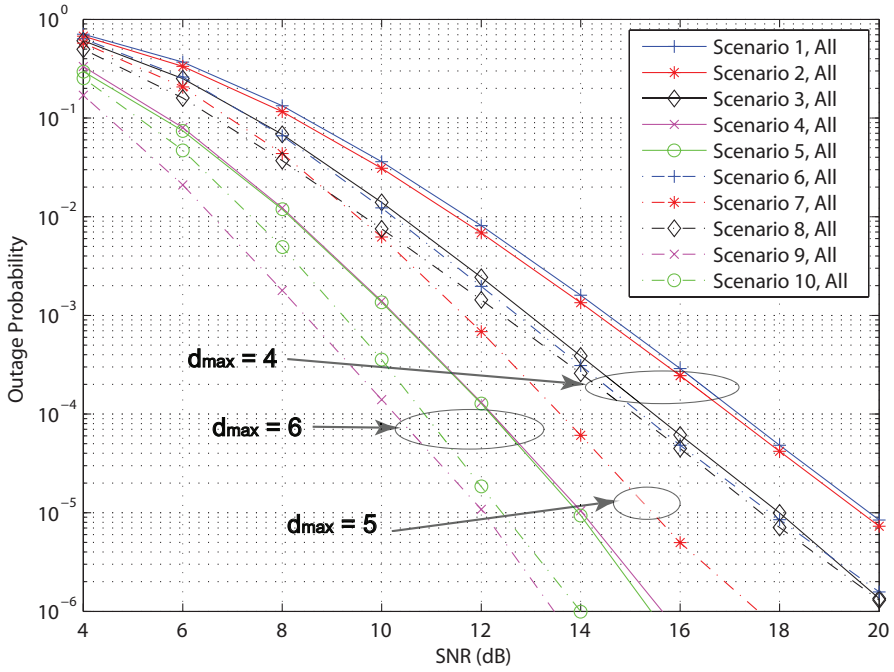

Figure 2.7: Simulated outage probability for all-decoding-relay method, $R = 2$ bits/s/Hz.

2.5.2 BER Performance

We further verify the performance of the transceiver designs with different relaying strategies. In the simulation, we use a block length $N = 32$ and Gray-mapped QPSK modulation. In Fig. 2.8 and Fig. 2.9, we consider FS fading channels with uniform power delay profile, i.e. each tap of each channel is i.i.d. fading with variance $1/L$ where L is the channel length. On both figures, we have also included the performance of the optimal maximum likelihood sequence estimator (MLSE) for comparison. As we can see from Fig. 2.8, with only 2 relays present in the system, the performance advantage of the best relay selection over the other two relaying strategies is negligible. This suggests that in systems with a relatively small number of relays, selection strategies that do not require feedback or CSI (such as the random relay selection and all-decoding-relay methods) may be preferred for their simplicity.

When as many as $K = 10$ relays are available, as shown in Fig. 2.9, the diversity order of the best relay selection may be significantly larger than the other two methods. In examining the power gain of the best relay selection over the other two relaying strategies, we note an interesting trend. When the fading channels contain $L = 2$ taps, the power gain of the best relay selection is about 6 dB at a bit error rate of 10^{-6}. When L increases to 4, however, the power gain of the best relay selection is only about 2 dB. Thus, when there is already sufficient frequency diversity in the system, the improvement in using sophisticated selection schemes which better exploit the spatial diversity is not as pronounced. Again, a system designer may favor one of the simpler selection schemes if it is known that the transmission environment has sufficient frequency diversity.

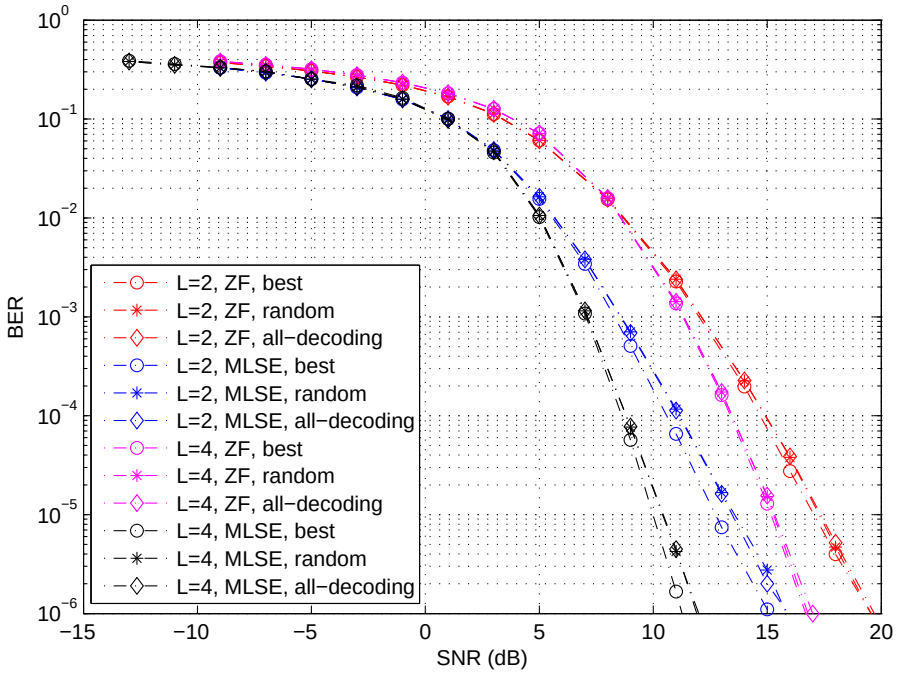

Figure 2.8: Simulated BER for i.i.d. fading channels, $K = 2$.

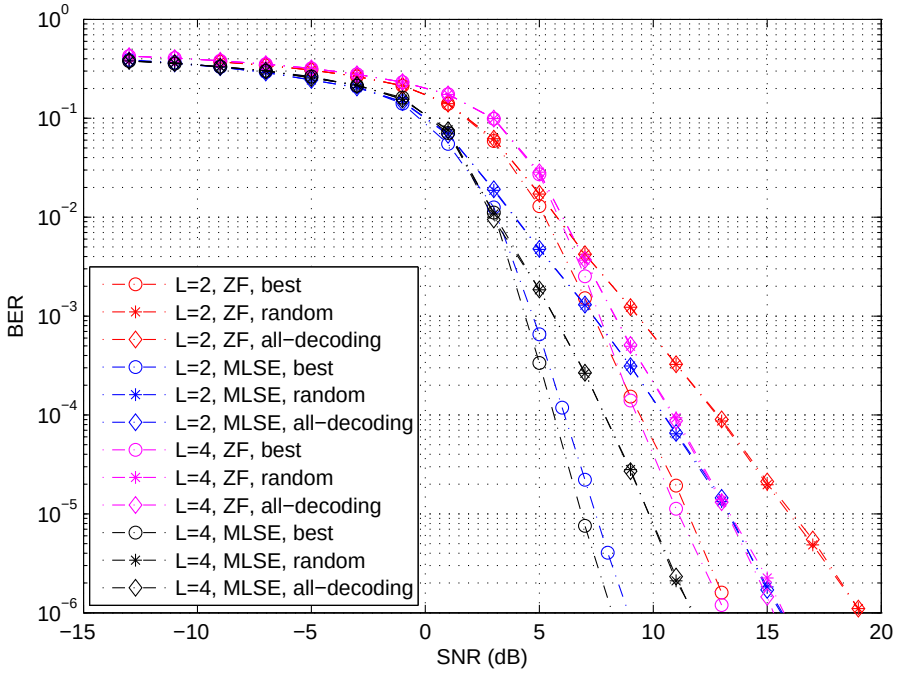

Figure 2.9: Simulated BER for i.i.d. fading channels, $K = 10$.

For transceivers which use linear ZFE, we consider the fourth relay selection method: the destination selects the decoding relay which has the largest average decision-point (DP) SNR, which is defined as the $\frac{NE_s}{E[\|\boldsymbol{z}\|^2]}$ where E_s is the symbol energy, N is the block length and $E[\|\boldsymbol{z}\|^2]$ is the total filtered noise variance defined in (2.46). As shown in Fig. 2.10, this new relay selection method has the larger average DP SNR than best relay selection in (2.14). Hence, it has the best BER performance, as we can see from Fig. 2.11. However, this performance improvement is achieved at the cost of higher computation complexity. It requires a matrix multiplication and a matrix inversion for each decoding relay where the matrices are of sizes no smaller than the block length. On the contrary, best relay selection just requires a few complex number multiplications, and the complexity is scaled by the channel lengths and the number of decoding relays.

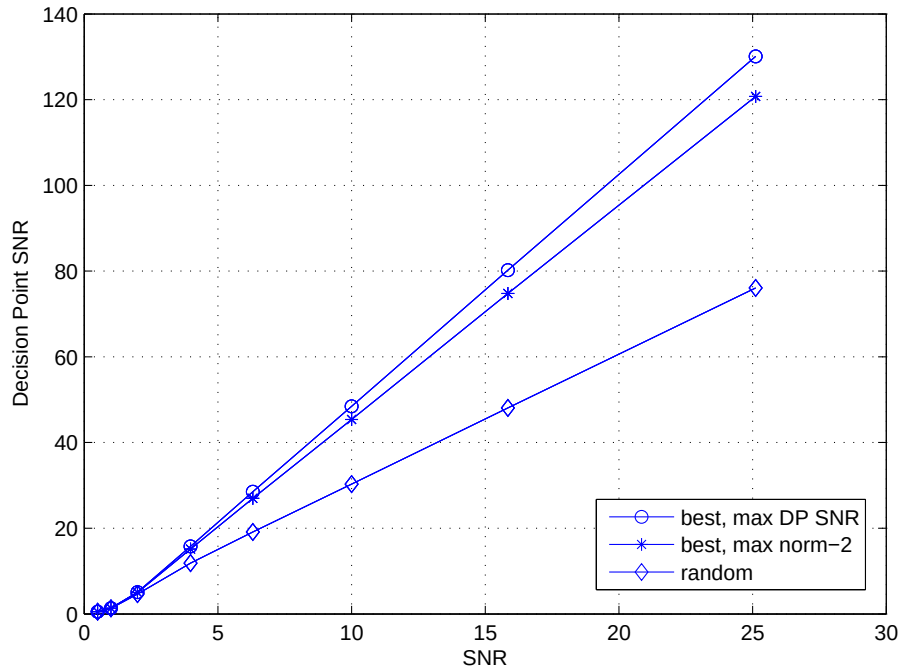

Figure 2.10: Average decision-point SNR for i.i.d. fading channels, $K = 10$ with transceivers based linear ZFE.

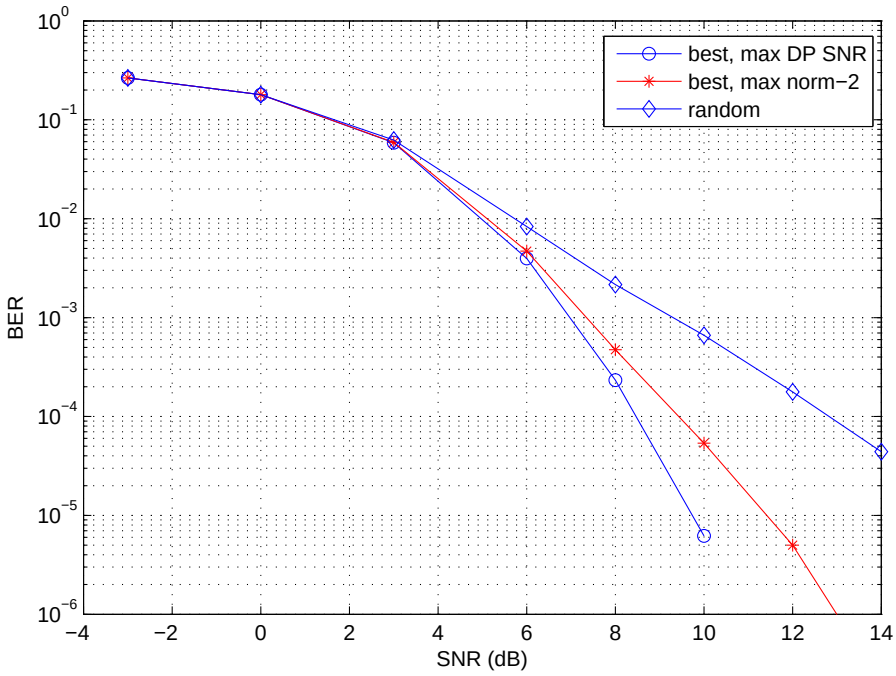

Figure 2.11: Simulated BER for i.i.d. fading channels, $K = 10$ with transceivers based linear ZFE.

We next compare the BER performance of different relaying strategies under i.i.d. and correlated fading. The i.i.d. fading channel used for comparison has uniform power delay profile, and its performance is shown in Fig. 2.8 and Fig. 2.9 with $L = 4$, and is referred to as "no correlation" in Fig. 2.12. To introduce the correlation in the channel taps, we model each channel in the system as a GSM typical rural channel [42] which has $L = 4$ underlying independent fading coefficients where each of the four path arrivals have power delay profile given by $[0, -2, -10, -20]$ dB and corresponding path arrival times $\boldsymbol{\tau}^T = [0, 0.2, 0.4, 0.6]\mu$s. We employ a square root raised cosine (SRRC) pulse shape $p(t)$ at the transmitting end with rolloff factor 0.4 which is truncated to a length of 8 symbol periods. The symbol period is taken to be $T = 0.278\mu s$ which, with QPSK transmission, corresponds to a data rate of 7.2Mbps. Together, these parameters determine

the tap autocovariance $\mathbf{\Gamma}_{jk}$ for each discrete baseband channel since each sampled channel $\boldsymbol{h}$ arises as

$$h[n] = h(t)|_{t=nT} = \sum_{\ell=0}^{L-1} \alpha_\ell p(t-\tau_\ell)p(-t)\Big|_{t=nT}$$

where the underlying independent fading coefficients $\boldsymbol{\alpha} \in \mathbb{C}^4$ are complex Gaussian with variance given by the GSM typical rural power delay profile. For fair comparison, we normalize the total average power in the underlying independent fading coefficients to 1. The resulting sampled channel with 4 independent path arrivals gives rise to a correlated discrete channel with 19 taps. As shown in Fig. 2.12, the simulated performance demonstrates that at finite SNR the receiver is not able to exploit the diversity offered by all 4 independent paths since the last path which has a power of -20 dB contributes very little to the received signal, an effect masked by the high-SNR analysis of the DMT. Nevertheless, the choice of relay selection method still has significant impact on system performance when the number of relays K is relatively large.

Fig. 2.13 shows the BER performance comparison of three different receiver designs when the best relay selection method is performed, and only 2 relays are present in the system. In Fig. 2.13, all BER curves of $L = 4$ have approximately equal negative slope around 6.3 and all BER curves of $L = 2$ have approximately equal negative slope around 4, which shows that all of the three schemes can exploit the FS diversity. Fig. 2.14 shows the BER performance of the three schemes with 10 relays in the system. We find that in Fig. 2.14 the negative slope is approximately 5 for all BER curves of $L = 2$ and 7.5 for all BER curves of $L = 4$. On both Fig. 2.13 and Fig. 2.14, while the diversity orders achieved by the three receivers are approximately the same, the receiver with finite-length MMSE-DFE

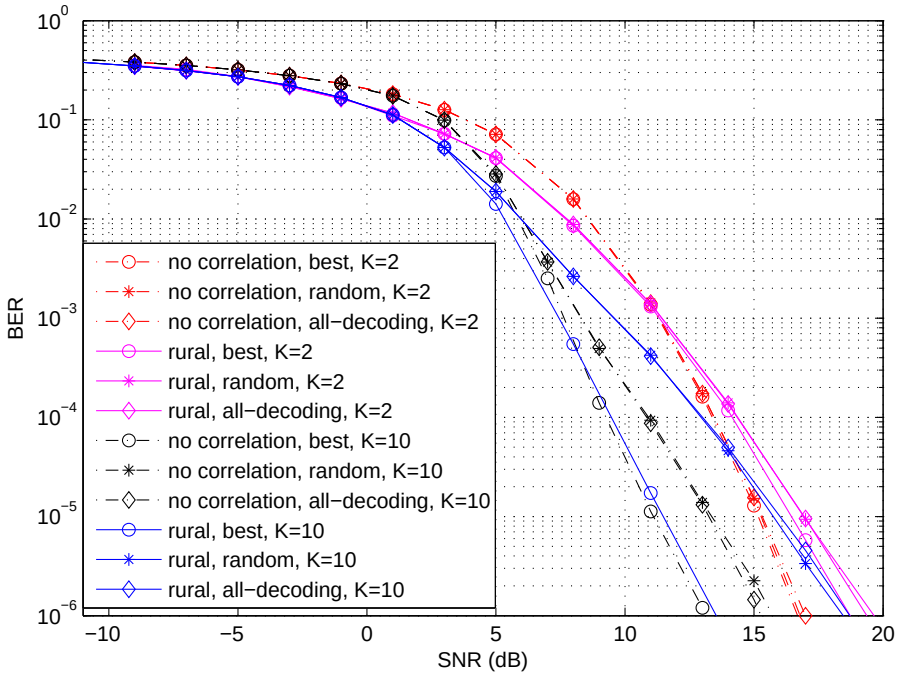

Figure 2.12: Simulated BER for correlated fading channels.

and receiver with MLSE have much larger coding gain than the receiver with linear ZFE. Comparing the two figures, we find that with an increased number of relays, the power gain is larger, and the diversity order is increasing, though it is not as predicted by the theoretical analysis due to finite SNR. This shows that the relay selection method is able to exploit the cooperative diversity offered by the relays.

We further compare BER performance between distributed space-frequency coding (DSFC) with OFDM transmission and best relay selection with SC transmission. Both employ QPSK modulation and ML decoding. For the OFDM transmission, we assume that the number of subcarriers is 32, the source uses the linear constellation precoding with the optimal grouping as [43] and the decoding relays perform the DSFC with random permutation as described in [44]. A detailed look into both system designs would reveal that DSFC has a higher com-

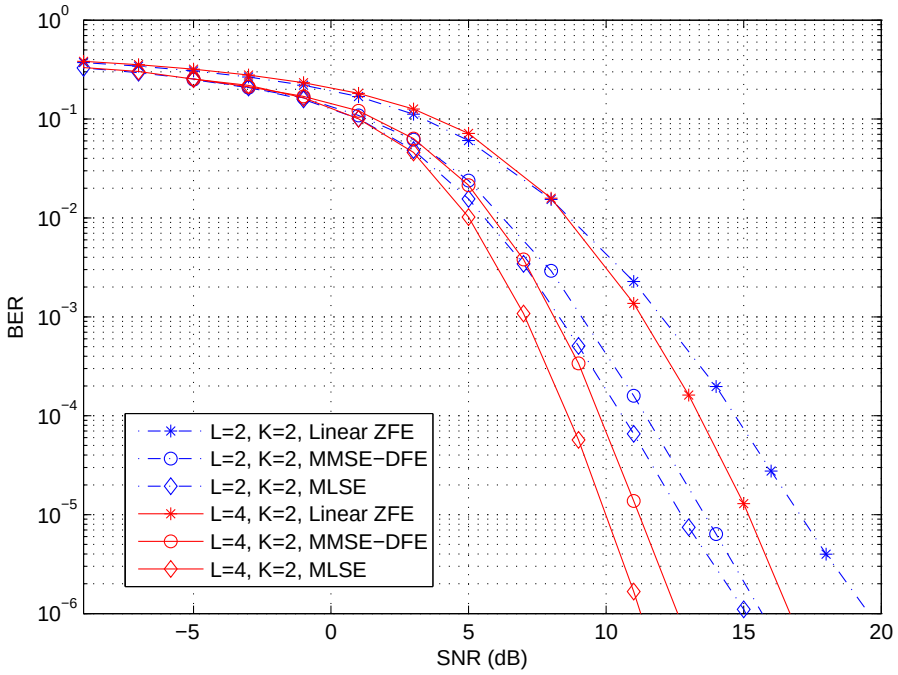

Figure 2.13: Simulated BER with 2 relays.

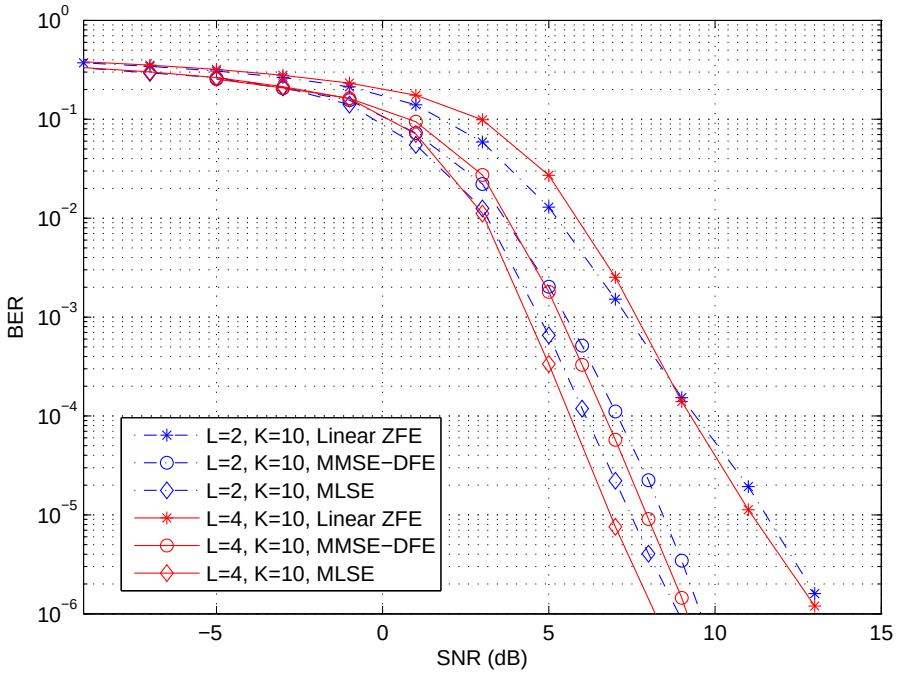

Figure 2.14: Simulated BER with 10 relays.

plexity than best relay selection. Specifically, the decoding complexity of DSFC is exponential with the sum of the length of each decoding-relay-to-destination, while the decoding complexity of best relay selection is exponential only with the length of the selected-decoding-relay-to-destination channel. On the other hand, DSFC does not require any CSIT at the decoding relays but the best relay selection requires the awareness of the decoding relay which has the best channel to the destination. As shown in Fig. 2.15, we see that the coding gain of using the best relay selection over DSFC is about 3.5dB at BER 10^{-5}. This is not surprising since zero-padded transmission is the linear precoding that can achieve maximal coding gain, as reported in [45]. More important, the relay selection method preserves this advantage. However, it should be noted that the DSFC scheme used for comparison requires only the number of decoding relays at the transmitters while our best relay selection requires the result of comparing multiple channel state information at the transmitter.

2.6 Conclusion

In this chapter, we have considered the relay selection problem for the orthogonal decode-and-forward system where correlated frequency selective fading is present. We analyzed the outage performance and derived the DMT for three relay methods: best relay selection, random relay selection, and the case where all decoding relays participate. Our analysis shows that the best relay selection performance dominates the other two schemes with respect to outage.

We further proposed a transceiver to realize the DMT offered by the best re-

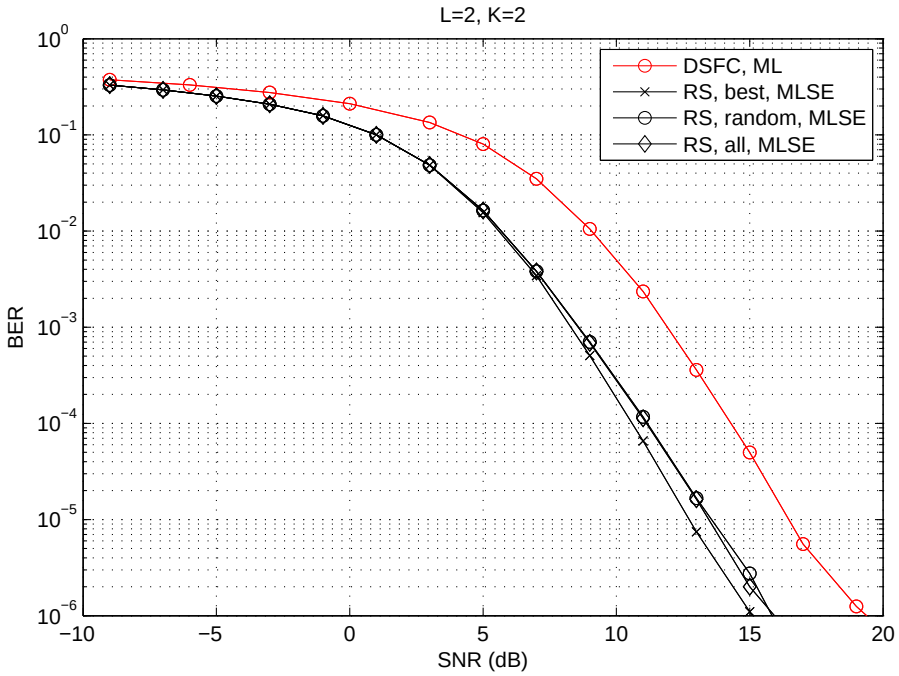

Figure 2.15: BER comparison between relay selection and distributed space-frequency codes for i.i.d. fading channels, $K = 2$, and $L = 2$.

lay selection with minimal complexity; the proposed scheme uses uncoded QAM transmission with guard times and uses linear ZFE at each node. The analysis and simulation results show that the proposed scheme asymptotically achieves the DMT. Additional analysis on the transceiver with ZF-DFE and the best relay selection is performed to show that the optimal DMT can also be achieved. Simulation results show that the best relay selection method combined with more practical finite-length MMSE-DFE receivers achieves full diversity, as well.

While the diversity offered by relay systems in flat fading channels is fairly well understood, the deployment of relay systems in ISI channels requires consideration of a variety of new issues in order to best exploit the available diversity. For example, we presented cases where random relay selection and the all-decoding-

relay method can achieve the same diversity as the best relay selection, which runs counter to the situation in flat fading channels where the best relay selection is always superior. We also find that only when the number of relays in the system is relatively large, the best relay selection offers a significant performance advantage over the other relaying strategies, though this tends to diminish with increased frequency diversity in the system. As the overhead of random relay selection is lower than that of the best relay selection, system designers may favor random relaying depending on the application and transmission environment.

The analytical work presented here focuses on the high-SNR regime, and is an important step toward understanding the diversity offered by relay systems in frequency selective fading channels. The relaying strategies presented in this chapter do not require sophisticated space-time coding; they have relaxed synchronization requirements, and are spectrally efficient; these advantages make the relay selection methods ready for implementation in today's distributed networks. Future work may consider the use of alternate forwarding protocols (such as amplify-and-forward or equalize-and-forward) as well as the overhead tradeoff of the various relay selection methods.

Chapter 3

Relay Selection in Amplify-and-Forward Cooperative Networks with Frequency Selective Fading

In this chapter, we consider the system model in Section 2.2 where the relays use amplify-and-forward protocols under a half-duplex constraint. In addition, to simplify notation, we assume that each channel in the system suffers i.i.d. frequency selective (FS) fading, i.e., $M_{jk} = L_{jk}$ and $\mathbf{\Gamma}_{jk}$ is diagonal. With techniques borrowed from the previous chapter, the analysis presented in this chapter can be extended to general cases with correlated fading. We first analyze the matched filter bound (MFB) of outage probability. We aim to find a relay selection method that can attain the optimal diversity-multiplexing tradeoff (DMT) in the presence of amplify-and-forward (AF) relays when only a single relay is selected in forwarding. The relay selection method developed in the outage analysis turns out to achieve full diversity when the maximum-likelihood sequential estimator (MLSE) is employed at the destination, as corroborated by simulation. However, in practice, MLSE may not be practical due to its high complexity. Hence, we also propose a new relay selection method based on the average decision-point (DP) SNR over the block for linear zero-forcing equalization (ZFE) at the destination to asymp-

totically achieve the optimal DMT. As we will see, while the MLSE has higher complexity in equalization, the two corresponding relay selection methods which can achieve full diversity do not require much computation; on the other hand, linear ZFE has lower complexity in equalization, but the corresponding selection method designed to achieve the optimal DMT requires higher computation (matrix inversion). Contrast to the DF relay selection, which has the same diversity order with different equalization methods, AF relay selection results in different diversity order with different equalization methods.

3.1 Outage Probability Analysis with Relay Selection

In this section, we aim to derive the relay selection method which can achieve the optimal DMT. We assume that each relay operates with the amplify-and-forward protocol, i.e., the relay scales what it receives before forwarding with an amplification factor in order to meet the transmission power constraint. To characterize the DMT upper bound of this AF relay channel, we use the MFB, and assume that a single symbol $x[0]$ is sent by the transmitter with energy $E[|x[0]|^2] = P/W$. We also assume that the total transmission time between the relay and the destination is only one symbol duration (if causality is ignored). This assumption is implicitly used in [36] for the optimal tradeoff curve characterization. As in Chapter 2, the transmission is divided into two phases. In the first phase, the source broadcasts the message to the destination and the relays, and the received

signals at the destination and at the ith relay are given by

$$\boldsymbol{y}_{sd} = \boldsymbol{h}_{sd}x[0] + \boldsymbol{w}_{sd}, \tag{3.1}$$

$$\boldsymbol{y}_{r_i} = \boldsymbol{h}_{sr_i}x[0] + \boldsymbol{w}_{sr_i}. \tag{3.2}$$

In the second phase, we assume only one selected relay forwards the scaled version of what it receives in the first phase to the destination. Assuming the selected relay is of subscript r_i, we have the received signal at the destination

$$\boldsymbol{y}_{r_id} = \beta\boldsymbol{H}_{r_id}(\boldsymbol{h}_{sr_i}x_0 + \boldsymbol{w}_{sd}) + \boldsymbol{w}_{r_id} \tag{3.3}$$

where the amplification factor $\beta_i = \sqrt{\frac{L_{sr_i}}{\|\boldsymbol{h}_{\boldsymbol{sr_i}}\|^2 + L_{sr_i}\rho^{-1}}}$, ρ is the discrete-time signal-to-noise ratio and is defined as $\rho \triangleq \frac{P}{WN_0}$, $\boldsymbol{H}_{r_id} \in \mathbb{C}^{(L_{sr_i}+L_{r_id}-1)\times L_{sr_i}}$ is the Tœplitz channel matrix corresponding to $\boldsymbol{h}_{r_id}$, e.g. $[\boldsymbol{H}_{r_id}]_{m,n} = \boldsymbol{h}_{r_id}[m-n]$. It should be noted that with this amplification factor β_i, the relay uses L_{sr_i} times as much transmit energy as the source.

We next aim to find the mutual information $I(x_0; \boldsymbol{y}_{sd}, \boldsymbol{y}_{r_id})$. This is the prerequisite step for finding the relay selection method which can maximize the mutual information between the sent symbol and the received signals over all possible ways of selecting a single relay. In the following, we first whiten the colored noise in the received signal at the second phase to simplify the calculation. With the assumption that the ith relay is selected, the noise covariance in $\boldsymbol{y}_{r_id}$ can be found as $N_0\boldsymbol{K}_i$ with

$$\boldsymbol{K}_i = \beta_i^2\boldsymbol{H}_{r_id}\boldsymbol{H}_{r_id}^H + \boldsymbol{I}.$$

As $\boldsymbol{K}_i$ is symmetric positive definite, its LU decomposition can be found as

$$\boldsymbol{K}_i = \boldsymbol{L}_i^H\boldsymbol{L}_i.$$

With the similar sufficient statistic argument as for [2, 5.26], we can write the mutual information as

$$\begin{aligned} I(x_0; \boldsymbol{y}_{sd}, \boldsymbol{y}_{r_i d}) &= I(x_0; \boldsymbol{y}_{sd}, \boldsymbol{L}_i^{-1} \boldsymbol{y}_{r_i d}) && (3.4) \\ &= \frac{1}{2} \log(1 + \rho \|\boldsymbol{h}_{sd}\|^2 + \mathrm{SNR}_{\mathrm{MFB},r_i}) && (3.5) \end{aligned}$$

where (3.4) follows that the invertible operation does not change the mutual information, and the SNR in the transformed signal is defined as

$$\mathrm{SNR}_{\mathrm{MFB},r_i} = \rho \beta_i^2 \boldsymbol{h}_{sr_i}^H \boldsymbol{H}_{r_i d}^H \boldsymbol{K}_i^{-1} \boldsymbol{H}_{r_i d} \boldsymbol{h}_{sr_i}.$$

As we want to maximize $I(x_0; \boldsymbol{y}_{sd}, \boldsymbol{y}_{r_i d})$, we need to select the relay $\mathbf{R}_*$ such that

$$\mathrm{SNR}_{\mathrm{MFB},r_*} = \arg \max_{i=1,\cdots,K} \mathrm{SNR}_{\mathrm{MFB},r_i}. \quad (3.6)$$

To help analyze the performance of the relay selection method (3.6), we use the singular value of $\boldsymbol{H}_{r_i d}$ to express $\mathrm{SNR}_{\mathrm{MFB},r_i}$. Define the singular value decomposition (SVD) of $\boldsymbol{H}_{r_i d}$ as $\boldsymbol{U}\boldsymbol{\Sigma}\boldsymbol{V}^H$, we can further write

$$\boldsymbol{K}_i = \boldsymbol{U}(\beta_i^2 \boldsymbol{\Sigma}\boldsymbol{\Sigma}^H + \boldsymbol{I})\boldsymbol{U}^H.$$

Hence the inverse of the noise covariance can be found as $\boldsymbol{K}_i^{-1} = \boldsymbol{U}(\beta_i^2 \boldsymbol{\Sigma}\boldsymbol{\Sigma}^H + \boldsymbol{I})^{-1}\boldsymbol{U}^H$, and

$$\begin{aligned} \mathrm{SNR}_{\mathrm{MFB},r_i} &= \rho \beta_i^2 \boldsymbol{h}_{sr_i}^H \boldsymbol{H}_{r_i d}^H \boldsymbol{K}_i^{-1} \boldsymbol{H}_{r_i d} \boldsymbol{h}_{sr_i} \\ &= \rho \sum_{k=0}^{L_{h_{sr_i}}-1} |\boldsymbol{h}'_k|^2 \frac{\beta_i^2 \lambda_k}{\beta_i^2 \lambda_k + 1} && (3.7) \end{aligned}$$

where $\boldsymbol{h}'_{sr_i} = \boldsymbol{V}\boldsymbol{h}_{sr_i}$ and λ_k is the square of kth singular value of $\boldsymbol{H}_{r_i d}$.

By definition, the outage probability can be expressed as

$$\begin{aligned} P_{out} &= Pr(I(x_0; \boldsymbol{y}_{sd}, \boldsymbol{y}_{r_*d}) < R) \\ &= Pr(\frac{1}{2}\log(1+\rho\|\boldsymbol{h}_{sd}\|^2 + \mathrm{SNR}_{\mathrm{MFB},r_*}) < R) \qquad (3.8) \\ &\dot{\leq} Pr((\max(\rho\|\boldsymbol{h}_{sd}\|^2, \mathrm{SNR}_{\mathrm{MFB},r_*}) < 2^{2R}-1) \\ &\doteq Pr(\|\boldsymbol{h}_{sd}\|^2 < \rho^{2r-1}) \prod_{i=1,\cdots,K} Pr(\mathrm{SNR}_{\mathrm{MFB},r_i} < 2^{2R}-1) \\ &= \rho^{(2r-1)(L_{sd}+\sum_{i=1}^{K}\min(L_{sr_i},L_{r_id}))} \qquad (3.9) \end{aligned}$$

where $r = \lim_{\rho\to\infty} \frac{\log R}{\log \rho}$, and (3.9) follows because

$$\begin{aligned} & \Pr(\mathrm{SNR}_{\mathrm{MFB},r_i} < 2^{2^R}-1) \\ =\ & \Pr(\sum_{k=0}^{L_{h_{sr_i}}-1} |\boldsymbol{h}'_k|^2 \frac{\beta_i^2\lambda_k}{\beta_i^2\lambda_k+1} < \rho^{2r-1}) \\ \doteq\ & \rho^{-\min(L_{sr_i},L_{r_id})}, \qquad (3.10) \end{aligned}$$

which is proven in Section 3.5.

The relay selection method defined in (3.6) selects the relay which has the largest processed SNR when only one symbol is transmitted. This method gives the best outage performance over all single relay selection method under the MFB. We define this method as "Max MFB SNR" method. As we will see in the simulation results, this relay selection method combined with the transmission scheme Section 3.2.1 and MLSE at the destination can achieve both frequency diversity and cooperative diversity. We also extend the relay selection method based on [12, equation (1)] and propose another relay selection method, namely "Max Min Norm-2", which selects the relay with the index

$$m = \arg\max_{i=1,\cdots,K} \min(\|\boldsymbol{h}_{sr_i}\|^2, \|\boldsymbol{h}_{r_id}\|^2). \qquad (3.11)$$

Both relay selection methods have the same outage probability, as will shown by simulation. Further BER performance with the transmission scheme described in Section 3.2.1 and MLSE at the destination is shown in Section 3.3; by simulation, both can achieve full diversity.

3.2 Optimal-DMT-Achieving Transceiver Based on Linear ZFE

In the previous section, we proposed two relay selection methods that can achieve full diversity with MLSE. We note that MLSE has a complexity which is exponentially increased with the number of fading taps in the channel, and this limits its application to devices with limited processing capability. If low-complexity processing is preferred at the destination, in order to achieve the full diversity, we need to develop a new relay selection method. We proceed by first describing the transmission scheme, then analyzing the BER when a specific relay is always selected without using any channel state information. Based on analysis of always preselecting a specific relay, we propose a relay selection method to asymptotically achieves the optimal DMT.

3.2.1 Transmission Scheme

The source and relays use the insertion of guard time between blocks of symbols, which can eliminate the possibility of inter-block interference, but not the possibility of inter-symbol interference. To specify the length of guard interval, we

define

$$L_{\max} \geq \max_{i \in 1,\ldots,K} \{L_{sr_i}, L_{r_i d}, L_{sd}\}$$

and it is essentially an upper bound on the length of all channels in the system. The transmission of a complete message is divided into two phases:

1. In phase one, after the source broadcasts $\boldsymbol{x}$, a block of N QAM-symbols to the destination and the relays, a guard interval of length $L_{\max} - 1$ zeros follows.

2. In phase two, the source is silent. The selected relay forwards its received signal to the destination under the constraint on transmit power, and then a guard interval of length $L_{\max} - 1$ follows.

The source and relays then alternate between these two phases; as quasi-static fading is assumed, for different message blocks, different relays might be selected to help the transmission. This is shown in Fig. 3.1 for the case where the relay $\mathbf{R}_2$ is selected in the second phase of transmission of the first block of the message and the fourth block of message. We note that the destination receives the composite signal corrupted by intersymbol interference and additive noise, but no inter-block interference due to the insertion of guard intervals. We also note that the interval of source transmission and the interval of relay transmission are different, as the transmitted signal by the relay has been extended through the source-to-relay channels.

In the proposed scheme, QAM-symbols transmitted by the source are drawn from a constellation of $M = \rho^{r'}$ points. We assume that M is a perfect square

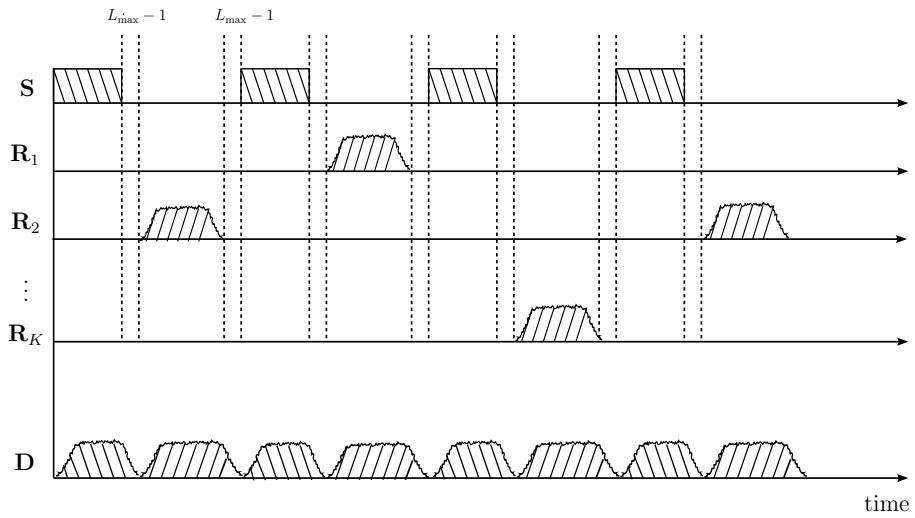

Figure 3.1: Transmission process.

so that the QAM constellation is well formed [36]. To find the multiplexing gain r' and also make a fair comparison with the cut-set bound on DMT, we want to make sure that

$$\frac{N}{2N+3L_{\max}-3}\log M = \frac{1}{2}r\log\rho,$$

thus we found that

$$r' = 1 - \frac{\frac{3}{2}L_{\max}-1}{N+\frac{3}{2}L_{\max}-\frac{3}{2}}. \tag{3.12}$$

Due to the insertion of guard time between alternating phases of source/relay transmission, we see from (3.12) that the system incurs a rate penalty that can be made arbitrarily small by increasing the block length N.

3.2.2 BER Analysis with Relay Selection

In this subsection, we first assume a single relay with index c is always selected without using any channel state information, and analyze the BER performance when linear ZFE is employed at the destination; then based on the the analysis,

we aim to develop a relay selection method that can exploit the spatial diversity.

The case that a single relay is always selected is equivalent to the case when only one relay is present in the system. In the first phase, the received signal at the destination is

$$\boldsymbol{y}_{sd} = \boldsymbol{H}_{sd}\boldsymbol{x} + \boldsymbol{w}_{sd}$$

where $\boldsymbol{H}_{sd} \in \mathbb{C}^{(N+L_{sd}-1)\times N}$ is the Tœplitz channel convolution matrix corresponding to $\boldsymbol{h}_{sd}$ and $\boldsymbol{w}_{sd}$ is the noise at the destination, and the received signal at the relay is

$$\boldsymbol{y}_{r_c} = \boldsymbol{H}_{sr_c}\boldsymbol{x} + \boldsymbol{w}_{r_c}$$

where $\boldsymbol{H}_{sr_c} \in \mathbb{C}^{(N+L_{sr_c}-1)\times N}$ is the Tœplitz channel convolution matrix corresponding to $\boldsymbol{h}_{sr_c}$ and $\boldsymbol{w}_{r_c}$ is the noise at the selected relay. The received signal in the second phase from the selected relay to the destination is

$$\begin{aligned}\boldsymbol{y}_{rd} &= \beta_c \boldsymbol{H}_{r_cd}\boldsymbol{y}_{r_c} + \boldsymbol{w}_{r_cd} \\ &= \beta_c \boldsymbol{H}_{r_cd}\boldsymbol{H}_{sr_c}\boldsymbol{x} + \beta_c \boldsymbol{H}_{r_cd}\boldsymbol{w}_{r_c} + \boldsymbol{w}_{r_cd}\end{aligned}$$

where the amplification factor

$$\beta_c = \sqrt{\frac{N + L_{sr_c} - 1}{N\|\boldsymbol{h}_{sr_c}\|^2 + (N + L_{sr_c} - 1)\rho^{-1}}},$$

$\boldsymbol{H}_{r_cd} \in \mathbb{C}^{(L_{sr_c}+L_{r_cd}+N-2)\times(L_{sr_c}+N-1)}$ is the Tœplitz channel convolution matrix corresponding to $\boldsymbol{h}_{r_cd}$, and $\boldsymbol{w}_{r_cd}$ is the noise at the destination when the selected relay transmits. The noise covariance matrix is $\boldsymbol{R}_{ww}N_0$ where $\boldsymbol{R}_{ww} = \beta_c^2 \boldsymbol{H}_{r_cd}\boldsymbol{H}_{r_cd}^H + \boldsymbol{I}$ and can be decomposed as $\boldsymbol{R}_{ww} = \boldsymbol{L}^H\boldsymbol{L}$ (i.e. Cholesky decomposition). After applying the whitening filter $\boldsymbol{L}^{-H}$ to $\boldsymbol{y}_{rd}$, we have

$$\begin{aligned}\tilde{\boldsymbol{y}}_{rd} &= \boldsymbol{L}^{-H}\boldsymbol{y}_{rd} \\ &= \beta_c \boldsymbol{L}^{-H}\boldsymbol{H}_{r_cd}\boldsymbol{H}_{sr_c}\boldsymbol{x} + \tilde{\boldsymbol{w}}\end{aligned}$$

where $\tilde{\boldsymbol{w}} = \boldsymbol{L}^{-H}(\beta_c \boldsymbol{H}_{r_c d}\boldsymbol{w}_{r_c} + \boldsymbol{w}_{d_c})$ is white. Denote $\boldsymbol{G}_c \triangleq \beta_c \boldsymbol{L}^{-H}\boldsymbol{H}_{r_c d}\boldsymbol{H}_{sr_c}$ and define

$$\boldsymbol{H}_{\text{eff},c} = \begin{bmatrix} \boldsymbol{H}_{sd} \\ \boldsymbol{G}_c \end{bmatrix}, \quad \boldsymbol{w}_{\text{eff}} = \begin{bmatrix} \boldsymbol{w}_{sd} \\ \tilde{\boldsymbol{w}} \end{bmatrix}.$$

Then the received signal to be equalized at the destination is then given by

$$\boldsymbol{y} = \boldsymbol{H}_{\text{eff},c}\boldsymbol{x} + \boldsymbol{w}_{\text{eff}}. \tag{3.13}$$

We note that this model includes the guard intervals inserted between the two transmission phases as can be seen by the dimensions of $\boldsymbol{H}_{sr_c}$, $\boldsymbol{H}_{sd}$, and $\boldsymbol{H}_{r_c d}$. We also note

$$\boldsymbol{H}_{\text{eff},c}^H \boldsymbol{H}_{\text{eff},c} = \boldsymbol{H}_{sd}^H \boldsymbol{H}_{sd} + \boldsymbol{G}_c^H \boldsymbol{G}_c. \tag{3.14}$$

Denote the minimum eigenvalue of $\boldsymbol{G}_c^H \boldsymbol{G}_c$ as $\lambda_{gc,\min}$, the minimum eigenvalue of $\boldsymbol{H}_{sd}^H \boldsymbol{H}_{sd}$ as $\lambda_{sd,\min}$, and the minimum eigenvalue of $\boldsymbol{H}_{\text{eff},c}^H \boldsymbol{H}_{\text{eff},c}$ as $\lambda_{\text{eff},\min}$. From (3.14) and the fact that these three matrices are Hermitian, Weyl's Inequality [37, Theorem 4.3.1] gives

$$\lambda_{\text{eff},\min} \geq \lambda_{sd,\min} + \lambda_{gc,\min}. \tag{3.15}$$

Since $\|\boldsymbol{h}_{sd}\|^2 \neq 0$ with probability 1 and due to [36, Lemma IV.1], $\lambda_{sd,\min} \geq \|\boldsymbol{h}_{sd}\|^2 \bar{\lambda}_{sd} > 0$ where

$$\bar{\lambda}_{sd} \;=\; \inf_{\boldsymbol{h}_{sd} \in \mathbb{C}^{L_{sd}}} \lambda_{sd,\min}(\bar{\boldsymbol{H}}_{sd}^H \bar{\boldsymbol{H}}_{sd}) > 0,$$

$$\bar{\boldsymbol{H}}_{sd} \;\triangleq\; \tfrac{\boldsymbol{H}_{sd}}{\|\boldsymbol{h}_{sd}\|}.$$

Thus we have $\lambda_{\text{eff},\min} > 0$ and $\boldsymbol{H}_{\text{eff},c}^H \boldsymbol{H}_{\text{eff},c}$ is invertible. The receiver at the destination processes the received signal with a ZF equalizer

$$\boldsymbol{F} = (\boldsymbol{H}_{\text{eff}}^H \boldsymbol{H}_{\text{eff},c})^{-1} \boldsymbol{H}_{\text{eff}}^H.$$

The filtered estimate of $\boldsymbol{x}$ at the receiver is then

$$\begin{aligned}\tilde{\boldsymbol{y}} &= \boldsymbol{F}\boldsymbol{y} \\ &= \boldsymbol{x} + (\boldsymbol{H}_{\text{eff},c}^H \boldsymbol{H}_{\text{eff},c})^{-1} \boldsymbol{H}_{\text{eff},c}^H \boldsymbol{w}_{\text{eff}}.\end{aligned}$$

The filtered noise $\boldsymbol{z} = (\boldsymbol{H}_{\text{eff},c}^H \boldsymbol{H}_{\text{eff},c})^{-1} \boldsymbol{H}_{\text{eff},c}^H \boldsymbol{w}_{\text{eff}}$ has total variance

$$\begin{aligned}E\left[\|\boldsymbol{z}\|^2\right] &= E[\boldsymbol{z}^H \boldsymbol{z}] \\ &= \text{tr}[(\boldsymbol{H}_{\text{eff},c}^H \boldsymbol{H}_{\text{eff},c})^{-1}] N_0.\end{aligned}$$

Assuming each symbol in the block is estimated separately, we find that the effective SNR for decoding the kth symbol is

$$\begin{aligned}\text{SNR}_{\text{eff}}(k) &= \frac{P}{WE[|z_k|^2]} \\ &\geq \frac{P}{WE\left[\|\boldsymbol{z}\|^2\right]} \\ &= \frac{\rho}{\text{tr}[(\boldsymbol{H}_{\text{eff},c}^H \boldsymbol{H}_{\text{eff},c})^{-1}]} \\ &= \frac{\rho}{\sum_{k=0}^{N-1} \lambda_{\text{eff},k}^{-1}} \\ &\geq N\rho\lambda_{\text{eff,min}} \\ &\geq \frac{1}{N}\rho(\lambda_{sd,\min} + \lambda_{gc,\min})\end{aligned} \tag{3.16}$$

where $\lambda_{\text{eff},k}$ is the kth eigenvalue for $\boldsymbol{H}_{\text{eff},c}^H \boldsymbol{H}_{\text{eff},c}$. We assume that the SVD for $\boldsymbol{H}_{r_c d}$ as $\boldsymbol{U}\boldsymbol{\Sigma}\boldsymbol{V}^H$ and $\sigma_i \triangleq [\boldsymbol{\Sigma}]_{i,i}$ with $0 \leq i \leq N + L_{sr_c} - 1$. Define the set

$$\mathcal{T} \triangleq \{\boldsymbol{a} \in \mathbb{C}^N : \|\boldsymbol{a}\| \geq 1\}. \tag{3.17}$$

The minimum eigenvalue of $\boldsymbol{G}_c^H \boldsymbol{G}_c$ can be found as

$$\begin{aligned}
\lambda_{gc,\min} &= \inf_{\boldsymbol{a}\in\mathcal{T}} \|\boldsymbol{G}_c\boldsymbol{a}\|^2 \\
&= \inf_{\boldsymbol{a}\in\mathcal{T}} \boldsymbol{a}^H \beta_c^2 \boldsymbol{H}_{sr_c}^H \boldsymbol{H}_{r_cd}^H \boldsymbol{R}_{ww}^{-1} \boldsymbol{H}_{r_cd} \boldsymbol{H}_{sr_c} \boldsymbol{a} \\
&= \inf_{\boldsymbol{a}\in\mathcal{T}} (\boldsymbol{V}^H \boldsymbol{H}_{sr_c}\boldsymbol{a})^H \beta_c^2 \boldsymbol{\Sigma}^H (\beta_c^2 \boldsymbol{\Sigma}\boldsymbol{\Sigma}^T + \boldsymbol{I})^{-1} \boldsymbol{\Sigma} (\boldsymbol{V}^H \boldsymbol{H}_{sr_c}\boldsymbol{a}) \qquad (3.18) \\
&= \inf_{\boldsymbol{a}\in\mathcal{T}} \sum_{i=0}^{\tilde{N}-1} \frac{\beta_c^2\sigma_i^2}{\beta_c^2\sigma_i^2+1} |[\boldsymbol{V}^H \boldsymbol{H}_{sr_c}\boldsymbol{a}]_i|^2 \\
&\geq \inf_{\boldsymbol{a}\in\mathcal{T}} \tilde{N} \frac{\beta_c^2 \|\boldsymbol{h}_{r_cd}\|^2 \bar{\lambda}_{r_cd}}{\beta_c^2 \|\boldsymbol{h}_{r_cd}\|^2 \bar{\lambda}_{r_cd}+1} \|\boldsymbol{V}^H \boldsymbol{H}_{sr_c}\boldsymbol{a}\|^2 \\
&= \tilde{N} \frac{\beta_c^2 \|\boldsymbol{h}_{r_cd}\|^2 \bar{\lambda}_{r_cd}}{\beta_c^2 \|\boldsymbol{h}_{r_cd}\|^2 \bar{\lambda}_{r_cd}+1} \inf_{\boldsymbol{a}\in\mathcal{T}} \|\boldsymbol{H}_{sr_c}\boldsymbol{a}\|^2 \\
&\geq \tilde{N} \frac{\beta_c^2 \|\boldsymbol{h}_{r_cd}\|^2 \bar{\lambda}_{r_cd}}{\beta_c^2 \|\boldsymbol{h}_{r_cd}\|^2 \bar{\lambda}_{r_cd}+1} \|\boldsymbol{h}_{sr_c}\|^2 \bar{\lambda}_{sr_c} \qquad (3.19)
\end{aligned}$$

where (3.18) follows by replaying $\boldsymbol{H}_{r_cd}$ with its SVD, $\tilde{N} = (N + L_{sr_c} - 1)$,

$$\begin{aligned}
\bar{\lambda}_{r_cd} &= \inf_{\boldsymbol{h}_{r_cd}\in\mathbb{C}^{L_{r_cd}}} \lambda_{r_cd,\min}(\bar{\boldsymbol{H}}_{r_cd}^H \bar{\boldsymbol{H}}_{r_cd}), \\
\bar{\lambda}_{sr_c} &= \inf_{\boldsymbol{h}_{sr_c}\in\mathbb{C}^{L_{sr_c}}} \lambda_{sr_c,\min}(\bar{\boldsymbol{H}}_{sr_c}^H \bar{\boldsymbol{H}}_{sr_c})
\end{aligned}$$

and

$$\bar{\boldsymbol{H}}_{r_cd} \triangleq \frac{\boldsymbol{H}_{r_cd}}{\|\boldsymbol{h}_{r_cd}\|}, \quad \bar{\boldsymbol{H}}_{sr_c} \triangleq \frac{\boldsymbol{H}_{sr_c}}{\|\boldsymbol{h}_{sr_c}\|}.$$

We have $\bar{\lambda}_{r_cd} > 0$ and $\bar{\lambda}_{sr_c} > 0$ due to [36, Lemma IV.1]. The error probability at the destination [36, Lemma VII.6] is

$$\begin{aligned}
P_e &\doteq \Pr[\mathrm{SNR}_{\mathrm{eff},c}(k) < \rho^{2r'}] \qquad (3.20) \\
&\leq \Pr[\frac{1}{N}\rho(\lambda_{sd,\min} + \lambda_{gc,\min}) < \rho^{2r'}] \\
&\leq \Pr[\frac{1}{N}\rho(\|\boldsymbol{h}_{sd}\|^2 \bar{\lambda}_{sd} + \tilde{N}\frac{\beta_c^2 \|\boldsymbol{h}_{r_cd}\|^2 \bar{\lambda}_{r_cd}}{\beta_c^2 \|\boldsymbol{h}_{r_cd}\|^2 \bar{\lambda}_{r_cd}+1} \|\boldsymbol{h}_{sr_c}\|^2 \bar{\lambda}_{sr_c}) < \rho^{2r'}]. \qquad (3.21)
\end{aligned}$$

We next use Lemma 3.6.1 to continue the calculation of (3.21) and find the upper bound on the error probability. First we find that

$$\Pr[\frac{1}{N}\rho\|\boldsymbol{h}_{sd}\|^2 \bar{\lambda}_{sd} < \rho^{2r'}] \dot{\leq} \rho^{-L_{sd}(1-2r')}. \qquad (3.22)$$

Next we calculate that

$$\begin{aligned}
& \Pr[\frac{\tilde{N}}{N}\rho\frac{\beta_c^2\|\boldsymbol{h}_{r_cd}\|^2\bar{\lambda}_{r_cd}}{\beta_c^2\|\boldsymbol{h}_{r_cd}\|^2\bar{\lambda}_{r_cd}+1}\|\boldsymbol{h}_{sr_c}\|^2\bar{\lambda}_{sr_c}<\rho^{2r'}] \\
\doteq\ & \Pr[\frac{\beta_c^2\|\boldsymbol{h}_{r_cd}\|^2\bar{\lambda}_{r_cd}}{\beta_c^2\|\boldsymbol{h}_{r_cd}\|^2\bar{\lambda}_{r_cd}+1}\|\boldsymbol{h}_{sr_c}\|^2\bar{\lambda}_{sr_c}<\rho^{2r'-1}] \\
\doteq\ & \Pr[\frac{\bar{\lambda}_{sr_c}\|\boldsymbol{h}_{sr_c}\|^2\|\boldsymbol{h}_{r_cd}\|^2\bar{\lambda}_{r_cd}}{\|\boldsymbol{h}_{sr_c}\|^2+\|\boldsymbol{h}_{r_cd}\|^2\bar{\lambda}_{r_cd}+\rho^{-1}}<\rho^{2r'-1}] \\
\leq\ & \Pr[\bar{\lambda}_{sr_c}\min(\|\boldsymbol{h}_{sr_c}\|^2,\|\boldsymbol{h}_{r_cd}\|^2\bar{\lambda}_{r_cd})\leq\rho^{2r'-1}+\rho^{r'-1}\sqrt{1+\rho^{2r'}}] \qquad (3.23) \\
=\ & 1-\Pr[\bar{\lambda}_{sr_c}\|\boldsymbol{h}_{sr_c}\|^2>\rho^{2r'-1}+\rho^{r'-1}\sqrt{1+\rho^{2r'}}]\cdot \\
& \qquad \Pr[\bar{\lambda}_{sr_c}\|\boldsymbol{h}_{r_cd}\|^2\bar{\lambda}_{r_cd}>\rho^{2r'-1}+\rho^{r'-1}\sqrt{1+\rho^{2r'}}] \\
\doteq\ & \Pr[\bar{\lambda}_{sr_c}\|\boldsymbol{h}_{sr_c}\|^2\leq\rho^{2r'-1}+\rho^{r'-1}\sqrt{1+\rho^{2r'}}]+ \\
& \qquad \Pr[\bar{\lambda}_{sr_c}\|\boldsymbol{h}_{r_cd}\|^2\bar{\lambda}_{r_cd}\leq\rho^{2r'-1}+\rho^{r'-1}\sqrt{1+\rho^{2r'}}] \\
\doteq\ & \rho^{-\min\{L_{sr_c},L_{r_cd}\}(1-2r')} \qquad (3.24)
\end{aligned}$$

where (3.23) follows due to [12, Lemma 4]. Using Lemma 3.6.1 to combine the results in (3.22) and (3.24), we find that

$$P_e\dot{\leq}\rho^{-(L_{sd}+\min\{L_{sr_c},L_{r_cd}\}(1-2r')}.$$

We see that preselection without any knowledge of channel state does not exploit any spatial diversity.

We next aim to find a single relay selection method which can exploit the distributed space diversity and hence asymptotically achieve the optimal DMT with linear ZFE. With the result in (3.24), it is intuitive to select the relay such that the lower bound on $\lambda_{g,\min}$, as shown in (3.19), is the largest. However, finding this lower bound is not easy as it is a function of the infimum of the squared minimum eigenvalue of the equivalent channel matrix for the relay-to-destination channel. As shown in Lemma 3.7.1, the infimum is a decreasing function of the

block length N. When N is large enough, the infimum is very small and the attempt of finding its numerical value would probably arrive at a value that is not accurate enough.

Hence, we focus on (3.20) and select the relay which can give the largest lower bound on the effective SNR as shown in (3.16), i.e., the relay with the index

$$m = \arg\max_i \frac{\rho}{\mathrm{tr}[(\boldsymbol{H}_{\mathrm{eff},i}^H \boldsymbol{H}_{\mathrm{eff},i})^{-1}]}. \tag{3.25}$$

It is equivalent to select the relay with the largest average decision-point (DP) SNR and is represented by "Max DP SNR" as it. With this relay selection method, we can calculate the error probability at the destination [36, Lemma VII.6] as

$$\begin{aligned}
P_e &\doteq \Pr[\mathrm{SNR}_{\mathrm{eff}}(k) < \rho^{2r'}] \\
&\leq \Pr[\max_{i=1,\cdots,K} \frac{\rho}{\mathrm{tr}[(\boldsymbol{H}_{\mathrm{eff},i}^H \boldsymbol{H}_{\mathrm{eff},i})^{-1}]} < \rho^{2r'}] \\
&\leq \Pr[\frac{\rho}{N}(\lambda_{sd,\min} + \max_{i=1,\cdots,K} \lambda_{gi,\min}) < \rho^{2r'}] \\
&\doteq \Pr[\frac{\rho}{N}\lambda_{sd,\min} < \rho^{2r'}]\Pr[\frac{\rho}{N} \max_{i=1,\cdots,K} \lambda_{gi,\min} < \rho^{2r'}] \qquad (3.26) \\
&= \Pr[\frac{\rho}{N}\lambda_{sd,\min} < \rho^{2r'}] \prod_{i=1,\cdots,K} \Pr[\frac{\rho}{N} \lambda_{gi,\min} < \rho^{2r'}] \\
&= \rho^{-(L_{sd}+\sum_{i=1}^K \min\{L_{sr_i}, L_{r_i d}\})(1-2r')} \qquad (3.27)
\end{aligned}$$

where (3.26) follows Lemma 3.6.1. Combining the result in (3.27) and the upper bound on DMT in (2.9), we have the following result on DMT of this multiple amplify-and-forward relay system

$$(L_{sd} + \sum_{i=1}^K \min(L_{sr_i}, L_{r_i d}))(1-2r') \dot{\leq} d(r) \dot{\leq} (L_{sd} + \sum_{i=1}^K \min(L_{sr_i}, L_{r_i d}))(1-2r).$$

It is obvious to see that such relay selection method can exploit cooperative diversity. As we can see in (3.12), as the block length N goes into infinity, r' is asymptotically equal to r. Thus, this relay selection method asymptotically achieves the upper bound on DMT with zero-forcing equalization at the destination.

So far we have developed the single best relay selection scheme as shown in (3.25). This selection requires full CSI and K matrix inversion; hence the computation complexity is relatively high. The implementation of relay selection can be completed in a distributed fashion by relays or a centralized fashion at the destination. However, in a distributed fashion, it should be noted that the CSI of the source-to-destination channel should be transmitted to each relay. It is interesting to note that in flat fading, this RS method and the method in (3.6) coincide.

3.3 Numerical Results

This section presents numerical examples of the outage probability of the proposed relay selection methods developed in Section 3.1 and the BER of the proposed relay selection methods developed in Sections 3.2. We remind the reader that in evaluating performance over finite SNRs, the diversity measured as the negative slope of each outage curve often does not coincide exactly with the predicted maximal diversity [14, 15]; the predicted diversity assumes that the SNR grows arbitrarily large to permit the analysis to be mathematically tractable.

Fig. 3.2 shows the outage probability where the rate $R = 2$ bits/s/Hz and each fading tap of $\boldsymbol{h}_{jk}$ is i.i.d. Rayleigh fading with variance 1 where the subscript jk can be sd, sr_i or r_id, In the figure, "Max MFB SNR" indicates the relay selection method in (3.6) and "Max Min Norm-2" indicates the relay selection method in (3.11). As we can see, both relay selection methods result in the same outage probability. As the number of relays increases, the negative slopes of the outage cures also increase. Hence both relay selection methods can exploit the space

diversity. As is shown, when the number of relay remains the same, the outage curves for $L = 1$ have smaller negative slopes than the the outage curves for $L = 2$. Thus, with increased frequency diversity, increased diversity order also shows in the outage curves. This indicates the frequency diversity can be exploited. Hence both relay selection methods can provide full diversity.

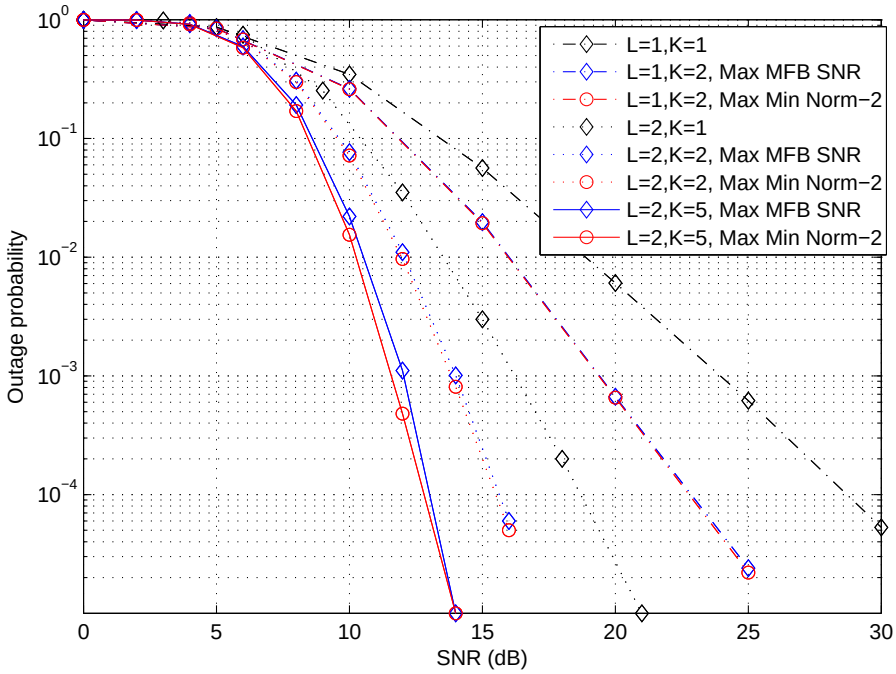

Figure 3.2: Simulated outage probability for relay selection "Max MFB SNR" and "Max Min Norm-2", $R = 2$ bits/s/Hz.

We further verify the BER performance of the transceiver designs with different relaying strategies. In the simulation, we use a block length $N = 32$. We assume each channel as a frequency selective channel with uniform power delay profile, i.e. each tap of each channel is i.i.d. fading with variance $1/L$ where L is the channel length.

We first consider the performance of MLSE at the destination with the "Max

MFB SNR" and "Max Min Norm-2" methods. As MLSE is only optimal with white noise, we employ a two-tap whitening filter before MLSE. Since it is of finite length, the optimality does not hold; however, it still has better performance than the one without whitening filter. Fig. 3.3 shows the BER performance of both relay selection methods when the input symbols are Gray-mapped QPSK symbols. With MLSE, both relay selection methods has better performance when more relays are present in the system. However, in the high SNR region, compared to the DF relay networks, such improvement with an increased number of relays is much less, since the best relay selection with DF protocol and 10 relay has a much larger power gain than "Max MFB SNR" selection with AF and 10 relays. We also note that in the lower SNR region, AF relay selection is better than DF relay selection. We further verify that MLSE with the two relay selection methods can exploit the frequency diversity by plotting the BER performance of $L = 2$ against that of $L = 4$, which is shown in Fig. 3.4.

We plot the BER performance of the transceiver design based on Linear ZFE in Fig. 3.5. The relay selection method in (3.25) is represented by "Max DP SNR" in the figure. As is shown, with an increased number of relays, it provides improved BER performance. It reaps the almost same diversity order as the best relay selection method shown in (2.14) in DF cooperative networks. Compared to the best relay selection with DF protocol, the "Max DP SNR" relay method with AF protocol has better BER performance at the cost of much more computation in performing relay selection. While the relay selection methods represented by "Max MFB SNR" and "Max Min Norm-2" can exploit spatial diversity with MLSE at the destination, both of them cannot exploit spatial diversity with linear ZFE. This is because of the small correlation between the selection criterion to the actual

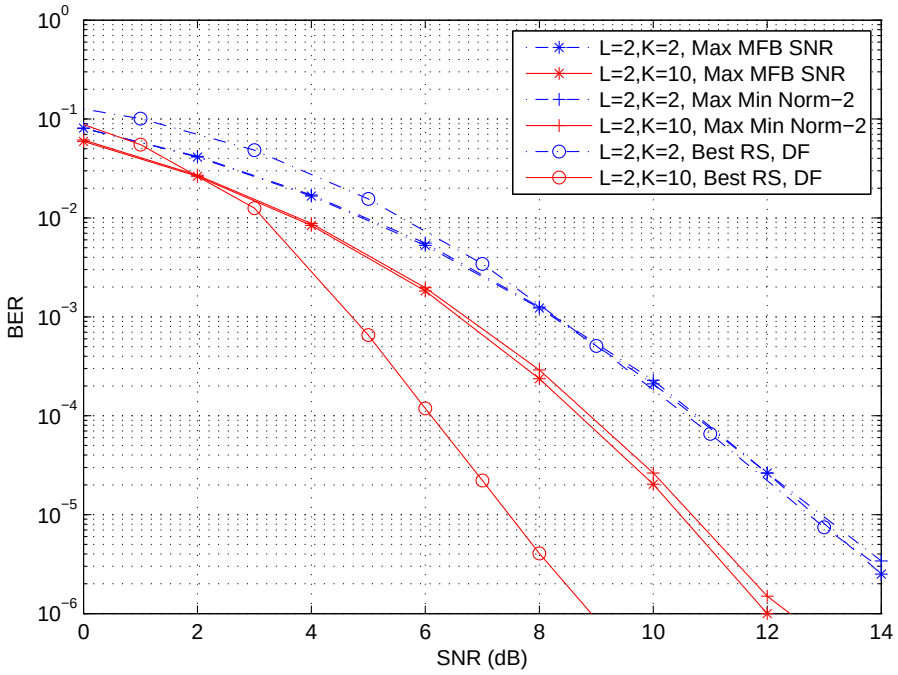

Figure 3.3: Simulated BER for i.i.d. fading channels with MLSE and QPSK.

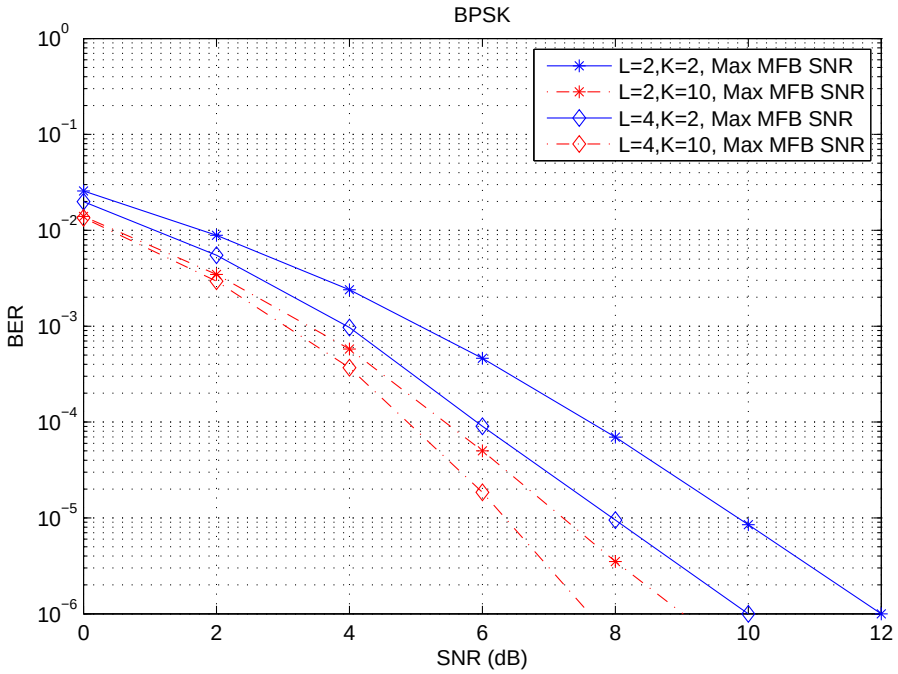

Figure 3.4: Simulated BER for i.i.d. fading channels with MLSE and BPSK.

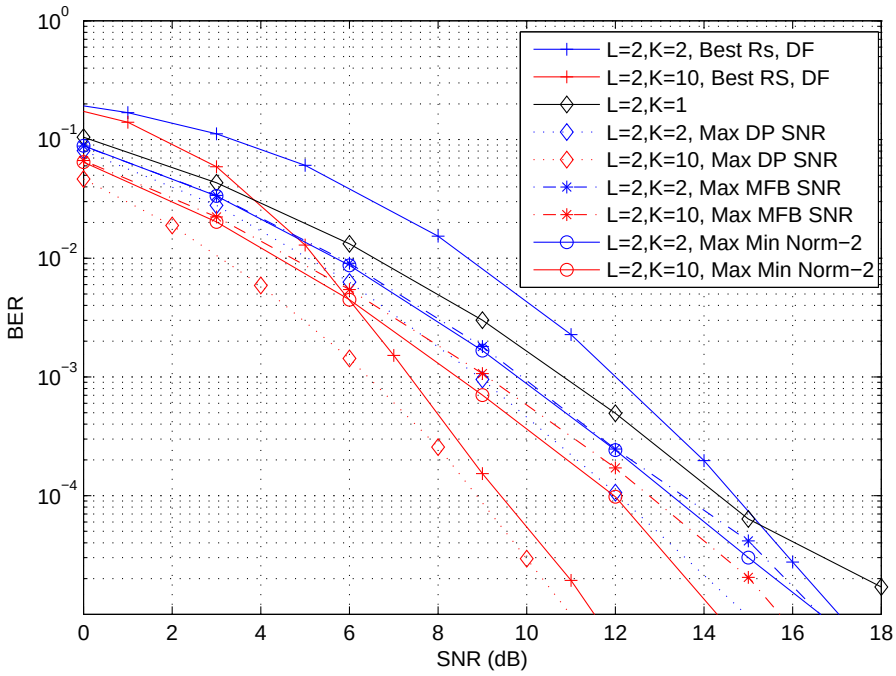

Figure 3.5: Simulated BER for i.i.d. fading channels with Linear ZFE and QPSK.

DP SNR which dictates the BER performance. This is also different from relay selection with DF protocol where the best relay selection method in [39] can achieve full diversity, no matter what equalization is used.

3.4 Conclusion

In this chapter, we considered the relay selection problem for the orthogonal amplify-and-forward system where i.i.d. frequency selective fading is present. We analyzed the outage performance based on MFB and developed a relay selection method that can provide a channel with the optimal DMT. The relay selection method selects the relay with the largest processed SNR at the destination when only one symbol is sent. This relay selection is useful in exploiting spatial diversity when MLSE is used at the destination, and this result is corroborated by simula-

tion. We also developed a relay selection method when the destination uses linear ZFE. It selects the relay with the largest average DP SNR. While this method is proven to asymptotically achieve the optimal DMT, the computation complexity is relatively high. This method requires a specific number of matrix inversions where the number of matrix inversions is up to the number of relays in the system, and the matrix dimension is up to the block length. Similar to relay selection with DF relays, we can perform low-complexity relay selections such as the random relay selection (Chapter 2), and there are cases when the random relay selection can achieve the maximal diversity with much lower overhead. As we know with DF relays, no matter what equalization is used, the same relay selection method can exploit cooperative diversity. However, with AF relays, if a different equalization method is used at the destination, a different relay selection needs to be used in order to achieve the optimal DMT. In other words, in order to exploit spatial diversity, the relay selection method is closely connected to the equalization method at the destination.

3.5 Appendix: Proof of (3.10)

To simplify notation, we make the following substitution of notations: $\boldsymbol{g} = \boldsymbol{h}_{r_i d}$, $\boldsymbol{h} = \boldsymbol{h}_{sr_i}$, $\boldsymbol{G} = \boldsymbol{H}_{r_i d}$, $L_h = L_{sr_i}$, $L_g = L_{r_i d}$, and $\boldsymbol{h}' = \boldsymbol{V}\boldsymbol{h}_{sr_i}$, where $\boldsymbol{V}$ is the in the SVD of $\boldsymbol{H}_{r_i d} =$

We define the diagonal matrix $\boldsymbol{\Lambda}$ where $\boldsymbol{\Lambda}_{k,k} = \lambda_k$, which is the square of the kth singular value of $\boldsymbol{G}$ where $0 \leq k \leq L_h$, and $\boldsymbol{Q} = \boldsymbol{G}^H\boldsymbol{G} = \boldsymbol{V}\boldsymbol{\Lambda}\boldsymbol{V}^H$. We find that $\boldsymbol{\Lambda} = \boldsymbol{V}^H\boldsymbol{Q}\boldsymbol{V}$. Since $\boldsymbol{G}$ is a Tœplitz convolution matrix containing $\boldsymbol{g}$,

$\boldsymbol{Q}_{k,k} = [\boldsymbol{G}^H \boldsymbol{G}]_{k,k} = \|\boldsymbol{g}\|^2$.

In order to analyze outage probability in high SNR region, we define $\alpha_h(k) \triangleq -\frac{\log |\boldsymbol{h}_k|^2}{log\rho}$ [46] which indicates the level of nullity of $|\boldsymbol{h}_k|^2$ (the larger $\alpha_h(k)$, the closer $|\boldsymbol{h}_k|^2$ is to 0). Similarly we define $\alpha_g(k) \triangleq -\frac{\log |\boldsymbol{g}_k|^2}{log\rho}$. It can be shown that $\|\boldsymbol{g}\|^2 \doteq \sum_{k=0}^{L_g-1} \rho^{-\alpha_g(k)} \doteq \rho^{-\min_k \alpha_g(k)}$ and

$$|\boldsymbol{Q}_{i,j}| = \sum_{k=0}^{L_g-1} \boldsymbol{g}_k^* \boldsymbol{g}_{k+i-j} \dot{\leq} \sum_{k=0}^{L_g-1} \rho^{-\frac{\alpha_g(k)}{2} - \frac{\alpha_g(k+i-j)}{2}} \dot{<} \rho^{-\min_k \alpha_g(k)}$$

if $i \neq j$. We can further derive that

$$\begin{aligned}
\lambda_i &= \sum_{k=0}^{L_h-1} \sum_{j=0}^{L_h-1} \boldsymbol{V}_{k,i}^* \boldsymbol{Q}_{k,j} \boldsymbol{V}_{j,i} \\
&= \sum_{k=0}^{L_h-1} \boldsymbol{V}_{k,i}^* \boldsymbol{Q}_{k,k} \boldsymbol{V}_{k,i} + \sum_{k=0}^{L_h-1} \sum_{j=0, j\neq k}^{L_h-1} \boldsymbol{V}_{k,i}^* \boldsymbol{Q}_{k,j} \boldsymbol{V}_{j,i} \\
&= \|\boldsymbol{g}\|^2 + \sum_{k=0}^{L_h-1} \sum_{j=0, j\neq k}^{L_h-1} \boldsymbol{V}_{k,i}^* \boldsymbol{Q}_{k,j} \boldsymbol{V}_{j,i} \\
&\doteq \rho^{-\min_l \alpha_g(l)}
\end{aligned} \tag{3.28}$$

with probability 1. Similarly we can derive that $|\boldsymbol{h}'[i]|^2 \doteq \rho^{-\min_l \alpha_h(l)}$ with probability 1.

To facilitate the derivation, we further define $m_g = \max |\boldsymbol{g}_k|^2$ and $m_h = \max |\boldsymbol{h}_k|^2$. The pdf for m_g is $f_{m_g}(\varepsilon_g) = L_g e^{-\varepsilon_g}(1 - e^{-\varepsilon_g})^{L_g-1}$ and the pdf for m_h is $f_{m_h}(\varepsilon_h) = L_h e^{-\varepsilon_h}(1 - e^{-\varepsilon_h})^{L_h-1}$. And we have $m_g \doteq \rho^{-\min_l \alpha_g(l)}$ and $m_h \doteq \rho^{-\min_l \alpha_h(l)}$.

To arrive at (3.10) , we calculate the following probability

$$\begin{aligned}
& \Pr\Big(\sum_{k=0}^{L_{h_{sr_i}}-1} |\boldsymbol{h}'_k|^2 \frac{\beta_i^2\lambda_k}{\beta_i^2\lambda_k+1} < \rho^{2r-1}\Big) \\
= \;& \Pr\Big(\sum_{k=0}^{L_h-1} |\boldsymbol{h}'_k|^2 \frac{L_h\lambda_k}{L_h\lambda_k+\|\boldsymbol{h}\|^2+\rho^{-1}} < \rho^{2r-1}\Big) \qquad (3.29) \\
\doteq \;& \Pr\Big[\frac{\rho^{-(\min_l \alpha_h(l)+\min_l \alpha_g(l))}}{\rho^{-\min_l \alpha_h(k)}+\rho^{-\min_l \alpha_g(l)}+\rho^{-1}} < \rho^{2r-1}\Big] \\
\doteq \;& \Pr\Big[\frac{m_h m_g}{m_h+m_g+\rho^{-1}} < \rho^{2r-1}, \max\{m_g,m_h\} > \rho^{-1}\Big] \\
& + \Pr[m_h m_g < \rho^{2r-2}, \max\{m_h,m_g\} \le \rho^{-1}] \qquad (3.30)
\end{aligned}$$

where (3.29) follows by the definition of β_i, and (3.30) follows as the interval over which the integration is performed is divided into two parts.

The first part in (3.30) can be further split as

$$\begin{aligned}
& \Pr\Big[\frac{m_g m_h}{m_h+m_g+\rho^{-1}} < \rho^{2r-1}, \max\{m_h,m_g\} > \rho^{-1}\Big] \\
\doteq \;& \Pr\Big[\frac{m_g m_h}{m_g+m_h} < \rho^{2r-1}, \max\{m_h,m_g\} > \rho^{-1}\Big] \\
\doteq \;& \Pr[m_h < \rho^{2r-1}, m_g > m_h, \max\{m_h,m_g\} > \rho^{-1}] \\
& + \Pr[m_g < \rho^{2r-1}, m_g < m_h, \max\{m_h,m_g\} > \rho^{-1}] \qquad (3.31)
\end{aligned}$$

where (3.31) follows as the interval over which the integration is performed is divided into two parts.

The first item in the summation of (3.31) can be further derived as

$$
\begin{aligned}
& \Pr[m_h < \rho^{2r-1}, m_g > m_h, \max\{m_h, m_g\} > \rho^{-1}] \\
= \; & \Pr[m_h < \rho^{2r-1}, m_g > m_h, m_g > \rho^{-1}] \\
\doteq \; & \int_{\rho^{-1}}^{\rho^{2r-1}} \int_{0}^{\varepsilon_g} f_{m_h}(\varepsilon_h) d\varepsilon_h f_{m_g}(\varepsilon_g) d\varepsilon_g \\
& + \int_{\rho^{2r-1}}^{+\infty} \int_{0}^{\rho^{2r-1}} f_{m_h}(\varepsilon_h) d\varepsilon_h f_{m_g}(\varepsilon_g) d\varepsilon_g \qquad (3.32) \\
= \; & \int_{\rho^{-1}}^{\rho^{2r-1}} f_{m_g}(\varepsilon_g)(1 - e^{-\varepsilon_g})^{L_h} d\varepsilon_g \\
& + (1 - e^{-\rho^{2r-1}})^{L_h}(1 - (1 - e^{-\rho^{2r-1}})^{L_g}) \\
= \; & \int_{e^{-\rho^{-1}}}^{e^{-\rho^{2r-1}}} L_g (1 - z)^{L_g - 1}(1 - z)^{L_h} dz \\
& + (1 - e^{-\rho^{2r-1}})^{L_h}(1 - (1 - e^{-\rho^{2r-1}})^{L_g}) \qquad (3.33) \\
= \; & \frac{L_g}{L_g + L_h}((1 - e^{-\rho^{-1}})^{L_g + L_h} - (1 - e^{-\rho^{2r-1}})^{L_g + L_h}) \\
& + (1 - e^{-\rho^{2r-1}})^{L_h}(1 - (1 - e^{-\rho^{2r-1}})^{L_g}) \\
\doteq \; & \rho^{L_h(2r-1)} \qquad (3.34)
\end{aligned}
$$

where (3.32) follows as the integrating range of m_g $[\rho^{-1}, +\infty]$ is divided into $[\rho^{-1}, \rho^{2r-1}]$ and $[\rho^{2r-1}, +\infty]$, (3.33) follows by substituting z for $e^{-\varepsilon_g}$.

The second item in the summation of (3.31) can be further derived as

$$
\begin{aligned}
& \Pr[m_g < \rho^{2r-1}, m_g < m_h, \max\{m_h, m_g\} > \rho^{-1}] \\
\doteq\ & \int_{\rho^{-1}}^{\rho^{2r-1}} \int_0^{\varepsilon_h} f_{m_g}(\varepsilon_g) d\varepsilon_g f_{m_h}(\varepsilon_h) d\varepsilon_h \\
& + \int_{\rho^{2r-1}}^{+\infty} \int_0^{\rho^{2r-1}} f_{m_g}(\varepsilon_g) d\varepsilon_g f_{m_h}(\varepsilon_h) d\varepsilon_h \qquad (3.35) \\
=\ & \int_{\rho^{-1}}^{\rho^{2r-1}} L_h e^{-\varepsilon_h} (1 - e^{-\varepsilon_h})^{L_h - 1} (1 - e^{-\varepsilon_h})^{L_g} d\varepsilon_h \\
& + (1 - e^{-\rho^{2r-1}})^{L_g} (1 - (1 - e^{-\rho^{2r-1}})^{L_h}) \\
=\ & \int_{e^{-\rho^{-1}}}^{e^{-\rho^{2r-1}}} L_h (1 - z)^{L_h - 1} (1 - z)^{L_g} dz \\
& + (1 - e^{-\rho^{2r-1}})^{L_g} (1 - (1 - e^{-\rho^{2r-1}})^{L_h}) \qquad (3.36) \\
=\ & \frac{L_h}{L_g + L_h} ((1 - e^{-\rho^{-1}})^{L_g + L_h} - (1 - e^{-\rho^{2r-1}})^{L_g + L_h}) \\
& + (1 - e^{-\rho^{2r-1}})^{L_g} (1 - (1 - e^{-\rho^{2r-1}})^{L_h}) \\
\doteq\ & \rho^{L_g(2r-1)}. \qquad (3.37)
\end{aligned}
$$

where (3.35) follows as the integrating range of m_g $[\rho^{-1}, +\infty]$ is divided into $[\rho^{-1}, \rho^{2r-1}]$ and $[\rho^{2r-1}, +\infty]$, (3.36) follows by substituting z for $e^{-\varepsilon_h}$.

The second part in (3.30) can be derived as

$$
\begin{aligned}
& \Pr[m_g m_h < \rho^{2r-2}, \max\{m_g, m_h\} \le \rho^{-1}] \\
= \; & \Pr[m_g m_h < \rho^{2r-2}, m_g \ge m_h, \max\{m_g, m_h\} \le \rho^{-1}] \\
& + \Pr[m_g m_h < \rho^{2r-2}, m_g < m_h, \max\{m_g, m_h\} \le \rho^{-1}] \qquad (3.38) \\
= \; & \Pr[m_g m_h < \rho^{2r-2}, m_g \ge m_h, m_g \le \rho^{-1}] \\
& + \Pr[m_g m_h < \rho^{2r-2}, m_g < m_h, m_h \le \rho^{-1}] \\
= \; & \int_0^{\rho^{-1}} \int_0^{\min\{\varepsilon_g, \rho^{2r-2}/\varepsilon_g\}} f_{m_h}(\varepsilon_h) f_{m_g}(\varepsilon_g) d\varepsilon_h d\varepsilon_g \\
+ \; & \int_0^{\rho^{-1}} \int_0^{\min\{\varepsilon_h, \rho^{2r-2}/\varepsilon_h\}} f_{m_h}(\varepsilon_h) f_{m_g}(\varepsilon_g) d\varepsilon_g d\varepsilon_h \\
= \; & \int_0^{\rho^{-1}} \int_0^{\varepsilon_g} f_{m_h}(\varepsilon_h) f_{m_g}(\varepsilon_g) d\varepsilon_h d\varepsilon_g \\
+ \; & \int_0^{\rho^{-1}} \int_0^{\varepsilon_h} f_{m_h}(\varepsilon_h) f_{m_g}(\varepsilon_g) d\varepsilon_g d\varepsilon_h \\
= \; & (1 - e^{-\rho^{-1}})^{L_g + L_h} \\
\doteq \; & \rho^{-(L_g + L_h)} \qquad (3.39)
\end{aligned}
$$

where (3.38) follows by dividing the integrating range into $m_g < m_h$ and $m_g \ge m_h$,

Collecting the results in (3.34), (3.37) and (3.39), and continuing the calculation from 3.30), we have

$$
\begin{aligned}
& \Pr\Big(\sum_{k=0}^{L_{h_{sr_i}} - 1} |\boldsymbol{h}'_k|^2 \frac{\beta_i^2 \lambda_k}{\beta_i^2 \lambda_k + 1} < \rho^{2r-1} \Big) \\
\doteq \; & \rho^{L_h(2r-1)} + \rho^{L_g(2r-1)} + \rho^{-(L_g + L_h)(2r-1)} \\
\doteq \; & \rho^{\min\{L_g, L_h\}(2r-1)}.
\end{aligned}
$$

3.6 Appendix: Asymptotic Summation Lemma

Lemma 3.6.1. *If random variables S and T are independent, and for any $u > 0$, $w > 0$, $\Pr[S < x] \doteq x^{L_S}$ for $0 < x < \rho^{-u}$ and $\Pr[T < x] \doteq x^{L_T}$ for $0 < x < \rho^{-w}$ where $\doteq$ is with respect to ρ,*

$$\Pr[S + T < \rho^{-v}] \doteq \rho^{-(L_S+L_T)v}$$

Proof. By taking the derivative of the c.d.f. of S and T, the p.d.f. for S is found as $f_S(x) \doteq x^{L_S-1}$ when $0 < x < \rho^{-u}$, and the p.d.f. of T is found as $f_T(x) \doteq x^{L_T-1}$ when $0 < x < \rho^{-w}$.

$$\begin{aligned}
\Pr[S + T < \rho^{-v}] &= \int_0^{\rho^{-v}} \int_0^{\rho^{-v}-x_S} f_S(x_S) f(x_T) dx_T dx_S \\
&\doteq \int_0^{\rho^{-v}} \int_0^{\rho^{-v}-x_S} x_S^{L_S-1} x_T^{L_T-1} dx_T dx_S \\
&= \int_0^{\rho^{-v}} x_S^{L_S-1} \frac{1}{L_T} (\rho^{-v} - x_S)^{L_T} dx_S \\
&\doteq \rho^{-(L_S+L_T)v} \qquad (3.40)
\end{aligned}$$

where (3.40) follows binomial theorem. ∎

3.7 Appendix: Lemma on the Infimum of Squared Minimum Singular Value of Tœplitz Channel Matrices

Lemma 3.7.1. *Denote $\boldsymbol{h} \in \mathbb{C}^L$ as a multipath channel. Define Tœplitz channel matrix of $\boldsymbol{h}$ of block length N as $\boldsymbol{H} \in \mathbb{C}^{(N+L-1)\times N}$ where $\boldsymbol{H}[i,j] = \boldsymbol{h}[i-j]$. Denote $\bar{\boldsymbol{H}} \triangleq \frac{\boldsymbol{H}}{\|\boldsymbol{h}\|}$ and denote $\lambda_{\min}(\bar{\boldsymbol{H}})$ as the minimum singular value of $\bar{\boldsymbol{H}}$. Define $\bar{\lambda} \triangleq \inf_{\boldsymbol{h}\in\mathbb{C}^L} \lambda^2_{\min}(\bar{\boldsymbol{H}})$. $\bar{\lambda}$ is decreasing with N.*

Proof. As proven by [36, Lemma IV.1], if with block length N, define Tœplitz channel matrix of $\boldsymbol{h}$ as $\boldsymbol{H}_N \in \mathbb{C}^{(N+L-1)\times N}$, we have

$$\bar{\lambda}_N = \inf_{\boldsymbol{h}\in\mathcal{S}} \inf_{\boldsymbol{a}\in\mathcal{T}_N} \|\boldsymbol{H}_N\boldsymbol{a}\|^2$$

where

$$\mathcal{S} \triangleq \{\boldsymbol{h} \in \mathbb{C}^L : \|\boldsymbol{h}\| = 1\}$$

and

$$\mathcal{T}_N \triangleq \{\boldsymbol{a} \in \mathbb{C}^N : \|\boldsymbol{a}\| \geq 1\}.$$

Assume block length is increased to $N+1$, define

$$\mathcal{T}_{N+1} \triangleq \{\boldsymbol{a} \in \mathbb{C}^{N+1} : \|\boldsymbol{a}\| \geq 1\},$$

we can derive that

$$\begin{aligned}
\bar{\lambda}_{N+1} &= \inf_{\boldsymbol{h}\in\mathcal{S}} \inf_{\boldsymbol{a}\in\mathcal{T}_{N+1}} \|\boldsymbol{H}_{N+1}\boldsymbol{a}\|^2 \\
&\leq \inf_{\boldsymbol{h}\in\mathcal{S}} \inf_{\boldsymbol{a}\in\mathcal{T}_{N+1},\boldsymbol{a}[N]=0} \|\boldsymbol{H}_{N+1}\boldsymbol{a}\|^2 \\
&\leq \inf_{\boldsymbol{h}\in\mathcal{S}} \inf_{\tilde{\boldsymbol{a}}\in\mathcal{T}_N} \|\boldsymbol{H}_N\tilde{\boldsymbol{a}}\|^2 \\
&= \bar{\lambda}_N.
\end{aligned}$$

■

Chapter 4

Diversity of Multi-Hop Cluster-Based Routing with Arbitrary Relay Selection

In this chapter, we extend the relay selection results from the two-hop networks to multi-hop networks. We study the routing problem in clustered multi-hop DF relay networks. In particular, we consider the effect of channel knowledge on exploiting diversity. We propose an opportunistic routing (or relay selection) algorithm for such networks. We first analyze the algorithm with flat fading assumption and then extend the analysis to frequency selective fading later. In addition, we also compare our proposed algorithm with two other routing algorithms, namely optimal routing and ad-hod routing, which require more channel knowledge.

4.1 Introduction

The two-hop system model, as studied in the previous two chapters, is insufficient when the communication ends cannot reach each other in two hops. For example, in mobile ad hoc networks (MANETS) where a group of mobile nodes need to communicate without requiring a fixed wireless infrastructure, the communication between nodes might be performed through multiple hop relays. Routing

algorithms for multi-hop systems [47, 48] have also been studied extensively, with the goal of optimizing various objectives. For example, at the higher network layers, routing algorithms have been proposed to maximize network lifetime [49] or minimize total power [50]. Traditional routing protocols for multi-hop wireless networks follow the routing paradigm in wired networks. Hence, it ignores the unreliability and also the broadcast nature of the wireless link. However, as seen in the two-hop model, the broadcast nature can help increase the reliability of transmission through the cooperation of relays. The use of cooperative communication in wireless multi-hop networks has attracted much interest for its promise of robustness against fading, increased data rates and improved energy-efficiency, among other benefits. Recognizing that the issues of routing and exploiting cooperative diversity are inherently linked, routing algorithms employing cross-layer design have also been proposed (see, for example [51]). For this latter class of algorithms, one of the major concerns is in developing routing algorithms that attain *full diversity*.

To provide scalable routing, meet quality-of-service requirements, and ease mobility management in multi-hop networks with a large number of mobile nodes, a hierarchical structure based on clustering has been considered since the early days of mobile packet radio [52]. Indeed, a wide range of algorithms exist for grouping the nodes into clusters based on some criteria, such as proximity or movement patterns [53, 54].

While a number of studies on the diversity attained by various multi-hop routing algorithms have been conducted [55, 56], less attention has been devoted to the diversity of routing algorithms in *clustered* multi-hop networks [57]. One notable

exception is [58] where several routing algorithms were proposed. In that work, an optimal routing algorithm was first considered, which assumes availability of global instantaneous channel state information (CSI), and performs a search over all possible routes at a central controller. Subsequently, a more practical routing algorithm called *ad-hoc* routing (AHR) was proposed, which generates routes in a hop-by-hop fashion, always routing the next hop through the node with the largest channel gain. While AHR does not require global channel state information, it does require channel state information between clusters so that each transmitting node can choose the best route. If all clusters in the multi-hop network have K nodes, both the optimal routing and AHR approaches were shown to yield a full diversity order of K, though the power gain of AHR was inferior to optimal approach.

Another related work which considers routing protocols and diversity in clustered multi-hop networks is [59]. The protocol employed in [59] requires two phases: one for intra-cluster communication, and another for inter-cluster communication. Then, multiple relays in each cluster transmit simultaneously to the next cluster using CDMA with RAKE receivers, though the end-to-end diversity is not explicitly computed. Lastly, in [60] the AHR protocol of [58] is modified by using an additional relay in each hop; this results in a performance improvement at the expense of an increase in complexity. However, all of these protocols [58–60] require instantaneous CSI at each transmitting node, and some of them even require full global CSI.

Here, we propose a simple opportunistic routing strategy which only requires CSI in the last hop, and selects an arbitrary node in the cluster to perform forwarding in all other hops. Quite remarkably, we show that this simple scheme can

achieve full diversity while exhibiting performance equal to the AHR approach. Furthermore, due to the flexibility in node selection in the intermediate hops, our scheme can also be adapted to optimize an external routing objective. By performing opportunistic routing – as opposed to pre-selecting a specific destination node in the next cluster before transmission – our scheme results in a significant complexity reduction and drastically reduced requirements on knowledge of CSI when compared with the existing routing protocols for clustered multi-hop networks [58–60]. Several works have investigated opportunistic routing at the higher network layers, e.g., [61, 62], though these works have not analyzed the attainable diversity. Our analysis starts with frequency flat fading and is extended to FS fading later.

4.2 System Model

We consider a wireless multi-hop network as illustrated in Fig. 4.1, where the wireless communication system consists of three kinds of nodes: a source node (**S**), clustered relay nodes, and a destination node (**D**). All nodes are assumed to be equipped with a single antenna, and we assume the relays operate in half-duplex mode so that they do not transmit and receive at the same time. Furthermore, we assume each relay node uses the decode-and-forward (DF) protocol and employs repetition coding. Only relays which correctly decode the message from the previous hop can participate in forwarding the decoded message in the next hop. We define such relays as *decoding relays* and they form a *decoding set*. In practice, the decision of whether the message is decoded successfully can be made with the help of a checksum (e.g. CRC) and we assume that relays which pass this checksum have

decoded the message error-free. To avoid interference, we consider time division

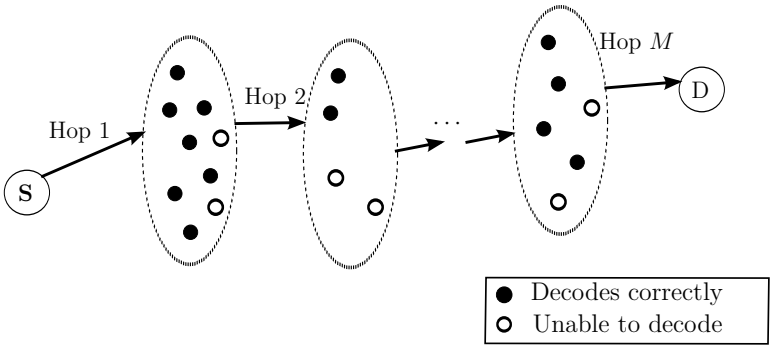

Figure 4.1: System model showing an example of the decoding set.

multiple access (TDMA) in the medium access control (MAC) layer, which allows each cluster to transmit its information in orthogonal time-domain subchannels.

We assume that the distance between relay clusters is much larger than that between nodes in any one cluster, so the point-to-point channels between two clusters are assumed to have i.i.d. Rayleigh fading statistics [2], and each channel coefficient is modelled as a complex Gaussian random variable with zero mean. Relay clusters are assumed to be spaced sufficiently far apart so that relays in a given cluster can only communicate with the neighboring cluster. Relaxation of this condition would permit combining multiple received copies at each hop, but would lead to overly optimistic results due to the high SNR analysis we employ. We note that the routing algorithm proposed in Section 4.3 can be readily extended to combine signals from multiple clusters, and this would of course improve performance.

We denote the number of total hops from the source to the destination as M. The $M-1$ relay clusters are located between the source and the destination. The relay cluster which receives in the mth-hop is denoted as $\mathcal{R}_m$ and contains K_m relays for $1 \leq m \leq M-1$. Each node in $\mathcal{R}_m$ is denoted as $\mathbf{R}_{j,m}$ where j denotes

its index in the cluster and $1 \leq j \leq K_m$. The decoding relays which can correctly decode the message from the mth hop consist of the decoding set $\mathcal{D}_m$ whose size is denoted as $|\mathcal{D}_m|$. In the subscript, we denote s as the source node $\mathbf{S}$, d as the destination $\mathbf{D}$ and $r_{i,m}$ as the ith relay in the relay cluster $\mathcal{R}_m$. The channels gains in the first hop are denoted as $h_{sr_{j,1}}$ with variance λ_1 where $1 \leq j \leq K_1$, the gains in the mth ($2 \leq m \leq M-1$) hops as $h_{r_{j,m-1}r_{k,m}}$ with variance λ_m where $1 \leq j \leq K_{m-1}$ and $1 \leq k \leq K_m$, and the gains at the last hop as $h_{r_{j,M-1}d}$ with variance λ_M where $1 \leq j \leq K_{M-1}$. We note that our system model is nearly identical to the one considered in [58], though our model is more general since each cluster can have different numbers of relays K_m. As in [58–60], we assume that cluster-level routing tables have been predetermined, and we focus on relay selection within each cluster.

To simplify the analysis, we assume that there is no power control and all nodes have the same average power constraint P watts and transmission bandwidth W Hz. In addition, all links have additive noise which is assumed to be mutually independent, zero-mean circularly symmetric complex Gaussian with variance N_0 and the discrete-time signal-to-noise ratio is defined as

$$\text{SNR} \triangleq \frac{P}{WN_0}.$$

We choose to treat the case of equal node powers and equal noise variances for simplicity; in the high SNR regime we are considering, the use of unequal powers would not change the final diversity result, though it would alter the power gain. While our model assumes all channels in the ith hop have equal variance λ_i, we note that even without the identical distribution assumption at each hop, the resulting diversity is the same. The diversity analysis below focuses on the SNR exponent

of the outage probability which is unaffected by relative node powers.

4.3 Best-Last Arbitrary-Rest Multi-hop Relaying

In this section, we propose a relaying algorithm called Best-Last Arbitrary-Rest (BLAR) which arbitrarily selects a single relay within the decoding set for the first $M-1$ hops, and then selects the best relay within the decoding set for the last hop. More sophisticated relay selection is required in the last hop; otherwise, the last hop would become a bottleneck with diversity order of 1 since there is only one antenna at the destination and spatial diversity could not be achieved. We note that arbitrary relay selection over the decoding set can be done deterministically, or randomly according to any prescribed probability mass function (pmf). For example, it can be uniformly distributed so that the relays are selected with equal probability, or it can be designed to optimize some performance objective. If the minimum latency route is desired, the decoding relay which is the first that occupies the channel to the next-hop cluster can be the actual forwarding relay with probability 1; or if we want to maximize network lifetime, the decoding relay with the largest available battery energy should be the forwarding relay. This method has the advantage that no channel state information at the transmitter (CSIT) is needed for the first $M-1$ hops, and only partial channel state information at the transmitter is needed for the final hop. In addition, we note that there is no intra-cluster communication required for this protocol.

At the first hop, after the source broadcasts the message, all the relays in the first relay cluster $\mathcal{R}_1$ try to decode the message. The relays which can decode the

message correctly form the decoding set $\mathcal{D}_1$. Each decoding relay in $\mathcal{D}_1$ takes the forwarding responsibility with probability predefined by the system as previously explained. For uniformly distributed random relay selection, each decoding relay in $\mathcal{D}_1$ waits for a random time which is uniformly distributed within a range with predefined maximum time, and the first to transmit becomes the chosen relay. For objective optimizing relay selection, the relay which optimizes the objective function within the decoding set waits for the minimal time and will be the first in the decoding set to send the decoded signal. At the next hop, the chosen relay works as the source in the first hop and the same random relaying procedure continues in the decoding set $\mathcal{D}_2$ up until $(M-1)$th hop.

In the last hop, the best relay is selected within $\mathcal{D}_{M-1}$, where the "best" relay is defined as the one with the largest channel amplitude from the relay in $\mathcal{D}_{M-1}$ to destination. The best relay selection process can be completed either centrally at the destination or in a distributed fashion by relays, as follows:

- **Centralized selection**: As each decoding relay $\mathcal{D}_{M-1}$ is aware that it has the direct link to the destination, in turn, each decoding relay transmits some known information to the destination, and the destination estimates each relay-to-destination channel. The destination chooses the relay with the largest relay-to-destination channel amplitude, and feeds back this information to the relays. The feedback requires $|\mathcal{D}_{M-1}|$ bits, and is assumed to be fed back reliably.

- **Distributed selection:** At the final hop, the relay-destination channel and the destination-relay channel are assumed to be the same due to reciprocity. For some decoding relay in $\mathcal{D}_{M-1}$ that knows it has the direct link to the

destination, it transmits a message indicating training needed to the destination. On receiving that information, the destination broadcasts training data, where each relay in $\mathcal{D}_{M-1}$ individually estimates its channel to the destination. Each relay in $\mathcal{D}_{M-1}$ waits for a time duration which is inversely proportional to its relay-destination channel amplitude before forwarding its decoded signal [12], so the relay with the largest channel amplitude will be the first to send the decoded signal to the destination. Before its actual transmission, the selected relay will first broadcast a flag message. Other decoding relays do not start transmission if they overhear the flag signal from the best relay. This flag signal is assumed known and can be detected without error.

We note that distributed selection in the last hop can yield smaller overhead and delay since the overhead of performing distributed selection is negligible compared with the training required for centralized selection. We also note that it is possible for the decoding set in any hop to be empty; in this case, the relaying procedure stops and the message cannot be transmitted to the destination successfully.

4.4 Outage Analysis with Frequency Flat Fading

In this section, we analyze the outage probability of the BLAR algorithm proposed in Section 4.3. The outage probability is defined as the probability that the mutual information I between source and destination falls below a certain rate R, and is denoted $\Pr[I < R]$. In multi-hop relaying the outage event can be caused by an outage at any intermediate hop (i.e. if $|\mathcal{D}_m| = 0$ for some m). Thus the outage

event can be expressed as the union of the following three disjoint events

$$\begin{aligned}\{I < R\} &= \{I < R \cap |\mathcal{D}_1| = 0\} \\ &\bigcup \cup_{m=2}^{M-1} \{I < R \cap |\mathcal{D}_m| = 0 \cap_{1 \le i < m} \{|\mathcal{D}_i| \neq 0\}\} \\ &\bigcup \{I < R \cap_{1 \le i \le M-1} \{|\mathcal{D}_i| \neq 0\}\}\end{aligned}$$

which correspond to conditioning on unsuccessful decoding in the first, intermediate (i.e. the mth), and final hops, respectively. As the outage probability conditioned on any empty decoding set is 1, we further have

$$\begin{aligned}\Pr[I < R \cap |\mathcal{D}_1| = 0] &= \Pr[I < R \big| \, |\mathcal{D}_1| = 0] \Pr[|\mathcal{D}_1| = 0] \\ &= \Pr[|\mathcal{D}_1| = 0]\end{aligned}$$

and similarly

$$\Pr[I < R \cap \, |\mathcal{D}_m| = 0 \cap_{1 \le i < m} \{|\mathcal{D}_i| \neq 0\}] = \Pr[|\mathcal{D}_m| = 0 \cap_{1 \le i < m} \{|\mathcal{D}_i| \neq 0\}].$$

Thus the outage probability can be written as

$$\begin{aligned}P_{out} &= \Pr[|\mathcal{D}_1| = 0] \\ &\quad + \sum_{m=2}^{M-1} \Pr[|\mathcal{D}_m| = 0 \cap_{1 \le i < m} \{|\mathcal{D}_i| \neq 0\}] \\ &\quad + \Pr[I < R \cap_{1 \le i \le M-1} \{|\mathcal{D}_i| \neq 0\}] \qquad (4.1)\end{aligned}$$

where the second term in (4.1) denotes the probability that the decoding set after mth hop is empty with non-empty previous decoding sets through the route, the third term denotes the outage probability at the last hop with non-empty previous decoding sets through the route. We next analyze the probability of the three events in (4.1) one by one.

As mentioned above, we will derive the diversity order by investigating the outage behavior in the high SNR regime. Toward that end, we use the notation $\doteq$ to denote asymptotic equality in the large SNR limit with $A \doteq B$ meaning

$$\lim_{\mathrm{SNR}\to\infty} \frac{\log A}{\log \mathrm{SNR}} = \lim_{\mathrm{SNR}\to\infty} \frac{\log B}{\log \mathrm{SNR}}.$$

4.4.1 Probability of An Empty Decoding Set After The First Hop

The first term in (4.1) corresponds to the probability of having an empty decoding set after the first hop. The mutual information between source and jth relay in $\mathcal{R}_1$ at the first hop is

$$I_{sr_{j,1}} = \log(1 + |h_{sr_{j,1}}|^2 \mathrm{SNR})$$

where $1 \leq j \leq K_1$. To calculate the probability of a given decoding set $\Pr[\mathcal{D}_1]$, first let

$$b \triangleq \frac{2^R - 1}{\mathrm{SNR}}.$$

The probability that ith relay node is in $\mathcal{D}_1$ is

$$\begin{aligned}
\Pr[\mathbf{R}_{j,1} \in \mathcal{D}_1] &= \Pr[I_{sr_{j,1}} > R] \\
&= \Pr[|h_{sr_{j,1}}|^2 > b] \\
&= \int_b^{+\infty} \lambda_1 e^{-\lambda_1 x} dx \\
&= e^{-\frac{b}{\lambda_1}}.
\end{aligned}$$

Since each relay independently decodes the message, and since the channels

from source to each relay in $\mathcal{R}_1$ are independent, the probability of a particular decoding set is

$$\begin{aligned}\Pr[\mathcal{D}_1] &= \prod_{\mathbf{R}_{i,1}\notin\mathcal{D}_1}(1-e^{-\frac{b}{\lambda_1}})\prod_{\mathbf{R}_{i,1}\in\mathcal{D}_1}e^{-\frac{b}{\lambda_1}} \\ &\doteq (\frac{b}{\lambda_1})^{K_1-|\mathcal{D}_1|} \qquad (4.2)\end{aligned}$$

where (4.2) follows when SNR is high, $e^{-\frac{b}{\lambda_1}} \doteq 1$ and $1-e^{-\frac{b}{\lambda_1}} \doteq \frac{b}{\lambda_1}$; as such, only terms of b with the smallest exponent in the polynomial are kept. Thus we have

$$\Pr[|\mathcal{D}_1|=0] \doteq (\frac{b}{\lambda_1})^{K_1}. \qquad (4.3)$$

4.4.2 Probability of An Empty Decoding Set in Intermediate Hops

We first analyze the probability of an empty decoding set after the second hop, and then generalize the argument to subsequent hops up to before the final hop. Given a non-empty decoding set $\mathcal{D}_1$, let $p_{j,i}$ be the chosen pmf for random selection after the ith hop for the jth relay in the decoding set. Thus, after the first hop, the distribution for random relay selection is $p_{1,1}$, $p_{2,1}$, $\cdots$, $p_{|\mathcal{D}_1|,1}$, and the probability of a specific decoding set after the second hop conditioned on $\mathcal{D}_1$ is

$$\Pr[\mathcal{D}_2\big|\{\mathcal{D}_1\cap|\mathcal{D}_1|\neq 0\}] = \sum_{\mathbf{R}_{j,1}\in\mathcal{D}_1} p_{j,1}\Pr[\mathcal{D}_2|\mathbf{R}_{j,1}] \qquad (4.4)$$

where $\Pr[\mathcal{D}_2|\mathbf{R}_{j,1}]$ denotes the probability of $\mathcal{D}_2$ given the forwarding relay is $\mathbf{R}_{j,1}$. With the i.i.d. assumption for each fading coefficient in the second hop, for any $\mathbf{R}_{j,1}\in\mathcal{D}_1$, a similar argument as for the decoding set of $\mathcal{D}_1$ gives

$$\Pr[\mathcal{D}_2|\mathbf{R}_{j,1}] \doteq (\frac{b}{\lambda_2})^{K_2-|\mathcal{D}_2|}. \qquad (4.5)$$

Substituting (4.5) into (4.4), we have

$$\Pr[\mathcal{D}_2 \big| \{\mathcal{D}_1 \cap |\mathcal{D}_1| \neq 0\}] \doteq (\frac{b}{\lambda_2})^{K_2 - |\mathcal{D}_2|}.$$

Applying the total probability theorem, we have

$$\begin{aligned} \Pr[\mathcal{D}_2 \cap |\mathcal{D}_1| \neq 0] &= \sum_{|\mathcal{D}_1| \neq 0} \Pr[\mathcal{D}_2|\mathcal{D}_1]\Pr[\mathcal{D}_1] \qquad (4.6) \\ &\doteq (\frac{b}{\lambda_2})^{K_2 - |\mathcal{D}_2|} \sum_{|\mathcal{D}_1| \neq 0} \Pr[\mathcal{D}_1] \\ &= (\frac{b}{\lambda_2})^{K_2 - |\mathcal{D}_2|}(1 - P[|\mathcal{D}_1| = 0]) \\ &\doteq (\frac{b}{\lambda_2})^{K_2 - |\mathcal{D}_2|}(1 - (\frac{b}{\lambda_1})^{K_1}) \\ &\doteq (\frac{b}{\lambda_2})^{K_2 - |\mathcal{D}_2|} \qquad (4.7) \end{aligned}$$

where the summation in (4.6) is over all possible decoding sets whose cardinality is non-zero at the first hop. We see from (4.7) that as long as $\mathcal{D}_1$ is not empty, with the random selection, the probability of the decoding set after the second hop is not affected by the decoding set at the first hop. This makes intuitive sense because no matter which decoding relay is selected, the total number of fading links in the next hop only depends on the number of receiving relays K_2 in the second cluster, and the probability of $|\mathcal{D}_2|$ only depends on the links which are in deep fade. We next generalize the results to $2 < m \leq M - 1$. Once the relay is selected, the probability of the decoding set in the next hop does not depend on the selected relay or the decoding sets in the previous hops. Hence we can conclude that

$$\begin{aligned} \Pr[\mathcal{D}_m \cap_{1 \leq i < m} \{|\mathcal{D}_i| \neq 0\}] &= \Pr[\mathcal{D}_m \cap |\mathcal{D}_{m-1}| \neq 0] \\ &\doteq (\frac{b}{\lambda_m})^{K_m - |\mathcal{D}_m|} \qquad (4.8) \end{aligned}$$

where (4.8) follows very similar steps as (4.6) to (4.7). Correspondingly, the probability of an empty decoding set at the mth hop is

$$\Pr[|\mathcal{D}_m| = 0 \cap_{1\leq i<m} \{|\mathcal{D}_i| \neq 0\}] \doteq (\frac{b}{\lambda_m})^{K_m}. \tag{4.9}$$

4.4.3 Outage Probability at Destination

If one of the decoding sets $\mathcal{D}_{1,\ldots,M-1}$ is empty, the outage probability is 1 as there is no path for the message to flow to the destination. Conditioning on non-empty sets for the first $M-1$ hops, and assuming that the destination selects the relay with the largest instant channel gain at the last hop, the conditional outage probability for the last hop is

$$\begin{aligned}
& \Pr[I < R \big| \cap_{1\leq i\leq M-1}\mathcal{D}_i \cap_{1\leq i\leq M-1} \{|\mathcal{D}_i| \neq 0\}] \\
= \; & \Pr[\log(1 + \max_{\mathrm{R}_{j,M-1}\in\mathcal{D}_{M-1}} |h_{r_{j,M-1}d}|^2 \mathrm{SNR}) < R] \\
= \; & \Pr[\max_{\mathrm{R}_{j,M-1}\in\mathcal{D}_{M-1}} |h_{r_{j,M-1}d}|^2 < b] \\
= \; & \prod_{\mathrm{R}_{j,M-1}\in\mathcal{D}_{M-1}} \Pr[|h_{r_{j,M-1}d}|^2 < b] \\
\doteq \; & (\frac{b}{\lambda_M})^{|\mathcal{D}_{M-1}|}.
\end{aligned} \tag{4.10}$$

Thus we have

$$\begin{aligned}
& \Pr[I < R \cap_{1\le i\le M-1} \{|\mathcal{D}_i| \neq 0\}] \\
= & \sum \Pr[I < R|\mathcal{D}_1 \cdots \mathcal{D}_{M-1}]\Pr[\mathcal{D}_1 \cdots \mathcal{D}_{M-1}] && (4.11)\\
\doteq & \sum (\frac{b}{\lambda_M})^{|\mathcal{D}_{M-1}|} \prod_{m=1}^{M-1} (\frac{b}{\lambda_m})^{K_m - |\mathcal{D}_m|} && (4.12)\\
= & \sum (\frac{b}{\lambda_M})^{|\mathcal{D}_{M-1}|} (\frac{b}{\lambda_{M-1}})^{K_{M-1} - |\mathcal{D}_{M-1}|} \prod_{m=1}^{M-2} (\frac{b}{\lambda_m})^{K_m - |\mathcal{D}_m|} && (4.13)\\
\doteq & [(\frac{1}{\lambda_M} + \frac{1}{\lambda_{M-1}})^{K_{M-1}} - (\frac{1}{\lambda_{M-1}})^{K_{M-1}}] b^{K_{M-1}} && (4.14)
\end{aligned}$$

where the summations in (4.11), (4.12) and (4.13) are over all possible combinations of non-empty decoding sets from the first hop to the $(M-1)$th hop, i.e. the set where $\cap_{1\le i\le M-1}\{|\mathcal{D}_i| \neq 0\}$. Equation (4.14) comes from the fact that the summation is dominated by the terms where b has the smallest exponent, which occurs when $|\mathcal{D}_m| = K_m$ for $1 \le m < M-1$.

4.4.4 End-to-End Outage and Comparison

Substituting equations (4.3), (4.9) and (4.14) into (4.1), the total outage probability is

$$\begin{aligned}
P_{out} & \doteq \sum_{m=1}^{M-2} (\frac{b}{\lambda_m})^{K_m} + (\frac{1}{\lambda_{M-1}} + \frac{1}{\lambda_M})^{K_{M-1}} b^{K_{M-1}} \\
& \doteq b^{d_{BLAR}} \sum_{m:K_m = d_{BLAR}} \beta_m^{d_{BLAR}} && (4.15)
\end{aligned}$$

where we denote $\beta_m \triangleq \frac{1}{\lambda_m}$, $\beta_{M-1} \triangleq \frac{1}{\lambda_M} + \frac{1}{\lambda_{M-1}}$, the summation in (4.15) is over all the hops that have the smallest number of relays in the cluster, and

$$d_{BLAR} \triangleq \min_{m=1,\cdots,M-1} K_m. \qquad (4.16)$$

From (4.16), the achievable diversity order (i.e. the SNR exponent) is bottlenecked by the minimum number of available relays over all relay clusters. Comparing (4.15) with (4.9), the major outage event is the empty decoding set at hops where the number of available receiving relays is the minimum over all relay clusters.

In the case where all clusters have the same number of nodes, i.e. $K_m = K$ for all $1 \leq m \leq M-1$, we have

$$P_{out} \doteq \left(\sum_{m=1}^{M-2} \lambda_m^K + (\lambda_{M-1} + \lambda_M)^K \right) b^K. \tag{4.17}$$

Comparing (4.17) with the result in [58, equations (20), (21)], we see that our algorithm can achieve outage performance identical to AHR in the high SNR regime, even though we arbitrarily choose the forwarding relays for the first $M-1$ hops.The flexibility of being able to arbitrarily select any relay in the decoding set for the first $M-1$ hops allows us to additionally optimize an external routing objective, if desired. The AHR approach [58] does not permit such flexibility since it always chooses the decoding relay which has the best channel gain. In this case, our proposed method and the AHR approach attain the same diversity order and power gain. However, for the optimal routing, the result in [58, equations (13)] can be further written as $(\lambda_1^K + \lambda_M^K)b^K$ by using the asymptotic equality. Hence, the optimal routing has a power gain of is $10\left(\log_{10} \frac{\sum_{m=1}^{M-2} \lambda_m^K + (\lambda_{M-1}+\lambda_M)^K}{\lambda_1^K + \lambda_M^K}\right)$dB over the AHR approach and our proposed scheme in the high SNR regime.

In other works which have investigated diversity in cluster-based multi-hop networks [58–60], the term *full diversity* is often used to used to describe a routing method which attains a diversity order equal to K, i.e. the number of nodes in all clusters. When the number of nodes in each cluster differs, however, the notion of full diversity is quite different. To explore this effect, let us reconsider our cluster-

based model with the optimal routing algorithm that uses global CSI in a central controller to preselect the best route [58]. Using the cut-set bound, the outage of any multi-hop routing scheme can be lower bounded by

$$P_{out}^{opt} \dot{\geq} \mathrm{SNR}^{-\min_{0\leq m\leq M-1} K_m K_{m+1}} \tag{4.18}$$

where by definition $K_0 = K_M = 1$ [33]. On the other hand, when performing optimal routing to select the path with the best worst-case link, there are at least $\min_{0\leq m\leq M-1} K_m K_{m+1}$ distinct bottleneck links in $\prod_{i=1,\cdots,M-1} K_i$ possible paths from source to relay. From equation [58, Lemma 2], the outage of optimal routing with different cluster sizes can be upper bounded by

$$P_{out}^{opt} \dot{\leq} \mathrm{SNR}^{-\min_{0\leq m\leq M-1} K_m K_{m+1}}. \tag{4.19}$$

Combining (4.18) and (4.19), we see that optimal routing can attain the maximum possible diversity order given by the cut-set bound and

$$d_{full} \triangleq \min_{0\leq m\leq M-1} K_m K_{m+1}. \tag{4.20}$$

While the authors in [58] claim that AHR attains full diversity, it can be shown that the AHR approach attains diversity order d_{BLAR}. This is further confirmed in the simulations that follow. The expressions in (4.16) and (4.20) show that the diversity order of BLAR is dominated by the diversity order of optimal routing, though we note that $d_{BLAR} = d_{full}$ in a wide variety of practical situations. For example, the BLAR and AHR schemes attain full diversity for any multi-hop system with fewer than 4 hops, which would result in full diversity $\min(K_1, K_2)$ for three hops and K_1 for two hops, as well as systems with a relatively even number of relays in each cluster.

4.5 Outage Analysis with Frequency Selective Fading

Next we extend our analysis to the case where the channels between different hops suffer FS fading. We assume at each hop all channels suffer the same FS fading as the nodes are clustered together. We use the vectors to represent FS fading channels. The channels in the first hop are denoted as $\boldsymbol{h}_{sr_{j,1}}$ with length L_1 and each tap is of variance λ_1 where $1 \leq j \leq K_1$; the channels in the mth $(2 \leq m \leq M-1)$ hops are denoted as $\boldsymbol{h}_{r_{j,m-1}r_{k,m}}$ with length L_m and each tap is of variance λ_m where $1 \leq j \leq K_{m-1}$ and $1 \leq k \leq K_m$; and the channels at the last hop are denoted as $\boldsymbol{h}_{r_{j,M-1}d}$ with length L_M and each tap is of variance λ_M where $1 \leq j \leq K_{M-1}$.

We continue to use the mutual information in the outage analysis. The mutual information between source and jth relay in $\mathcal{R}_1$ at the first hop is

$$I_{sr_{j,1}} = \log(1 + \|\boldsymbol{h}_{sr_{j,1}}\|^2 \text{SNR})$$

where $1 \leq j \leq K_1$. The probability that the ith relay node is in $\mathcal{D}_1$ is

$$\begin{aligned} \Pr[\mathbf{R}_{j,1} \in \mathcal{D}_1] &= \Pr[I_{sr_{j,1}} > R] \\ &= \Pr[\|\boldsymbol{h}_{sr_{j,1}}\|^2 > b] \\ &= \int_{\frac{b}{\lambda_1}}^{+\infty} \frac{x^{L_1-1}}{L_1!} e^{-x} dx \\ &= e^{-\frac{b}{\lambda_1}} \sum_{k=0}^{L_1-1} \frac{b^k}{\lambda_1^k k!} \end{aligned} \tag{4.21}$$

as $\frac{\|\boldsymbol{h}_{sr_{j,1}}\|^2}{\lambda_1/2}$ is chi-square distributed with L_1 degrees of freedom.

Similar to (4.2), we find that the probability of a particular decoding set is

$$\Pr[\mathcal{D}_1] \doteq (\frac{b}{\lambda_1})^{L_1(K_1 - |\mathcal{D}_1|)},$$

and

$$\begin{aligned}\Pr[\mathcal{D}_m \cap_{1\le i<m} \{|\mathcal{D}_i| \neq 0\}] &= \Pr[\mathcal{D}_m \cap |\mathcal{D}_{m-1}| \neq 0] \\ &\doteq (\frac{b}{\lambda_m})^{L_m(K_m-|\mathcal{D}_m|)}\end{aligned}$$

In the final hop, we assume that the destination selects the decoding relay with the largest sum-square of the relay-to-destination channel. Hence the conditional outage probability for the last hop is

$$\begin{aligned}&\Pr[I < R \big| \cap_{1\le i\le M-1}\mathcal{D}_i \cap_{1\le i\le M-1} \{|\mathcal{D}_i| \neq 0\}] \\ \doteq\ & (\frac{b}{\lambda_M})^{L_M|\mathcal{D}_{M-1}|},\end{aligned}$$

and

$$\begin{aligned}&\Pr[I < R \cap_{1\le i\le M-1} \{|\mathcal{D}_i| \neq 0\}] \\ \doteq\ & [((\frac{b}{\lambda_M})^{L_M} + (\frac{b}{\lambda_{M-1}})^{L_{M-1}})^{K_{M-1}} - (\frac{b}{\lambda_{M-1}})^{K_{M-1}L_{M-1}}].\end{aligned}$$

The end-to-end outage probability is

$$\begin{aligned}P_{out} &\doteq \sum_{m=1}^{M-2}(\lambda_m b)^{K_m L_m} + \left((\frac{b}{\lambda_M})^{L_M} + (\frac{b}{\lambda_{M-1}})^{L_{M-1}}\right)^{K_{M-1}} \\ &\doteq b^{d_{BLAR,FS}}\end{aligned}$$

where

$$d_{BLAR,FS} = \min(\min_{m=1,\cdots,M-1} K_m L_m, K_{M-1}L_M). \tag{4.22}$$

As for ad-hoc routing, we apply the similar results in (4.21) and use [58, equation (20)] to calculate the end-to-end outage probability where the outage probability in each of the first $M-2$ hops is the probability of a null decoding set. We conclude that the maximal diversity can be achieved by ad-hoc routing is equal to $d_{BLAR,FS}$.

We next derive the full diversity that achieved by optimal routing in the presence of FS fading. Using the cut-set bound, we find that the outage of any routing scheme can be lower bounded by

$$P_{out,FS}^{opt} \dot{\leq} \mathrm{SNR}^{-\min_{0\leq m\leq M-1} K_m K_{m+1} L_m}. \tag{4.23}$$

Since the optimal routing selects the path with the best worse-case link, we can divide the space $\boldsymbol{W}$, which contains all possible paths, into M subspace $\boldsymbol{W}_m$ where each space contains the path where the worse-case link is at the mth hop for $1 \leq m \leq M$. Denote the mutual information on the mth hop of path $\boldsymbol{v}$ as $I_{m,v}$ and v_{ind} as the index of path $\boldsymbol{v}$ in the whole space $\boldsymbol{W}$. Then the end-to-end outage probability can be written as

$$\begin{aligned} P_{out,FS}^{opt} &= \Pr[\max_{\boldsymbol{v}\in\boldsymbol{W}} \min_{m=1,\cdots,M} I_{m,v_{ind}} < R] \\ &\leq \sum_{m=1}^{M} \Pr[\max_{\boldsymbol{v}\in\boldsymbol{W}_m} \min_{m=1,\cdots,M} I_{m,v_{ind}} < R] \\ &\dot{\leq} \sum_{m=1}^{M} \mathrm{SNR}^{-K_m K_{m+1} L_m} \\ &\doteq \mathrm{SNR}^{-\min_{0\leq m\leq M-1} K_m K_{m+1} L_m} \end{aligned} \tag{4.24}$$

Combining (4.23) and (4.24), we can conclude that at presence of FS fading, the optima routing achieves diversity

$$d_{full,FS} = \min_{0\leq m\leq M-1} K_m K_{m+1} L_m. \tag{4.25}$$

Comparing (4.22) and (4.25), we find that the diversity order of BLAR is dominated by the diversity order of optimal routing. As in flat fading case, we note that $d_{BLAR,FS} = d_{full,FS}$ in some practical situations. However, in FS fading, not only the size of each cluster but also the number of fading taps in each hop

Table 4.1: Simulation scenarios.

Scenario	Hops (M)	Nodes per cluster	d_{BLAR}	d_{full}
1	6	$K_1 = 5$, $K_2 = 3$, $K_3 = K_4 = 2$, $K_5 = 6$	2	4
2	10	$K_i = 3, 1 \leq i \leq 9$	3	3
3	4	$K_i = 3, 1 \leq i \leq 3$	3	3
4	3	$K_1 = K_2 = 3$	3	3
5	4	$K_1 = 3$, $K_2 = 2$, $K_3 = 3$	2	3
6	3	$K_1 = 2$, $K_2 = 3$	2	2
7	4	$K_1 = 8$, $K_2 = 6$, $K_3 = 8$	6	8

influence the result. For example, the BLAR and AHR schemes attain full diversity for any multi-hop system with fewer than 4 hops and the number of fading taps in the intermediate hops is no less than that of the first or last hop.

4.6 Numerical Results

We now present numerical performance results to validate the analysis in Section 4.4 and Section 4.5. We first present the results in the presence of flat fading. In Table 4.1, 7 simulation scenarios are listed where the d_{BLAR} column shows the achievable diversity by the BLAR and AHR methods, while the d_{full} column shows the full diversity achievable by optimal routing.

The curves in Fig. 4.2 show the outage performance of the three routing methods in scenarios 1 through 3. For BLAR routing, we employ a random approach for the arbitrary selection where all decoding nodes are equally likely to be selected.

The diversity is represented by the negative slope of outage probability curve in Fig. 4.2. As expected, optimal routing has a larger diversity than the other two methods in scenario 1 while in scenario 2 and 3 the three have the same diversity. The outage performance of AHR and BLAR routing are almost the same for all scenarios 1 through 3. This agrees with our analysis that relay selection without channel knowledge in all but the last hop does not affect the achievable diversity. Thus with no diversity penalty, the proposed BLAR algorithm offers the flexibility of incorporating an additional routing objective in the first $M-1$ hops.

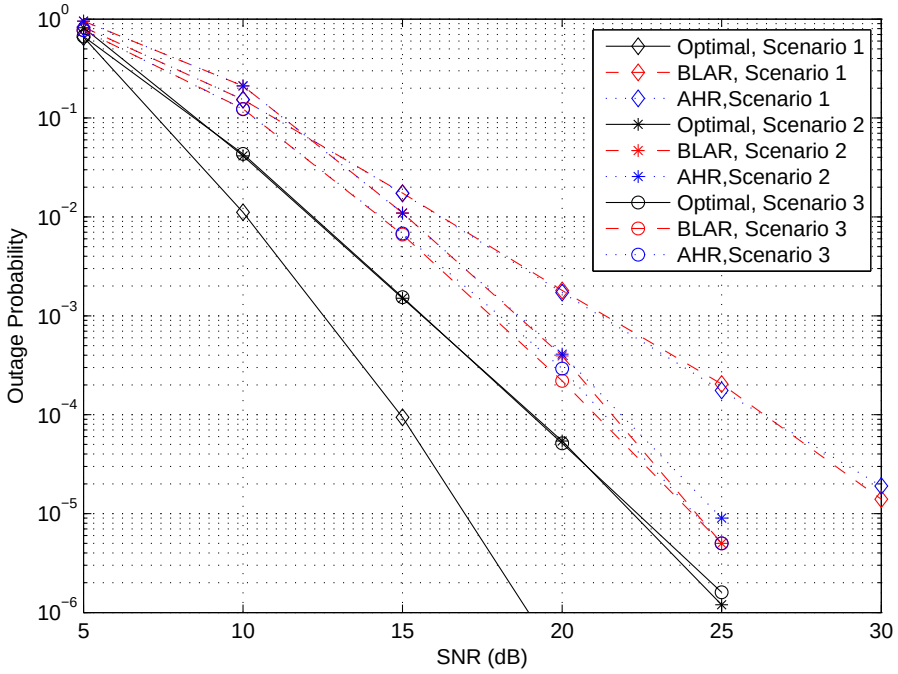

Figure 4.2: Outage comparison of optimal routing, BLAR and AHR, $R = 2$ bits/s/Hz, and $\lambda_{r_m} = 1$ for all $1 \leq m \leq M$.

We next consider the last three scenarios listed in Table 4.1 to show that the arbitrary relay selection in the first $M-1$ hops does not affect outage performance. The curves in Fig. 4.3 show the outage performance of BLAR algorithm with three implementations for arbitrary relay selection. The first implementation is to select

one of the decoding relays with uniform distribution in the first $M-1$ hops. The second implementation is to maximize the network lifetime. As only one source-destination pair is considered in this chapter, even use of each relay in the first $M-1$ clusters will help achieve this objective [63]. Thus we assume each relay in the first $M-1$ clusters has a counter to record the times that it has forwarded for the source-destination transmission. In each cluster, the decoding relay with the smallest counter number will be the actual forwarding relay. The third implementation is to minimize the routing latency where each decoding relay in the first $M-1$ clusters waits for a random duration uniformly distributed between 0 and the maximum waiting time and the one waiting for the least time in each cluster is chosen as the actual forwarding relay. Both the second and third relay selection implementations result in outage performance that is almost the same as the one with a uniform distribution, which shows that arbitrary relay selection in the first $M-1$ hops does not affect the diversity.

We use Scenario 7 as an example of high diversity order and to study the effect on outage probability of the distance between clusters. In this case, we assume that the distance between the source and the destination equals 4 unit lengths and the relay clusters are located along the line between the source and the destination. The numerical examples for the distance between clusters are shown in Table 4.2 where d_m is the distance between the $m-1$th cluster and its next cluster and the mean channel strength is determined as $\lambda_m = d_m^{-3}$. We first focus on the outage performance where $\lambda_m = 1$ for all $1 \leq m \leq 4$, which is shown in Fig. 4.4 for $R = 2$ bit/s/Hz and in Fig. 4.5 for $R = 4$ bit/s/Hz with the legend "Example 1". Both outage performances are very similar, except that there exists a power gain approximately equal to 7dB for $R = 2$ bit/s/Hz over $R = 4$ bit/s/Hz. At finite

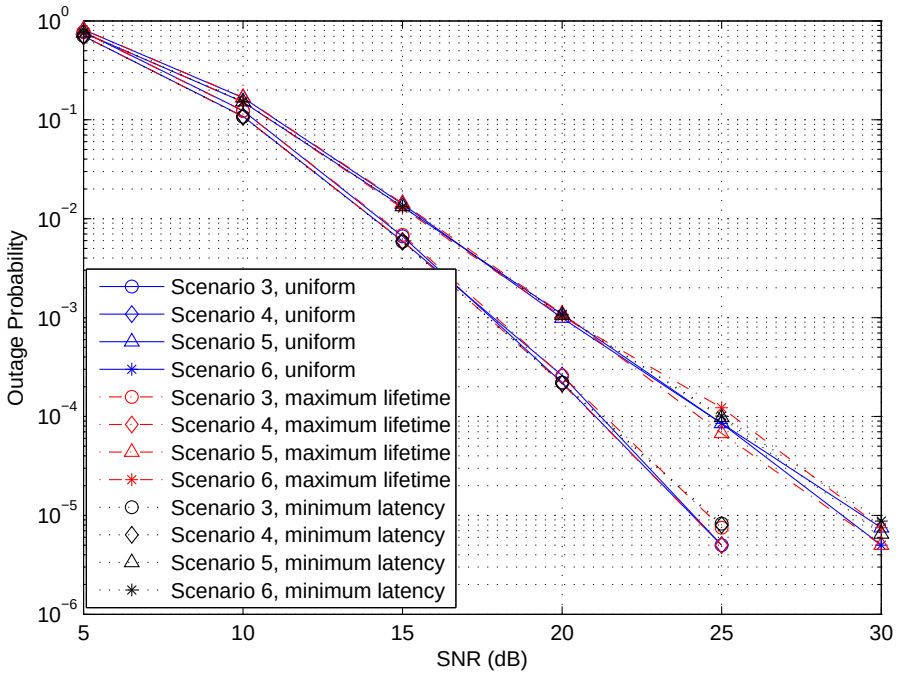

Figure 4.3: Outage comparison of three implementations for arbitrary relay selection, $R = 2$ bits/s/Hz, and $\lambda_{r_m} = 1$ for all $1 \leq m \leq M$.

SNR regime, with increased number of relays in each cluster, the full diversity does not show up and the diversity benefit of the optimal routing over the AHR and BLAR routing is diminishing. We next study the effect on outage probability of the distance between clusters. For the AHR and BLAR routing, even placement of clusters (Example 1) results in a power gain when compared to uneven placement of clusters (Example 2 and 3). However, for optimal routing, the effect of uneven placement of clusters is more complicated. As shown in [58, equations (13)], the power gain of the optimal routing is only closely related to λ_1 and λ_M where $M = 4$ in this case. Compared to Example 1, the larger distance in the first hop and the last hop in Example 3 results in a lower power gain of the optimal routing. As Example 2 has a shorter distance in the first hop and the last hop, Example 2 has the smallest outage probability over the three examples and the outage curve

Table 4.2: Cluster distance examples for Scenario 7 (4 hops).

Example	Distance
1	$d_1 = d_2 = d_3 = d_4 = 1$
2	$d_1 = d_4 = 0.5$, $d_2 = d_3 = 1.5$
3	$d_1 = d_4 = 1.5$, $d_2 = d_3 = 0.5$

of Example 2 goes eventually under that of Example 1. Compared to the outage curve of Example 1 and Example 3, the outage curve of Example 2 has a much steeper slope, which means a higher diversity at the shown SNR regime. This can be explained as the result of a shorter distance: the shorter the distance in the first hop and the last hop, the higher λ_1 and λ_M, the lower the SNR regime where the full diversity shows up. This also explains why in Example 3 the diversity order of optimal routing is almost equal to that of the AHR and BLAR routing.

We next present the simulation results for the cases with FS fading. In Table 4.3, simulation scenarios are listed with different frequency diversity at each hop and each fading tap in each channel at each hop suffers is i.i.d. Rayleigh fading with variance 1. In the table, the $d_{BLAR,FS}$ column shows the achievable diversity by the BLAR and AHR methods, while the $d_{full,FS}$ column shows the full diversity achievable by optimal routing. For both scenarios, we assume the size per cluster is as $K_1 = 3$, $K_2 = 2$, $K_3 = 4$.

The curves in Fig. 4.6 show the outage performance of the three routing methods in scenarios 1 and 2. For BLAR routing, we employ a random approach for the arbitrary selection where all decoding nodes are equally likely to be selected. The diversity is represented by the negative slope of outage probability curve in

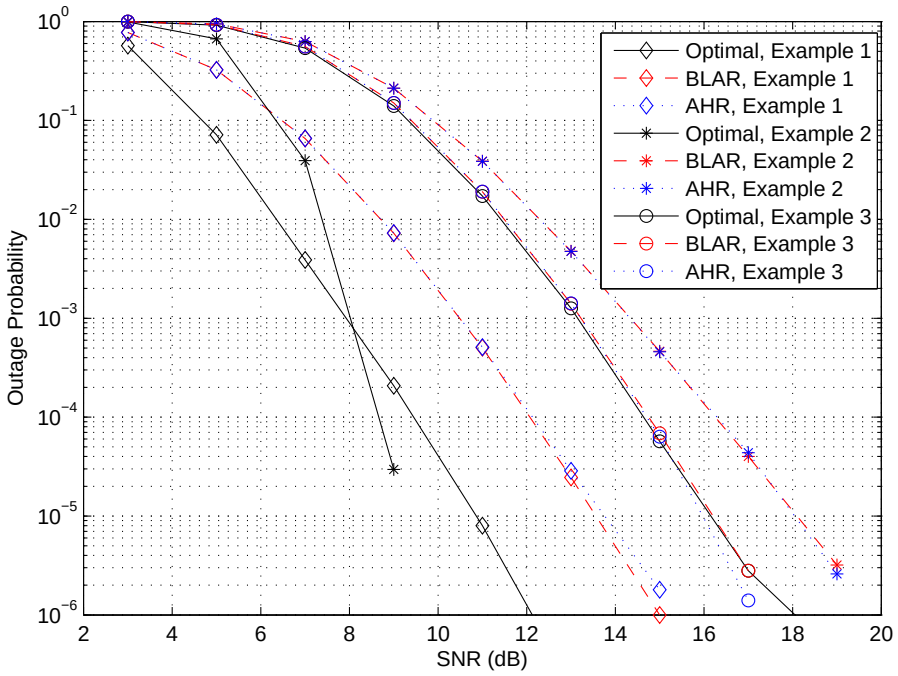

Figure 4.4: Outage comparison of optimal routing, BLAR and AHR for Scenario 7, $R = 2$bits/s/Hz and $\lambda_{r_m} = d_m^{-3}$ for all $1 \leq m \leq M$.

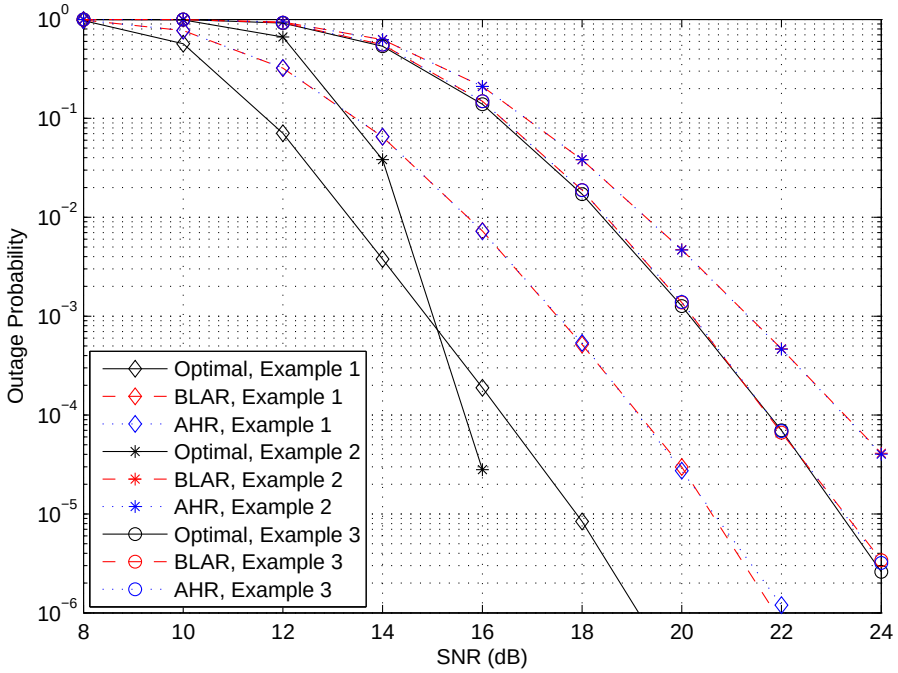

Figure 4.5: Outage comparison of optimal routing, BLAR and AHR for Scenario 7, $R = 4$ bits/s/Hz. and $\lambda_{r_m} = d_m^{-3}$ for all $1 \leq m \leq M$.

Table 4.3: Simulation scenarios for frequency selective fading.

Scenario	Hops (M)	Channel length per hop	$d_{BLAR,FS}$	$d_{full,FS}$
1	4	$L_1 = 3$, $L_2 = 2$, $L_3 = 2$, $L_4 = 2$,	4	8
2	4	$L_1 = 3$, $L_2 = 1$, $L_3 = 2$, $L_4 = 2$	2	6

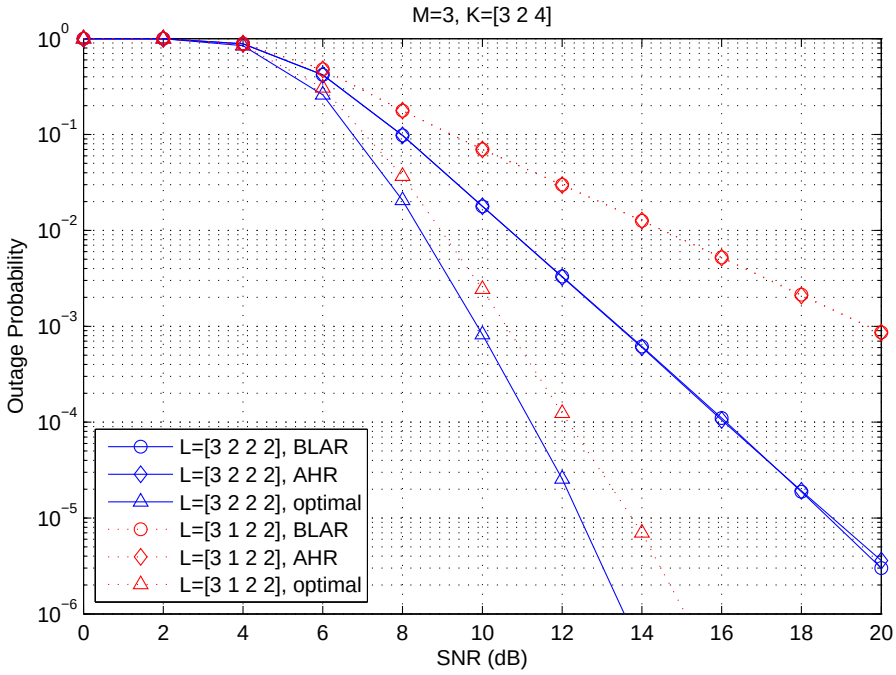

Figure 4.6: Outage comparison of optimal routing, BLAR and AHR with presence of frequency selective fading, $R = 2$ bits/s/Hz.

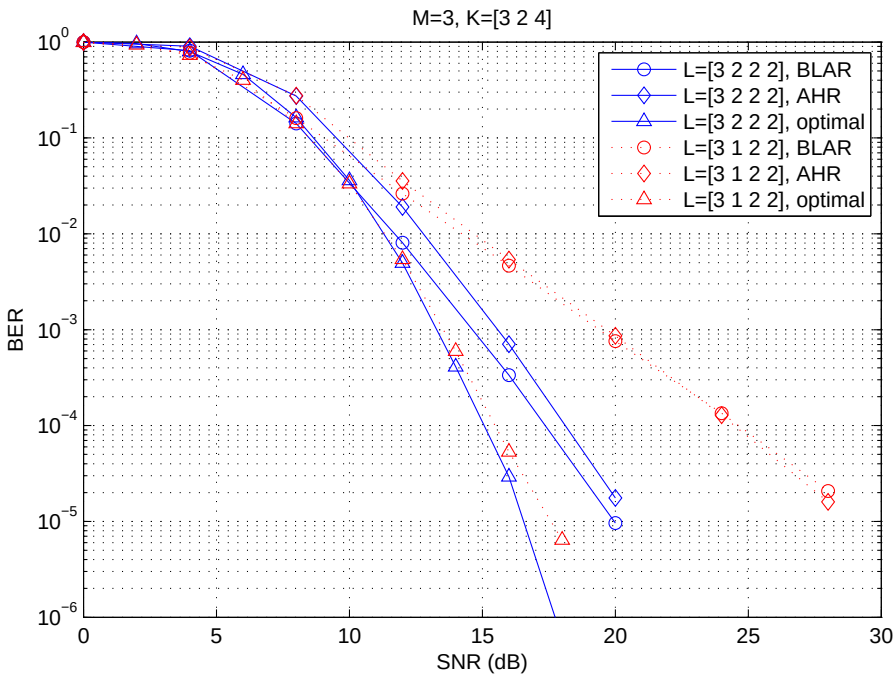

Figure 4.7: BER comparison of optimal routing, BLAR and AHR with presence of frequency selective fading and MMSE-DFE , $R = 2$ bits/s/Hz.

Fig. 4.6. As expected, optimal routing has a larger diversity than the other two methods in both scenarios. The outage performance of AHR and that of BLAR routing are almost the same. This agrees with our analysis that relay selection without channel knowledge in all but the last hop does not affect the achievable diversity. Thus, compared to AHR, the proposed BLAR algorithm offers the flexibility of incorporating an additional routing objective in the first $M-1$ hops with no diversity penalty.

We further compare the BER performance of different routing algorithms for scenarios 1 and 2 shown in Table 4.3. We note that the BER analysis can be done for routing algorithms by extending the analysis in Section 2.4.2 and 2.4.3 in the similar way as in Section 4.4. We skip this analysis and conclude that with zero-

padded transmission and linear ZFE or ZF-DFE at each receiver, the diversity order shown by outage analysis with the MFB assumption can be achieved by each routing algorithm. As the MMSE-DFE outperforms linear ZFE, the routing algorithm with MMSE-DFE at the receiver of each node should attain the same diversity as the same routing algorithm with linear ZFE. Fig. 4.7 shows the BER performance when the receiver at each node uses MMSE-DFE. As expected, BLAR routing achieves the same diversity order as AHR routing.

4.7 Conclusion

In this chapter, we proposed an opportunistic routing algorithm for clustered multi-hop networks which arbitrarily selects a decoding relay in the first $M-1$ hops, and only requires channel state information for selection in the final hop. This algorithm is shown to achieve the same outage performance as *ad-hoc* routing [58], and additionally achieves the maximum diversity offered by the channel for a variety of network cluster topologies. In fact, the proposed algorithm can attain the same diversity offered by an optimal scheme which requires global CSI and performs an exhaustive search over all possible routes. Furthermore, the proposed algorithm is very simple, and has the flexibility of supporting additional, higher-layer routing objectives without any loss in diversity. This algorithm has implications for the design of future multi-hop networks, as it demonstrates that full diversity can be achieved without full channel state information. Future work in the area could incorporate the issue of network flows, and include multiple sources and destinations as well as the effect of interference from other transmissions.

Chapter 5

Adaptive Channel Estimation in Decode and Forward Relay Networks

In wireless communications, channels vary with time and frequency due to changes in the dynamic transmission environment or the mobility of the transmitter or receiver. Channel knowledge is very important for exploiting diversity in the system. This chapter considers the channel estimation problem in relay networks. In particular, we consider estimating the relay-to-destination channel in decode-and-forward (DF) relay systems for which the presence of training data is probabilistic since it is unknown whether the relay participates in the forwarding round. To reduce the forwarding delay, short block lengths are preferred, and adaptive estimation through multiple blocks is required. A new LMS algorithm is proposed which combines adaptation and detection, for which a proper threshold is set through maximizing a heuristic objective function to improve the convergence speed and reduce the estimation error.

5.1 Introduction

Cooperative relay networks have emerged as a powerful technique to combat multipath fading and increase energy efficiency [16]. To reap the benefits of cooperative diversity, accurate channel state information is required at the transmitter or receiver, or both. Much of the current literature assumes perfect channel information; however, channel estimation in relay systems is a practical challenge that must be addressed. Some pioneering works on relay channel estimation are [9, 10] for amplify-and-forward (AF) relay channels and [64] for decode-and-forward (DF) relay channels. These works assume quasi-static Rayleigh flat fading channels, which means that the channel remains constant within one block but varies independently from block to block. While the block fading assumption renders nice analytical results, it may not be applicable to practical situations. Under this assumption, the training in each block is assumed long enough for channel estimation. Since the training data usually comprises a relatively small proportion of the whole block, the total duration of one block could be very long. As each block is processed individually at the end of transmission for relaying, large delay results. To reduce the delay and computation, short block lengths are preferred, and the training data should be spread across each block. In this situation, training data is periodic for AF channel estimation [65]. However, the DF relay only forwards the signal it receives from the source when it can correctly decode the message (verified, for example, by using cyclic redundancy check). As such, the DF relay switches between forwarding and silence, so the presence of training data in each block for the relay-to-destination channel is therefore probabilistic. We aim to determine if the adaptive algorithm combining detection and LMS algorithm

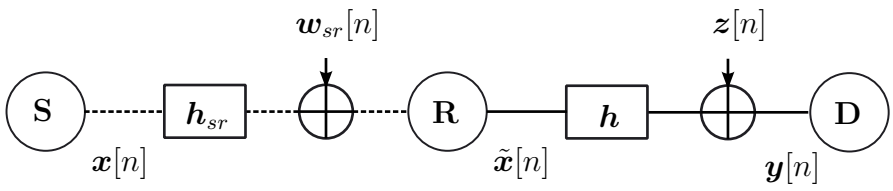

Figure 5.1: System model.

converges and what the average convergence rate is. We also study the impact of the detector threshold on convergence speed and estimation error.

5.2 System Model

We investigate a system as shown in Fig. 5.1, which consists of a source node (**S**), a relay node (**R**), and a destination node (**D**). We consider pilot-assisted estimation of the relay-to-destination channel $\boldsymbol{h}$, which is assumed to be static from block to block. The relay operates in half-duplex mode, and thus does not transmit and receive at the same time. In addition, the relay node and the source use the same transmission bandwidth but employ time division so that the relay transmits on a channel orthogonal to that the source transmits on. We assume that the transmitted symbol block from the source is $\boldsymbol{x}[n] \in \mathbb{C}^{N\times 1}$ where n is the block index. To have independent receiving blocks at the destination, we assume that transmission takes place with guard intervals. We do not put any assumption on the source-to-relay channel $\boldsymbol{h}_{sr}$ and the noise at the relay $\boldsymbol{w}_{sr}$ but assume the probability that the relay can correctly decode the message from the source is P. Without loss of generality, we assume that the length of $\boldsymbol{h}$ is larger than the length of $\boldsymbol{h}_{sr}$ and that the transmitter knows the length of the channel L_h and becomes silent for $L_h - 1$ symbol duration after it transmits $\boldsymbol{x}[n]$. Hence the input

to the relay-to-destination channel $\tilde{\boldsymbol{x}}[n]$ is probabilistic as $\Pr(\tilde{\boldsymbol{x}}[n] = \boldsymbol{x}[n]) = P$ and $\Pr(\tilde{\boldsymbol{x}}[n] = \boldsymbol{0}) = 1 - P$. The corresponding output $\boldsymbol{y}[n]$ is also probabilistic as

$$\Pr(\boldsymbol{y}[n] = \boldsymbol{X}[n]\boldsymbol{h} + \boldsymbol{z}[n]) = P$$

and

$$\Pr(\boldsymbol{y}[n] = \boldsymbol{z}[n]) = 1 - P$$

where $\boldsymbol{z}[n] \sim \mathcal{N}(0, \sigma^2 \boldsymbol{I}_{N+L_h-1})$ is i.i.d. noise, and $\boldsymbol{X}[n] \in \mathbb{C}^{(N+L_h-1)\times L_h}$ is a tall Tœplitz matrix with $X_{i,j}[n] = x_{i-j}[n]$. The transmission of a complete message is divided into two phases:

1. In phase one, the source broadcasts the message to the destination and the relay. The relay attempts to decode the message.

2. In phase two, the source is silent. If the relay can successfully decoded the message, it forwards the message to the destination. Otherwise, it remains silent.

The source and relay then alternate between these two phases. As shown in Fig. 5.2, the relay does not participate in the second phase of the second block, and the destination receives the composite signal corrupted by intersymbol interference and additive noise, but not by the interblock interference.

5.3 Combining Detection and Adaptation

In this section, we propose an adaptive algorithm to estimate the relay-to-destination channel. The algorithm is based on the LMS algorithm and combines detection

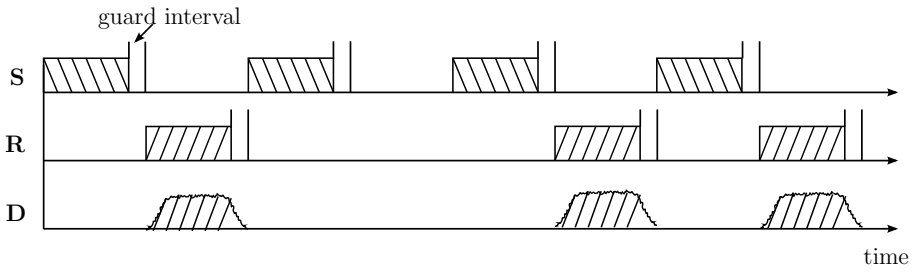

Figure 5.2: Transmission process.

and adaptation so that the adaptation happens only when the detector determines there is training data in the received signal. We develop the condition of convergence in the mean square. We emphasize that the updating proceeds in a block-by-block fashion, as the blocks are made mutually independent by transmission with guard intervals, which is useful for detection of the presence of training and is sometimes referred to as the "Periodic LMS algorithm" [66]. An alternative could be updating channel estimate in a symbol-by-symbol fashion. However, due to the guard-interval, the input process is not stationary but cyclostationary, and subsequently the convergence analysis for symbol-by-symbol updating LMS algorithm is complicated and more onerous [67].

Because of the probabilistic transmission, the receiver needs to decide whether it should use the observation to update the channel estimate. Mathematically, the detector is used to make a decision between the following two hypotheses

$$\begin{aligned} \mathcal{H}_0 \quad &: \qquad \boldsymbol{y}[n] = \boldsymbol{z}[n] \\ \mathcal{H}_1 \quad &: \quad \boldsymbol{y}[n] = \boldsymbol{X}[n]\boldsymbol{h} + \boldsymbol{z}[n]. \end{aligned} \tag{5.1}$$

As shown in Fig. 5.3, the observation used for updating is

$$\hat{\boldsymbol{y}}[n] = \begin{cases} \boldsymbol{y}[n] & \text{if } \mathcal{H}_1 \text{ is decided} \\ \boldsymbol{0} & \text{otherwise,} \end{cases}$$

and the input to the channel estimate $\hat{\boldsymbol{h}}[n]$ at time n is

$$\hat{\boldsymbol{x}}[n] = \begin{cases} \boldsymbol{x}[n] & \text{if } \mathcal{H}_1 \text{ is decided} \\ \mathbf{0} & \text{otherwise.} \end{cases}$$

The LMS update equation is

$$\hat{\boldsymbol{h}}[n+1] = \hat{\boldsymbol{h}}[n] + \mu \hat{\boldsymbol{X}}^H[n](\hat{\boldsymbol{y}}[n] - \boldsymbol{d}[n]) \tag{5.2}$$

where μ is the stepsize, $\boldsymbol{d}[n] = \hat{\boldsymbol{X}}[n]\hat{\boldsymbol{h}}[n]$ is the filtered output. The estimation error is defined as $\boldsymbol{e}[n] = \hat{\boldsymbol{y}}[n] - \boldsymbol{d}[n]$. If $\mathcal{H}_0$ is decided, the channel estimate remains unchanged since adaptation does not take place.

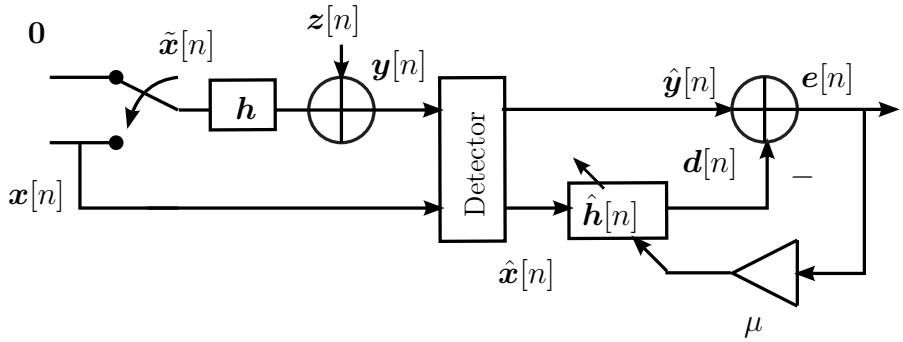

Figure 5.3: Block diagram of LMS-based adaptive algorithm.

The hypothesis testing problem defined in (5.1) is a composite hypothesis testing problem. Before we proceed with specific the detector, we use an abstract detector to analyze the algorithm. We defined an abstract detector with $\Pr(\mathcal{H}_i|\mathcal{H}_j)$ as the probability of deciding $\mathcal{H}_i$ when $\mathcal{H}_j$ is true. Hence the probability of detection is $P_D = \Pr(\mathcal{H}_1|\mathcal{H}_1)$ and the probability of false alarm is $P_{FA} = \Pr(\mathcal{H}_1|\mathcal{H}_0)$. Thus the probability that the detector decides $\mathcal{H}_1$ is

$$P_u = PP_D + (1-P)P_{FA}. \tag{5.3}$$

Then we have $\Pr(\hat{\boldsymbol{x}}[n] = \boldsymbol{x}[n]) = P_u$, and $\Pr(\hat{\boldsymbol{x}}[n] = \mathbf{0}) = 1 - P_u$.

We focus on the update behavior of the algorithm and define the mean squared error (MSE) as

$$\begin{aligned} J[n] &= E[\|\boldsymbol{e}[n]\|^2] = E[\|\hat{\boldsymbol{y}}[n] - \boldsymbol{d}[n]\|^2] \\ &= E[\|\boldsymbol{X}[n]\boldsymbol{h} + \boldsymbol{z}[n] - \boldsymbol{X}[n]\hat{\boldsymbol{h}}[n]\|^2]P_s \\ &+ E[\|\boldsymbol{z}[n] - \boldsymbol{X}[n]\hat{\boldsymbol{h}}[n]\|^2](1 - P_s) \end{aligned} \tag{5.4}$$

where

$$P_s = \frac{PP_D}{P_u} \tag{5.5}$$

is the probability that the receiver correctly uses the received signal when updating the channel estimate, and the first item in (5.4) is the mean square error when a detection occurs and the second item in (5.4) is the mean square error when a false alarm occurs. Taking the derivative of $J[n]$ with respect to $\hat{\boldsymbol{h}}[n]$ and setting it to zero, the Weiner solution $\boldsymbol{h}_o$ which minimizes the mean squared error $J[n]$ is given by

$$\boldsymbol{h}_o = P_s\boldsymbol{h}.$$

It should be noted that the Weiner solution is a scaled version of the true channel. The minimum mean squared error is

$$J_{\min} = (N + L_h - 1)\sigma^2 + P_s(1 - P_s)\boldsymbol{h}^H\boldsymbol{K}_x\boldsymbol{h}$$

where $\boldsymbol{K}_x = E[\boldsymbol{X}^H[n]\boldsymbol{X}[n]]$ is the autocorrelation matrix of the Tœplitz matrix of the training data. We note that the minimum mean squared error $J_{\min}$ achieves its minimum at both $P_s = 0$ and $P_s = 1$. This situation arises from the nature of this channel estimation problem. Because of the probabilistic transmission of the training data, the observation at the receiver may be just noise, from which the channel estimate is $\mathbf{0}$. Naturally we want P_s as large as possible, so a proper

alternative formulation could be to the minimize J with the constraint $P_s > 1/2$. The reason for requiring $P_s > 1/2$ is that we want the LMS channel estimate to be updated more by the observations with training data than by the noise. As P_s is only related to the detector, we leave this problem for the next section.

It is interesting to note that the cost function $J[n]$ in (5.4) in this case can be viewed as a weighted composition of two cost functions: one when the training data is always present, i.e., $\boldsymbol{y}[n] = \boldsymbol{X}[n]\boldsymbol{h} + \boldsymbol{z}[n]$, and other when only noise is present, i.e., $\boldsymbol{y}[n] = \boldsymbol{z}[n]$. Fig. 5.4 illustrates the situation. When the training data is always present, the Weiner solution $\boldsymbol{h}_o$ is equal to the true channel $\boldsymbol{h}$. On the other hand, when only noise is present, the Weiner solution is at the origin. It is not surprising then, that the minimum of the combined cost function is in between both solutions, being a scaled version of $\boldsymbol{h}$.

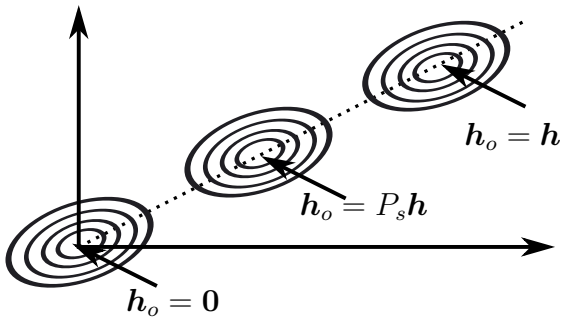

Figure 5.4: Cost functions.

5.3.1 Convergence Condition

For convergence analysis, we focus on the statistical behavior of the input random process $\hat{\boldsymbol{x}}[n]$ when an update happens, i.e., when $\mathcal{H}_1$ is decided. In this case, the input random process to this LMS-based block-updating algorithm with an ab-

stract detector is still stationary and the input correlation matrix is $\boldsymbol{K}_x$. Hence, according to the small-step-size statistical theory, the channel estimate $\hat{\boldsymbol{h}}[n]$ converges to $P_s\boldsymbol{h}$ in the mean squared sense and the ensemble-average learning curve of the block LMS filter can be proven to converge to some constant value, with the following condition on the step-size parameter:

$$0 < \mu < \frac{2}{\max \lambda_i}$$

where λ_i is the ith eigenvalue of $\boldsymbol{K}_x$.

5.3.2 Average Time Constant

The average time constant τ_{av}, which reflects the average convergence speed, was originally defined to fit to the geometric series where the unit of time lasts the duration of one iteration cycle [68]. As the overall update probability is P_u, to make one update happen, the average number of iteration is $1/P_u$, hence the unit of time for an update lasts $1/P_u$ times the duration of one iteration cycle. And the τ_{av} is chosen such that

$$(1 - \mu\lambda_{av})^{2/P_u} = \exp\left(-\frac{1}{\tau_{av}}\right)$$

where $\lambda_{av} = \frac{1}{L_h}\sum_{i=1}^{L_h} \lambda_i$. The average time constant can be further expressed as

$$\tau_{av} = \frac{-1}{2P_u \ln(1 - \mu\lambda_{av})}.$$

When the step-size μ is very small, i.e., $\mu \ll 1$, then τ_{av} can be approximated as

$$\tau_{av} \approx \frac{1}{2P_u\mu\lambda_{av}}. \tag{5.6}$$

Hence the higher P_u, which is the probability of deciding $\mathcal{H}_1$, the faster the convergence speed. If the orthogonal transmission between source and relay is taken into consideration, τ_{av} will be doubled.

5.4 Adaptation with Generalized Likelihood Ratio Test

In the previous section, we developed the general framework of applying LMS theory with an abstract detector to the situation where the presence of input training is probabilistic as described. It is generally known that there is no uniformly most powerful test for the composite hypothesis testing problem defined in (5.1). Hence we resort to the generalized likelihood ratio test (GLRT) [69] for the hypothesis testing problem and propose a heuristic approach for finding a "good" threshold which is used for hypothesis testing when the channel is unknown. Specifically, the hope is that the choice of threshold leads to improved convergence speed while minimizing estimation error. Without loss of generality, we assume that the training data at each block is the same, i.e., $\boldsymbol{x}[n] = \boldsymbol{x}$, and $\boldsymbol{X}$ is the tall Tœplitz matrix with $X_{i,j} = x_{i-j}$. The pdf of the observation $\boldsymbol{y}[n]$ under $\mathcal{H}_1$ is

$$p(\boldsymbol{y}[n]; \boldsymbol{h}, \mathcal{H}_1) = \frac{1}{(\pi\sigma^2)^{(N+L_h-1)}} \exp\left(-\frac{1}{\sigma^2}(\boldsymbol{y}[n] - \boldsymbol{X}\boldsymbol{h})^H(\boldsymbol{y}[n] - \boldsymbol{X}\boldsymbol{h})\right) \tag{5.7}$$

and under $\mathcal{H}_0$ is

$$p(\boldsymbol{y}[n]; \mathcal{H}_0) = \frac{1}{(\pi\sigma^2)^{(N+L_h-1)}} \exp\left(-\frac{1}{\sigma^2}\boldsymbol{y}^H[n]\boldsymbol{y}[n]\right).$$

5.4.1 Generalized Likelihood Ratio Test

The GLRT decides $\mathcal{H}_1$ if

$$\frac{p(\boldsymbol{y}[n];\tilde{\boldsymbol{h}},\mathcal{H}_1)}{p(\boldsymbol{y}[n];\mathcal{H}_0)} > \gamma$$

where γ is such that P_{FA} does not exceed some maximum value, $\tilde{\boldsymbol{h}} = (\boldsymbol{X}^H\boldsymbol{X})^{-1}\boldsymbol{X}^H\boldsymbol{y}$ is the maximum likelihood estimate of $\boldsymbol{h}$ under $\mathcal{H}_1$ and $p(\boldsymbol{y}[n];\tilde{\boldsymbol{h}},\mathcal{H}_1)$ is similarly defined as in (5.7) by replacing $\boldsymbol{h}$ with $\tilde{\boldsymbol{h}}$. It is equivalent to say that the GLRT decides $\mathcal{H}_1$ if

$$T[n] > \log\gamma$$

where

$$\begin{aligned} T[n] &= \frac{-\tilde{\boldsymbol{h}}^H\boldsymbol{X}^H\boldsymbol{X}\tilde{\boldsymbol{h}} + 2\mathrm{Re}(\tilde{\boldsymbol{h}}^H\boldsymbol{X}^H\boldsymbol{y}[n])}{\sigma^2} \\ &= \frac{\boldsymbol{u}^H[n]\boldsymbol{u}[n]}{\sigma^2} \end{aligned}$$

with $\boldsymbol{u}[n] = (\boldsymbol{X}^H\boldsymbol{X})^{-1/2}\boldsymbol{X}^H\boldsymbol{y}[n]$. When $\mathcal{H}_0$ is true, $\boldsymbol{u}[n] \sim \mathcal{CN}(0,\sigma^2\boldsymbol{I})$ and $T[n]$ is Gamma distributed, i.e., $T[n] \sim \Gamma(L_h,1)$. Define $P_{FA,\max}$ as the maximum probability of false alarm, i.e.,

$$\frac{1}{(L_h-1)!}\int_{\log\gamma}^{+\infty} t^{L_h-1}e^{-t}dt < P_{FA,\max}.$$

The threshold of $\log\gamma$ can be found by reversing the integration. When $\mathcal{H}_1$ is true, $\boldsymbol{u}[n] \sim \mathcal{CN}(\boldsymbol{X}\boldsymbol{h},\sigma^2\boldsymbol{I})$, and $2T[n]$ is non-central chi-squared distributed with $2L_h$ degrees of freedom and mean $2T_{half}$ where

$$T_{half} = \frac{(\boldsymbol{X}\boldsymbol{h})^H(\boldsymbol{X}\boldsymbol{h})}{\sigma^2}. \tag{5.8}$$

The analysis of the distribution of the test statistic T_{half} is further verified in Fig. 5.5. For the same training symbols at each block, we can calculate the theo-

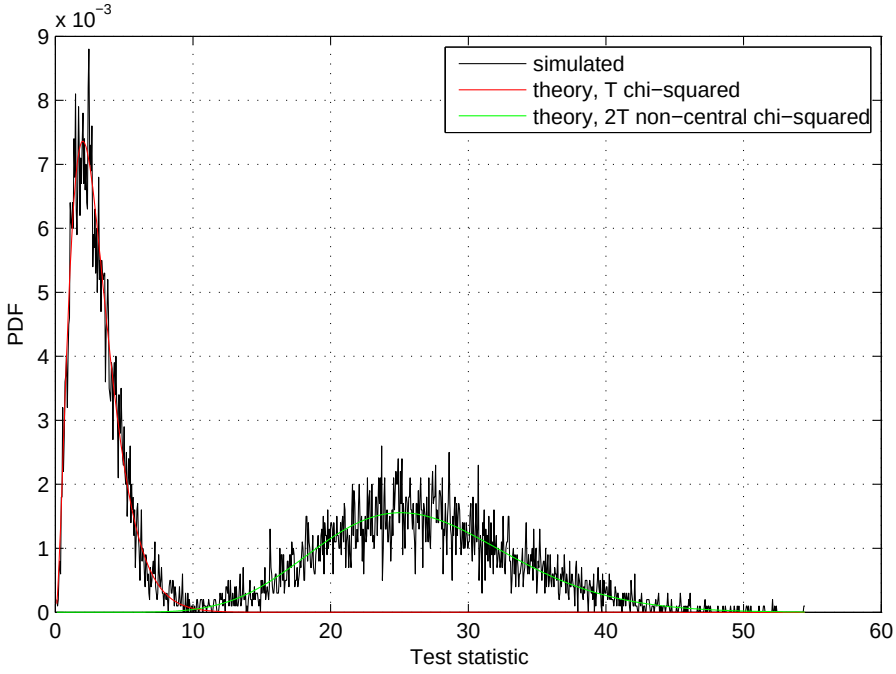

Figure 5.5: PDF of the test statistic T_{half} when $P = 0.5, N = 2$, normalized $\boldsymbol{h} = [0.5 + 1i \quad 4 + 3i \quad 0.75 + 2.7i]$, SNR $= 5dB$, and $\boldsymbol{x} = \frac{1}{\sqrt{2}}[-1 - 1i \quad 1 - 1i]$.

retical probability of detection (PD) by using the Marcum Q-function. As can be seen in Fig. 5.6, the simulated PD and theoretical PD agree with each other very well, as expected.

5.4.2 Finding the Proper Threshold $\log \gamma$

In this subsection, we assume there is no constraint on maximum probability of false alarm $P_{FA,\max}$ and consider finding the proper threshold $\log \gamma$ which can achieve a fast convergence rate given the same estimate performance. As previously mentioned, the Wiener solution for (5.4) is a scaled version of the actual channel $P_s\boldsymbol{h}$. To have an estimate of the true channel, either an estimate of P_s is required or an estimate of the channel gain, which is computed as the sum-square of the

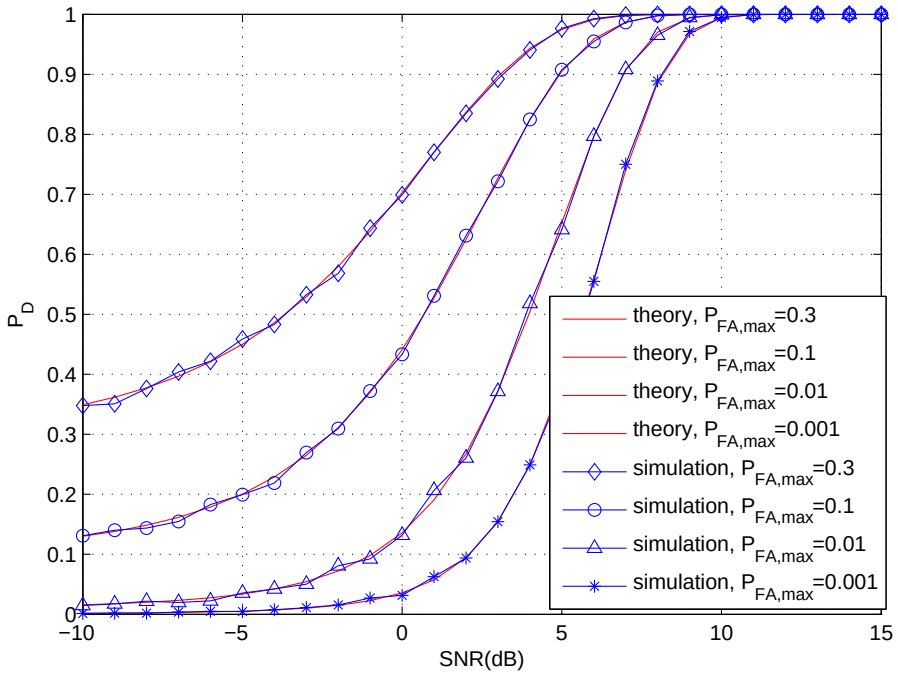

Figure 5.6: Probability of detection with parameters as in Fig. 5.5.

channel. We leave the accurate estimation of P_s or the estimation of the channel gain as separate problems and use the following performance metric [70]:

$$\xi(\boldsymbol{h}, \hat{\boldsymbol{h}}[n]) = E\left[\left\| \frac{\hat{\boldsymbol{h}}[n]}{\|\hat{\boldsymbol{h}}[n]\|} - \frac{\boldsymbol{h}}{\|\boldsymbol{h}\|} \right\|^2\right]. \tag{5.9}$$

This performance metric measures how close $\boldsymbol{h}[n]$ is to $\boldsymbol{h}$ in terms of the shape of the impulse response. For this performance metric, it makes intuitive sense that the larger P_s is, the smaller the minimum mean performance metric is.

On one hand, P_s determines where the update equation in (5.2) converges to and the estimation performance. On the other hand, as shown in (5.6), the convergence speed is dependent on P_u. Ideally for a fixed P, we want both P_s and P_u as large as possible. However, there are situations in which we cannot make both P_s and P_u as large as possible at the same time. As shown in Fig. 5.7, P_s is increasing with $\log\gamma$ and P_u is decreasing with $\log\gamma$. Hence an appropriate

threshold $\log \gamma$ should be chosen to balance the convergence speed and the accuracy of channel estimate.

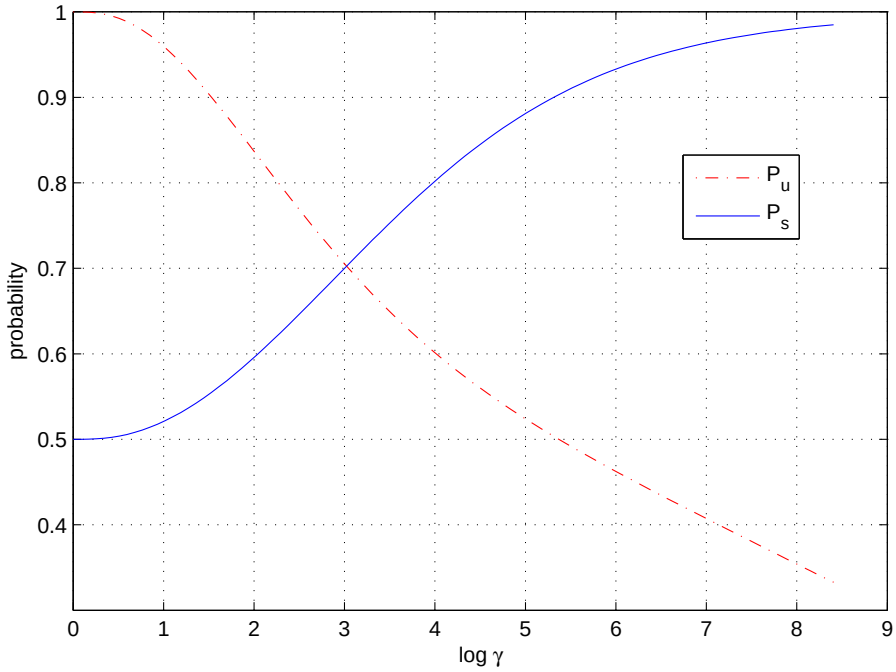

Figure 5.7: P_u and P_s with parameters as in Fig. 5.5.

As it is mathematically intractable to find the optimal threshold $\log \gamma$ in general, we need to find a proper function of P_u and P_s which reflects how the threshold affects the convergence speed and the estimation performance. Based on the intuition about P_u and P_s, we propose the following heuristic approach to finding a good threshold:

$$\arg \max_{\log \gamma \in [0,+\infty]} P_u(P_s - 0.5). \tag{5.10}$$

As P_u affects convergence speed and P_s affects the accuracy of channel estimate, the threshold which gives the maximum of the product of P_u and $P_s - 0.5$ attempts to achieve a balance. In the function to be maximized, i.e., $P_u(P_s - 0.5)$, we use a term containing $P_s - 0.5$ rather than just P_s for the following two reasons. First, by using $P_s - 0.5$, the threshold which results in $P_s < 0.5$ is eliminated as a choice since

P_u is never less than 0. Hence the condition $P_s > 0.5$ is automatically satisfied. Secondly, if we were to just use $P_u P_s$ as the heuristic, this would be equivalent to maximizing PP_D which can be made equal to P if P_D is 1. To make $P_D = 1$, we can always set the threshold 0, which is not necessarily a good choice at all situations.

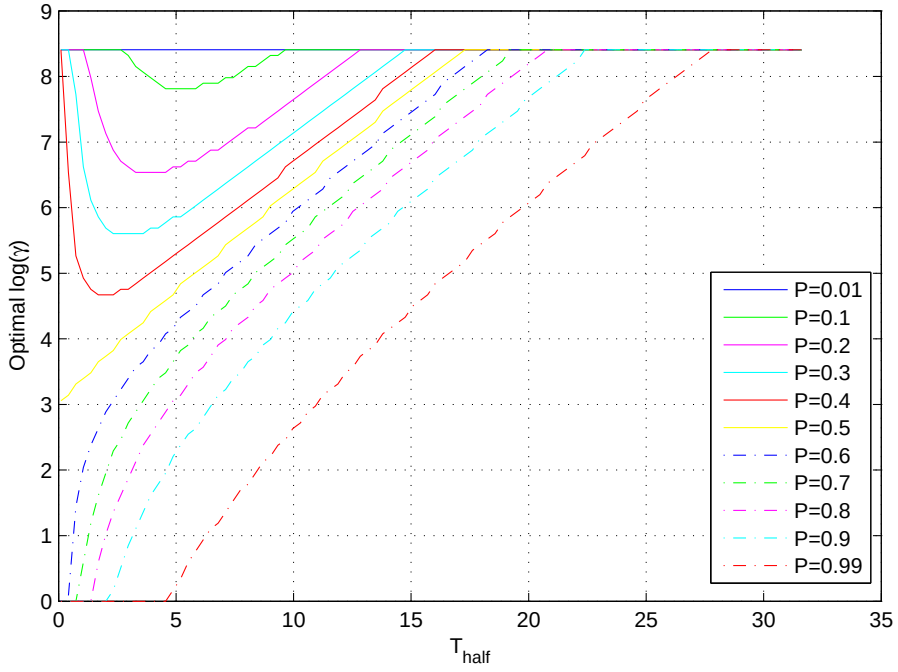

Figure 5.8: Simulated proper threshold $\log\gamma$ versus T_{half} with $L_h = 3$ for maximizing $P_u(P_s - 0.5)$.

As can be seen from distribution of T under different hypotheses, $P_D(P_s - 0.5)$ is only related to P, $\log\gamma$, L_h and T_{half}, which is originally defined in (5.8) and is half of the mean of $2T$ when $\mathcal{H}_1$ is true. Hence we plot in Fig. 5.8 the proper $\log\gamma$ versus T_{half} with different transmission probability P, where the proper $\log\gamma$ maximizes $P_u(P_s - 0.5)$. In calculating P_s, we use $P_{FA,\max}$ as for P_{FA} as an approximation. The plot makes intuitive sense: when P is small, e.g., $P = 0.01$, rather than setting a low threshold to make $P_D = 1$, a proper threshold should be large to also make the

$P_{FA,\max}$ small such that the updating is not primarily by noise; when P is large, for a small T_{half}, e.g., $P = 0.99$ and $T_{half} = 3$, we use the threshold $\log\gamma = 0$ which makes both $P_D = P_{FA\max} = 1$, as the proportion of updating by noise, $(1-P)P_{FA,\max}$, is very small. Another observation is that when T_{half} is large, no matter what the transmission probability is, the proper threshold is always high. Of course there are undoubtedly numerous other approaches of finding a "good" threshold; yet the proposed one shows a good performance as will be seen in the simulation of an extensive number of scenarios.

To calculate P_D for computing P_u and P_s, it requires the knowledge of T_{half}, which is generally unknown before the channel estimation. In the following, we use a function of the mean of T to estimate T_{half}. The mean of $T[n]$ can be calculated as $T_{mean} = E[T[n]] = PT_{half} + L_h$. Hence $T_{half} = (E[T[n]] - L_h)/P$. In the implementation of the LMS algorithm, we use a moving average to represent $E[T]$. Hence a heuristic adaptive algorithm for the channel estimation problem is as follows:

Step 1: Compute the proper $\log\gamma$ *for the known* P *according to (5.10) offline. Initialize the channel estimate* $\hat{\boldsymbol{h}}[0]$.

Step 2: Compute the estimate of $\hat{T}_{half}[n] = (\hat{T}_{mean}[n] - L_h)/P$ *where* $\hat{T}_{mean}[n] = (\hat{T}_{mean}[n-1](n-1) + T[n])/n$ *is the estimate of the mean of* $T[n]$.

Step 3: Find the proper $\log\gamma$ *for* $\hat{T}_{half}[n]$*; If* $T[n]$ *is greater than the found proper* $\log\gamma$*, the channel estimate* $\hat{\boldsymbol{h}}[n]$ *is updated by (5.2); otherwise, the channel estimate remains the same* $\hat{\boldsymbol{h}}[n] = \hat{\boldsymbol{h}}[n-1]$.

Step 4: Increase n *by* 1*. Check if* n *is greater the total number of training blocks. If yes, the algorithm stops; otherwise, go to Step 2.*

5.5 Numerical Results

In this section, we plot the error measure in (5.9) and we are primarily interested in the performance improvement of using the proper threshold for *GLRT*. For purpose of comparison, we define the *genie-aided* LMS algorithm, in which we assume that the receiver knows if the observation contains training. In this ideal case, the destination can perfectly detect whether training data exists or not, thus $P_D = 1$, $P_{FA} = 0$, and subsequently $P_u = P$ and $P_s = 1$. The Weiner solution for the *genie-aided* LMS algorithm is $\boldsymbol{h}$, which is exactly the true channel.

In the simulation, we specify the parameter T_{half} to aid comparison. We use the normalized $\boldsymbol{h} = [0.5 + 1i\ 4 + 3i\ 0.75 + 2.7i]$, $N = 2$, and the input training is $\boldsymbol{x} = \frac{1}{\sqrt{2}}[-1 - 1i \quad 1 - 1i]$, to calculate the noise covariance $\sigma^2 = \frac{(\boldsymbol{Xh})^H \boldsymbol{Xh}}{T_{half}}$. It should be noted that we can specify any combination of the block length N and the noise covariance σ^2 for a certain normalized channel to achieve the preset T_{half}. We compare the performance of the heuristic algorithm using the proper threshold with the performance of the adaptive algorithms with GLRT using the fixed threshold $\log\gamma = 0$ ($P_{FA,\max} = 1$) and $\log\gamma = 8.4059$ ($P_{FA,\max} = 0.01$). We consider transmission probabilities $P \in \{0.1, 0.5, 0.8, 0.99\}$. The performance is shown in Fig. 5.9 for $T_{half} = 2$, Fig. 5.10 for $T_{half} = 8$ and Fig. 5.11 for $T_{half} = 20$. With the increased transmission probability and increased T_{half}, the performance of the adaptive algorithm with the proper threshold becomes closer to the performance of the *genie-aided* algorithm. In Fig. 5.9 at a low $T_{half} = 2$, for low transmission probability, $P = 0.1$, the fixed threshold $\log\gamma = 8.4059$, gives better performance than the fixed threshold $\log\gamma = 0$ while for $P = 0.8$ and $P = 0.99$, the fixed threshold $\log\gamma = 0$ gives better performance than the fixed threshold $\log\gamma = 8.4059$. For

all these different transmission probabilities, the proper threshold always arrives at the threshold which gives better performance. For the 12 scenarios shown from Fig. 5.9 to Fig. 5.11, we see that to arrive at the same final estimation error, the heuristic algorithm with the proper threshold gives faster convergence speed than the algorithms with the fixed thresholds. This means that the proper threshold which maximizes $P_u(P_{FA} - 0.5)$ can improve the convergence speed.

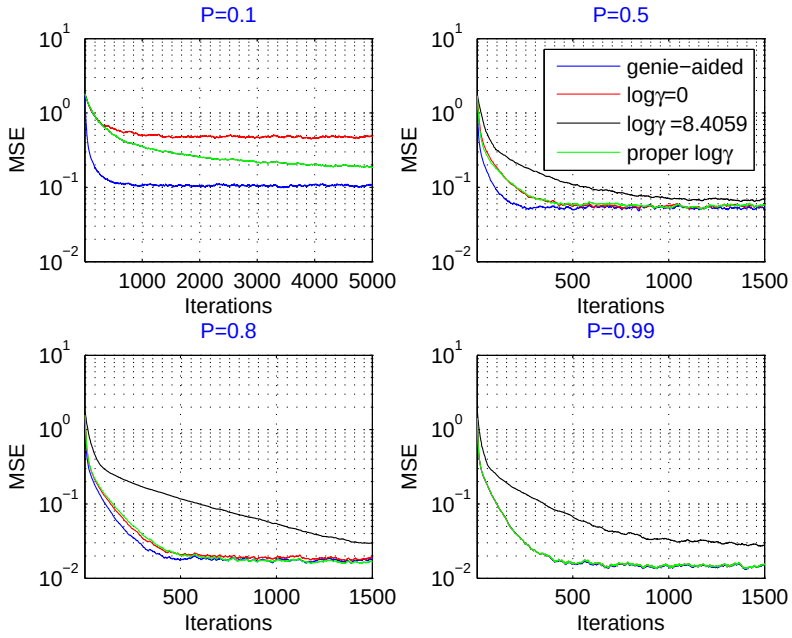

Figure 5.9: Mean error measure with $T_{half} = 2$ and different P.

5.6 Conclusion

A new adaptive algorithm is proposed for the relay-to-destination channel estimation in DF relay networks when the presence of an input training sequence is probabilistic as a Bernoulli random variable. The adaptive algorithm combines a detector and the classical LMS adaptation. For each observation, detection of

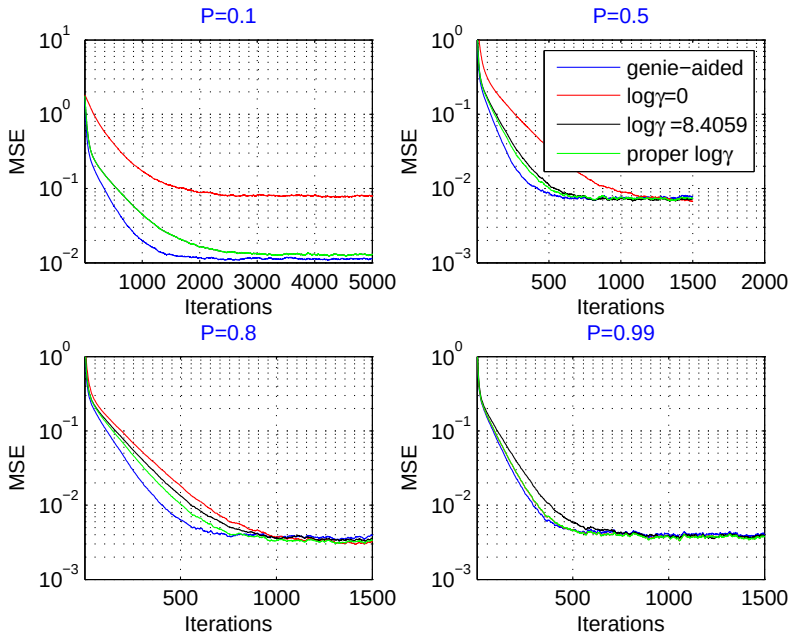

Figure 5.10: Mean error measure with $T_{half} = 8$ and different P.

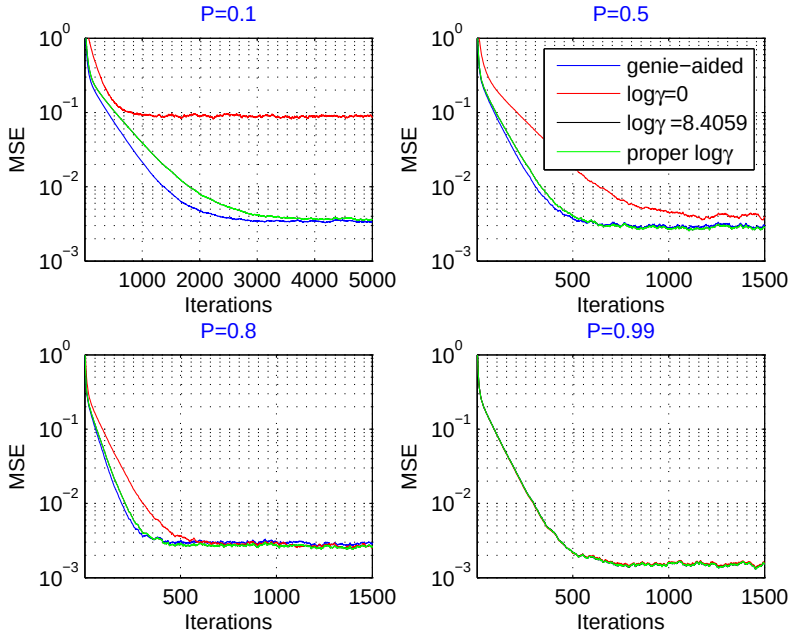

Figure 5.11: Mean error measure with $T_{half} = 20$ and different P.

the presence of input training is performed before updating, as the update only happens with a positive decision. The threshold which the detector uses to make a decision is critical to balance the convergence speed and estimation error. On one hand, a low threshold increases the probability of deciding the presence of input training and results in increased convergence speed. On the other hand, the estimation performance is only related to the portion of correctly deciding the presence of input training and might require a high threshold. Hence, a heuristic objective function is proposed to capture the balance of convergence speed and estimation error. The objective function consists of the probability that the relay is forwarding, the probability of false alarm and the probability of detection, which is estimated in turn by using a moving average of the test statistic. Numerical results show that by using the proper threshold which maximizes the proposed objective function, the adaptive algorithm has faster convergence speed than by using fixed thresholds.

Chapter 6

Conclusions and Future Work

6.1 Summary

Diversity techniques are effective methods to combat fading. The main focus of this dissertation was to exploit cooperative diversity or distributed spatial diversity provided by relays and frequency diversity (in the context of high data-rate communications, in which the underlying wireless channels suffer frequency selective (FS) fading) . As the majority of cooperative communication research focuses on flat fading, our results led to several novel and effective communication techniques. A brief summary of our work follows.

We studied the relay selection problem of a two-hop, multi-relay system in Chapter 2 and 3, where Chapter 2 assumes decode-and-forward (DF) relays and Chapter 3 assumes amplify-and-forward (AF) relays. We characterized the upper bound of diversity-multiplexing tradeoff (DMT) of the general system model without specifying the relay protocol or the cooperative scheme. This result is useful because it provides us with the best overall performance from such a system. For DF relay networks, we presented and analyzed three relay selection methods. These three relay selection methods require different channel state information (CSI), cause different overhead, and achieve different DMT or BER. Among the

three relay selection methods, the best relay selection requires most CSI, most overhead, and can achieve the upper bound of DMT of the system, while the other two can achieve this only in certain settings. With zero-padded transmission, the receivers at the relays and destination with different equalizers can asymptotically achieve the same DMT with the same relay selection methods. However, for AF relay networks, we find that there is no universal relay method that can achieve full diversity for different equalizers at the destination. We proposed two relay selection methods. The first relay selection method is based on the matched filter bound (MFB) and is shown to achieve the optimal DMT through outage analysis. With a receiver at the destination employing maximum-likelihood sequential estimation (MLSE), the relay selection can achieve full diversity, as corroborated by simulation. The second relay selection method works for a receiver at the destination employing linear zero-forcing equalization (ZFE) and can achieve the optimal DMT through BER analysis. However, it should be mentioned that the relay selection corresponding to linear ZFE, has a much higher complexity than the relay selection which can also achieve full diversity if MLSE is used.

In Chapter 4, we studied the relay selection problem of a multi-hop system where relays at each hop are clustered and employ DF protocol. We studied the effect of channel knowledge on the diversity by comparing three routing algorithms. The first algorithm is the optimal routing algorithm which assumes availability of global instantaneous channel state information (CSI) and performs a search over all possible routes at a central controller. The second algorithm is the *ad-hoc* routing algorithm which generates routes in a hop-by-hop fashion, always routing the next hop through the node with the largest channel gain. The last algorithm is our proposed algorithm which uses any decoding relays in the first few hops, and only

at the last hop routes through the node with the largest channel gain. We also extended the analysis of these algorithms from flat fading to FS fading. Though our algorithm has a diversity loss, which makes intuitive sense as it only requires channel state information in the final hop, we demonstrate through analysis and simulation that under certain conditions, on the cluster sizes and frequency diversity orders, our proposed routing algorithm attains the same full diversity as more complicated approaches that require full channel state information. In addition to exploiting the available diversity, our simple cross-layer algorithm has the flexibility to simultaneously satisfy an additional routing objective such as maximization of network lifetime.

In Chapter 5, we studied the channel estimation problem in the decode-and-forward channel. In particular, we focused on estimating the relay-to-destination channel coefficients because the probabilistic nature of the training data poses a challenge. We assumed small block lengths to meet the short delay constraints. We also assumed that the amount of training inside one block is not sufficient for the required estimation accuracy. We proposed a new adaptive algorithm which combines the least mean square (LMS) algorithm and a detector so that an LMS update is made only when the detector decides the presence of training data. In terms of the probability of false alarm and the probability of detection of the detector, we gave the expression of the average time constant which measures the convergence speed and the misadjustment which measures the accuracy of the channel estimate. We proposed an intuitive method for setting the threshold of the detector to achieve a satisfactory tradeoff between convergence speed and error performance on the channel estimate. Extensive numerical results show the performance of using this threshold, as opposed to fixed thresholds, to be superior.

6.2 Future Research Directions

The following is a list of interesting research topics that can be pursued as an extension of this dissertation:

- In Chapter 2, 3, and 4, we assume CSI is perfect when the relay selection or routing is performed. It is essential to characterize the performance degradation in relay selection because of the imperfect CSI estimation [71]. This would lead to better guidance in system design with respect to complexity/overhead and performance tradeoff.

- In Chapter 3, we focused on equalizers at two extremes: MLSE with highest equalization complexity, and linear ZFE with lowest equalization complexity. However, the relay selection methods corresponding to these two equalizers require different computation complexity. While the optimal-DMT-achieving relay selection method for linear ZFE at the destination requires inversion of matrices with dimensions up to a specific block length, the relay selection method for MLSE at the destination requires a small number of operations. If we seek to lower the combined computation in the selection and equalization, it is necessary to develop relay selection methods corresponding to minimum mean-square error (MMSE) equalization and decision-feedback equalization (DFE), and study the performance and complexity.

- In Chapter 2, 3, and 4, we focused on the performance of a single-source, single-destination system and use relay selection to exploit the cooperative diversity to combat fading. When we have a network where multiple pairs of source-destination communicate, the routing method which maximizes the

performance of a single pair does not necessarily always maximize the network performance. Hence it is imperative to study routing for multiple pairs of source-destination to achieve better network performance. This might be much more complicated as more issues are involved, such as interference, cooperation assignment, handoff, fairness of the system, and other issues.

- In Chapter 2, the proposed relay selection chooses either a single relay or chooses all the decoding relays. It would be intriguing to see the performance improvement when multiple relays are selected under certain criteria [72] (e.g. maximizing the received SNR) with unit total transmission power constraint. It should be kept in mind that as multiple relays are selected in forwarding, multiple relays transmit at the same time; the possible radio collision may require modification in the media-access-control (MAC) layer.

BIBLIOGRAPHY

[1] A. Goldsmith, *Wireless communications*. Cambridge Univ Pr, 2005.

[2] D. Tse and P. Viswanath, *Fundamentals of Wireless Communication*. Cambridge University Press, 2005.

[3] G. Foschini and M. Gans, "On limits of wireless communications in a fading environment when using multiple antennas," *Wireless personal communications*, vol. 6, no. 3, pp. 311–335, 1998.

[4] J. Laneman, D. Tse, and G. Wornell, "Cooperative diversity in wireless networks: Efficient protocols and outage behavior," *IEEE Trans. Inf. Theory*, vol. 50, no. 12, pp. 3062–3080, Dec. 2004.

[5] 3GPP, "Evolved universal terrestrial radio access (e-utra); relay architectures for e-utra (lte-advanced) (release 9)," 3rd Generation Partnership Project (3GPP), TS 36.806, Apr. 2010. [Online]. Available: http://www.3gpp.org/ftp/Specs/html-info/36806.htm

[6] R. Nabar, H. Bolcskei, and F. Kneubuhler, "Fading relay channels: performance limits and space-time signal design," *IEEE J. Sel. Areas Commun.*, vol. 22, no. 6, pp. 1099–1109, Aug. 2004.

[7] J. Laneman and G. Wornell, "Distributed space-time-coded protocols for exploiting cooperative diversity in wireless networks," *IEEE Trans. Inf. Theory*, vol. 49, no. 10, pp. 2415–2425, Oct. 2003.

[8] Y. Shang and X.-G. Xia, "Shift-full-rank matrices and applications in space-time trellis codes for relay networks with asynchronous cooperative diversity," *IEEE Trans. Inf. Theory*, vol. 52, no. 7, pp. 3153–3167, Jul. 2006.

[9] C. Patel and G. Stuber, "Channel estimation for amplify and forward relay based cooperation diversity systems," *IEEE Trans. Wireless Commun.*, vol. 6, no. 6, pp. 2348–2356, Jun. 2007.

[10] F. Gao, T. Cui, and A. Nallanathan, "On channel estimation and optimal training design for amplify and forward relay networks," *IEEE Trans. Wireless Commun.*, vol. 7, no. 5, pp. 1907–1916, May 2008.

[11] S. Shakkottai, T. Rappaport, and P. Karlsson, "Cross-layer design for wireless networks," *Communications Magazine, IEEE*, vol. 41, no. 10, pp. 74–80, 2003.

[12] A. Bletsas, A. Khisti, D. Reed, and A. Lippman, "A simple cooperative diversity method based on network path selection," *IEEE J. Sel. Areas Commun.*, vol. 24, no. 3, pp. 659–672, Mar. 2006.

[13] L. Zheng and D. Tse, "Diversity and multiplexing: A fundamental tradeoff in multiple-antenna channels," *IEEE Trans. Inf. Theory*, vol. 49, no. 5, pp. 1073–1096, May 2003.

[14] R. Narasimhan, "Finite-SNR diversity-multiplexing tradeoff for correlated Rayleigh and Rician MIMO channels," *IEEE Trans. Inf. Theory*, vol. 52, no. 9, pp. 3965–3979, Sep. 2006.

[15] K. Azarian and H. El Gamal, "The throughput–reliability tradeoff in block-fading MIMO channels," *IEEE Trans. Inf. Theory*, vol. 53, no. 2, pp. 488–501, Feb. 2007.

[16] A. Sendonaris, E. Erkip, and B. Aazhang, "User cooperation diversity— Part I: System description," *IEEE Trans. Commun.*, vol. 51, no. 11, pp. 1927–1938, Nov. 2003.

[17] ——, "User cooperation diversity— Part II. implementation aspects and performance analysis," *IEEE Trans. Commun.*, vol. 51, no. 11, pp. 1939–1948, Nov. 2003.

[18] A. Host-Madsen and J. Zhang, "Capacity bounds and power allocation for wireless relay channels," *IEEE Trans. Inf. Theory*, vol. 51, no. 6, pp. 2020–2040, Jun. 2005.

[19] K. Azarian, H. El Gamal, and P. Schniter, "On the achievable diversity-multiplexing tradeoff in half-duplex cooperative channels," *IEEE Trans. Inf. Theory*, vol. 51, no. 12, pp. 4152–4172, Dec. 2005.

[20] A. Bletsas, A. Khisti, and M. Win, "Opportunistic cooperative diversity with feedback and cheap radios," *IEEE Trans. Wireless Commun.*, vol. 7, no. 5, pp. 1823–1827, May 2008.

[21] E. Beres and R. Adve, "On selection cooperation in distributed networks," in *40th Annual Conference on Information Sciences and Systems*, Mar. 2006, pp. 1056–1061.

[22] A. Bletsas, H. Shin, and M. Win, "Cooperative communications with outage-optimal opportunistic relaying," *IEEE Trans. Wireless Commun.*, vol. 6, no. 9, pp. 3450–3460, Sep. 2007.

[23] H. Mheidat, M. Uysal, and N. Al-Dhahir, "Equalization techniques for distributed space-time block codes with amplify-and-forward relaying," *IEEE Trans. Signal Process.*, vol. 55, no. 5, pp. 1839–1852, May 2007.

[24] W. Zhang, Y. Li, X.-G. Xia, P. Ching, and K. Ben Letaief, "Distributed space-frequency coding for cooperative diversity in broadband wireless ad hoc networks," *IEEE Trans. Wireless Commun.*, vol. 7, no. 3, pp. 995–1003, Mar. 2008.

[25] B. Gui, L. Cimini, and L. Dai, "OFDM for cooperative networking with limited channel state information," in *Military Communications Conference (MILCOM'06)*, Oct. 2006, pp. 1–6.

[26] L. Dai, B. Gui, and L. Cimini, "Selective relaying in OFDM multihop cooperative networks," in *Wireless Communications and Networking Conference*, Mar. 2007, pp. 963–968.

[27] Z. Wang and G. Giannakis, "Complex-field coding for OFDM over fading wireless channels," *IEEE Trans. Inf. Theory*, vol. 49, no. 3, pp. 707–720, Mar. 2003.

[28] Y. Ding and M. Uysal, "Amplify-and-forward cooperative OFDM with multiple-relays: performance analysis and relay selection methods," *IEEE Trans. Wireless Commun.*, vol. 8, no. 10, pp. 4963–4968, Oct. 2009.

[29] M. Gastpar and M. Vetterli, "On the capacity of large Gaussian relay networks," *IEEE Trans. Inf. Theory*, vol. 51, no. 3, pp. 765–779, Mar. 2005.

[30] A. Medles and D. Slock, "Optimal diversity vs multiplexing tradeoff for frequency selective MIMO channels," in *International Symposium on Information Theory (ISIT'05)*, Sep. 2005, pp. 1813–1817.

[31] S. Zhou and G. Giannakis, "Space-time coding with maximum diversity gains over frequency-selective fading channels," *IEEE Signal Process. Lett.*, vol. 8, no. 10, pp. 269–272, Oct. 2001.

[32] T. Cormen, C. E. Leiserson, D. L. Rivest, and C. Stein, *Introduction to algorithms*. The MIT press, 2001.

[33] S. Yang and J. Belfiore, "Diversity of MIMO multihop relay channels," submitted to *IEEE Trans. Inf. Theory [arXiv:0708.0386v1]*, 2007.

[34] I. Gradshteyn, I. Ryzhik, A. Jeffrey, and D. Zwillinger, *Table of integrals, series and products*. Academic press, 2007.

[35] S. Wei, D. Goeckel, and M. Valenti, "Asynchronous cooperative diversity," *IEEE Trans. Wireless Commun.*, vol. 5, no. 6, pp. 1547–1557, Jun. 2006.

[36] L. Grokop and D. Tse, "Diversity-multiplexing tradeoff in ISI channels," *IEEE Trans. Inf. Theory*, vol. 55, no. 1, pp. 109–135, Jan. 2009.

[37] R. Horn and C. Johnson, *Matrix analysis*. Cambridge University Press, 1990.

[38] J. R. Barry, E. Lee, and D. Messerschmitt, *Digital communication*. Springer Netherlands, 2004.

[39] Q. Deng and A. Klein, "Relay Selection in Cooperative Networks with Frequency Selective Fading," *EURASIP Journal on Wireless Communications and Networking*, 2011.

[40] A. Medles and D. Slock, "Achieving the optimal diversity-versus-multiplexing tradeoff for MIMO flat channels with QAM space ndash;time spreading and DFE equalization," *IEEE Trans. Inf. Theory*, vol. 52, no. 12, pp. 5312 –5323, Dec. 2006.

[41] N. Al-Dhahir and A. Sayed, "The finite-length multi-input multi-output mmse-dfe," *IEEE Trans. Signal Process.*, vol. 48, no. 10, pp. 2921 –2936, oct 2000.

[42] 3GPP, "Technical specification group GSM/EDGE radio access network; radio transmission and reception (release 10)," 3rd Generation Partnership Project (3GPP), TS 45.005, May 2011. [Online]. Available: http://www.3gpp.org/ftp/Specs/html-info/45005.htm

[43] Z. Liu, Y. Xin, and G. Giannakis, "Linear constellation precoding for OFDM with maximum multipath diversity and coding gains," *Communications, IEEE Transactions on*, vol. 51, no. 3, pp. 416– 27, Mar. 2003.

[44] W. Su, Z. Safar, and K. Liu, "Full-rate full-diversity space-frequency codes with optimum coding advantage," *Information Theory, IEEE Transactions on*, vol. 51, no. 1, pp. 229 –249, Jan. 2005.

[45] Z. Wang and G. Giannakis, "Complex-field coding for OFDM over fading wireless channels," *IEEE Trans. Inf. Theory*, vol. 49, no. 3, pp. 707–720, Mar. 2003.

[46] A. Tajer and A. Nosratinia, "Diversity order in ISI channels with single-carrier frequency-domain equalizers," vol. 9, no. 3, pp. 1022 –1032, Mar. 2010.

[47] D. S. J. D. Couto, D. Aguayo, J. Bicket, and R. Morris, "a high-throughput path metric for multi-hop wireless routing," *Wireless Networks*, vol. 11, pp. 419–434, 2005, 10.1007/s11276-005-1766-z. [Online]. Available: http://dx.doi.org/10.1007/s11276-005-1766-z

[48] M. S. Obaidat, S. K. Dhurandher, P. Jindal, R. Chavli, and S. Valecha, "PMH: A stability based predictive multi-hop routing protocol for vehicular ad hoc networks," *Journal of Internet Technology*, vol. 11, no. 4, pp. 437–449, Jul. 2010.

[49] C. Pandana, W. Siriwongpairat, T. Himsoon, and K. Liu, "Distributed cooperative routing algorithms for maximizing network lifetime," in *Proc. IEEE Wireless Communications and Networking Conf. (WCNC'06)*, vol. 1, Apr. 2006, pp. 451–456.

[50] F. Li, K. Wu, and A. Lippman, "Energy-efficient cooperative routing in multi-hop wireless ad hoc networks," in *Proc. IEEE Intl. Performance, Computing, and Communications Conf. (IPCCC'06)*, Apr. 2006, pp. 215–222.

[51] R. Babaee and N. Beaulieu, "Cross-layer design for multihop wireless relaying networks," *IEEE Trans. Wireless Commun.*, vol. 9, no. 11, pp. 3522–3531, Nov. 2010.

[52] D. Baker, A. Ephremides, and J. Flynn, "The design and simulation of a mobile radio network with distributed control," *IEEE J. Sel. Areas Commun.*, vol. 2, no. 1, pp. 226–237, Jan. 1984.

[53] C. Lin and M. Gerla, "Adaptive clustering for mobile wireless networks," *IEEE J. Sel. Areas Commun.*, vol. 15, no. 7, pp. 1265–1275, Sep. 1997.

[54] S. Banerjee and S. Khuller, "A clustering scheme for hierarchical control in multi-hop wireless networks," in *Proc. IEEE Conf. Computer and Communications Societies (INFOCOM 2001)*, vol. 2, Apr. 2001, pp. 1028–1037.

[55] J. Boyer, D. Falconer, and H. Yanikomeroglu, "Multihop diversity in wireless relaying channels," *IEEE Trans. Commun.*, vol. 52, no. 10, pp. 1820–1830, Oct. 2004.

[56] S.-H. Chen, U. Mitra, and B. Krishnamachari, "Cooperative communication and routing over fading channels in wireless sensor networks," in *Proc. Intl. Conf. on Wireless Networks, Communications and Mobile Computing (WiCOM'05)*, vol. 2, Jun. 2005, pp. 1477–1482.

[57] Q. Tian, S. Bandyopadhyay, and E. J. Coyle, "Designing directional antennas to maximize spatio-temporal sampling rates in multi-hop clustered sensor networks," *Journal of Internet Technology*, vol. 8, no. 1, pp. 1–10, Jan. 2007.

[58] B. Gui, L. Dai, and L. Cimini, "Routing strategies in multihop cooperative networks," *IEEE Trans. Wireless Commun.*, vol. 8, no. 2, pp. 843–855, Feb. 2009.

[59] B. Azimi-Sadjadi and A. Mercado, "Diversity gain for cooperating nodes in multi-hop wireless networks," in *Proc. IEEE Vehicular Technology Conf. (VTC'04)*, vol. 2, Sep. 2004, pp. 1483–1487.

[60] I.-T. Lin and I. Sasase, "Distributed ad hoc cooperative routing in cluster-based multihop networks," in *Proc. IEEE Intl. Symp. on Personal, Indoor and Mobile Radio Communications (PIMRC'09)*, Sep. 2009, pp. 2643–2647.

[61] S. Biswas and R. Morris, "ExOR: opportunistic multi-hop routing for wireless networks," *SIGCOMM Comput. Commun. Rev.*, vol. 35, pp. 133–144, Oct. 2005.

[62] K. Zeng, W. Lou, J. Yang, and D. Brown III, "On throughput efficiency of geographic opportunistic routing in multihop wireless networks," *ACM Mobile Networks and Applications (MONET)*, vol. 12, no. 5, pp. 347–357, Dec. 2007.

[63] C.-K. Toh, "Maximum battery life routing to support ubiquitous mobile computing in wireless ad hoc networks," *IEEE Commun. Mag.*, vol. 39, no. 6, pp. 138–147, Jun. 2001.

[64] F. Gao, T. Cui, and A. Nallanathan, "Optimal training design for channel estimation in decode-and-forward relay networks with individual and total power constraints," *IEEE Trans. Signal Process.*, vol. 56, no. 12, pp. 5937–5949, Dec. 2008.

[65] X. Zhou, T. Lamahewa, and P. Sadeghi, "Kalman filter-based channel estimation for amplify and forward relay communications," in *Signals, Systems and Computers, 2009 Conference Record of the Forty-Third Asilomar Conference on*, Nov. 2009, pp. 1498–1502.

[66] S. Werner, M. de Campos, and P. Diniz, "Partial-update NLMS algorithms with data-selective updating," *IEEE Trans. Signal Process.*, vol. 52, no. 4, pp. 938–949, Apr. 2004.

[67] D. McLernon, "Analysis of LMS algorithm with inputs from cyclostationary random processes," *Electronics Letters*, vol. 27, no. 2, pp. 136–138, Jan. 1991.

[68] S. Haykin, *Adaptive Filter Theory*. Prentice Hall, 2003.

[69] S. Kay, *Fundamentals of Statistical Signal Processing, Volume II: Detection Theory*. Prentice Hall, 1993.

[70] D. Morgan, J. Benesty, and M. Sondhi, "On the evaluation of estimated impulse responses," *IEEE Signal Process. Lett.*, vol. 5, no. 7, pp. 174–176, Jul. 1998.

[71] M. Seyfi, S. Muhaidat, and J. Liang, "Performance analysis of relay selection with feedback delay and channel estimation errors," *IEEE Signal Process. Lett.*, vol. 18, no. 1, pp. 67–70, Jan. 2011.

[72] M. Pun, D. Brown III, and H. Poor, "Opportunistic collaborative beamforming with one-bit feedback," *IEEE Trans. Wireless Commun.*, vol. 8, no. 5, pp. 2629–2641, May 2009.